1-1-1991

Phase transitions of lyotropic liquid crystalline polymers :: effect of fluctuations and disorder/

Mark D. Dadmun
University of Massachusetts Amherst

Phase Transitions of Lyotropic Liquid Crystalline Polymers:

Effect of Fluctuations and Disorder

A Dissertation Presented

by

MARK D. DADMUN

Submitted to the Graduate School of the
University of Massachusetts in partial fulfillment
of the requirements for the degree of

DOCTOR OF PHILOSOPHY

September 1991

Department of Polymer Science and Engineering

Phase Transitions of Lyotropic Liquid Crystalline Polymers:

Effect of Fluctuations and Disorder

A Dissertation Presented

by

MARK D. DADMUN

Approved as to style and content by:

M. Muthukumar, Chair

R. S. Stein, Member

W. J. MacKnight, Member

S. W. Barton, Member

W.J. MacKnight, Department Head
Polymer Science and Engineering Dept.

DEDICATION

This thesis is dedicated to my family; my brothers Jim, Jeff, and Tom, my wife Jayne, and especially my parents, without whose constant encouragement, pride and support this work would not have been possible.

ACKNOWLEDGEMENTS

I would first like to acknowledge the members of my committee, Professor Stein, Professor MacKnight, and Professor Barton for their guidance and advise on the work of this thesis. I would especially like to thank Professor Muthukumar. He has introduced me to many exciting and interesting problems in polymer physics, only a portion of which are in this thesis. In my opinion, he has been everything a doctoral research advisor should be, a teacher, a mentor, and a friend.

Professor T. Springer and Dr. Schwahn of the KFA in Jülich, Dr. Ibel of the ILL in Grenoble, and Dr. Han of NIST are all extended a special thanks for their help and guidance in the completion of the small angle neutron scattering experiments and introducing me to this experimental technique. Thanks also go to Dr. Hempelmann of Jülich for his help and explanation of the quasi-elastic neutron scattering experiment. I would also like to thank Dr. Tereoaka for his help on completion of the low angle light scattering experiments and Jeff Kollodge for his interest and aid in completing the differential scanning calorimetry studies.

I would like to thank all of my friends who have made these four years fun. These include, but are not limited to, Tim, Nicole, Keith, Hiro, Gregg, Bill, Michele, Molly and Mardye. A special thanks goes to Warren, Jeff, and Howard; your friendships have made coming into work every day something to look forward to instead of dreading. Each of you, in your own way, have reminded me that it is not only possible, but imperative to enjoy yourself, even while working. I would also like to

thank Guido, Stefan and Jörg for their friendship while I was in Germany. You introduced me to a different and wonderful culture that I will never forget, Vielen Dank. I would also like to thank the members of Muthu's group, Cristina, Mike, Jim, Rob, Dumont, Scott, Kleanthes, and Mahesh for their interest, comments, and questions concerning my research. Your interest has helped me better understand the problems and results of this work.

I would like to thank my family, Jim, Jeff, Tom, Mom and Dad. You have put up with a perpetual student and your encouragement, pride, and financial and emotional support have not only made this work possible, but also worth doing.

Finally I would like to thank my wife Jayne. You have put your career on hold for two years so that we could be together. Thank you for supporting a poor, starving graduate student in Worcester, Jülich, Paris, London, Rüdesheim, Innsbruck, Munich, Berlin, Grenoble, Amsterdam, and Amherst. Your love, pride and encouragement have made these last two years seem easy.

ABSTRACT

PHASE TRANSITIONS OF LYOTROPIC LIQUID CRYSTALLINE POLYMERS: EFFECT OF FLUCTUATIONS AND DISORDER

SEPTEMBER 1991

MARK D. DADMUN, B.S., UNIVERSITY OF MASSACHUSETTS

Ph.D., UNIVERSITY OF MASSACHUSETTS

Directed by: Professor M. Muthukumar

When a solution of rod-like polymers is subjected to a reduction in solvent quality, it is theoretically predicted that a biphasic system will result. This is not what is observed however as the result is gelation; the formation of a three dimensional self-supporting polymer rich network. The lyotropic system of poly (γ-benzyl l-glutamate) (PBLG) in benzyl alcohol (BA) has been studied on a molecular level as the system is brought from the high temperature phases towards the gel in hopes of understanding the processes that occur that result in gelation.

Low angle light scattering and small angle neutron scattering were used to monitor the configuration of the PBLG molecule as the system was brought from the isotropic to gel phase and to study the gel itself. Quasi-elastic neutron scattering was utilized to measure the local dynamics of the PBLG molecule as the system is brought from the cholesteric to the gel phase.

The results show that an aggregation of PBLG molecules exists up to 80 °C in the isotropic phase and the size of the aggregate changes little as the gelation threshold is approached. As gelation occurs, the size of the aggregate increase substantially. The thermal history of the solution in the isotropic phase also affects the local structure of the resultant gel. Short annealing times result in an open structure similar to an aggregate that is formed via the clustering of clusters mechanism and longer annealing times allow the aggregate to relax and results in a denser, more compact structure. Quasi-elastic neutron scattering demonstrated that the local dynamics of the polymer are continuous and unhindered in the cholesteric phase, but become more constrained and jump like as the system enters the gel phase.

The effect of quenched disorder on the nematic to isotropic transition of a liquid crystal has also been studied. Using Monte Carlo simulation and differential scanning calorimetry, it was seen that quenched disorder will interrupt the ability of the liquid crystal to correlate and this will lower the transition temperature, round and lower the heat capacity peak, and possibly change the order of the transition.

TABLE OF CONTENTS

LIST OF TABLES

LIST OF FIGURES

CHAPTER 1

INTRODUCTION

Statement of Problem and Objective

Rapid reduction of solvent quality of solutions of rod-like polymers plays an important role in the processing of high-strength polymer materials. Dry-jet wet spinning is a method used in processing rod-like polymers into fibers.[1] This method increases the orientation of the fibers over wet spinning. By spinning the polymer dope through an air gap briefly before it is drawn through a coagulation bath where gelation occurs, a greater amount of molecular order results. In this way, stronger fiber mechanical properties are realized. Poly (phenylenebenzobisthiazole), PBT, poly(phenyleneterephthalamide) PPTA, and poly (*p*-phenylenebenzobisoxazole), PBO are three examples of rod-like polymers that are processed in this manner in industry. Gelation has also been performed with PBT in the presence of nylon.[2] There were many problems with the resulting composite including void formation, phase separation, and layer formation. Due to these defects, the mechanical properties of the final product were inferior to the pure materials, but it was much more machinable. Optimization of product characteristics could result from a composite of rod-like and random coil polymers formed from gelation. Another product formed from the reduction of solvent quality of a solution of rod-like polymers is a

microcellular foam. By sublimation of solvent after gelation of a solution of rod-like polymers, Jackson *et. al.*[3,4] and Mustafa *et. al.*[5] have created microcellular foams that have smaller cell sizes than comparable foams created from conventional thermoplastic foam extrusion.[6] As a foam generated from rod-like polymers, these specimens will be chemically, thermally, and mechanically stable and may have superior mechanical properties to random coil gels, as well as other unique properties. They have potential use as artificial skin and blood vessels, filters, catalytic substrates, and model porous media. In order to optimize the use of solutions of rod-like polymers in polymer applications, a better understanding of the process of gelation of rod-like polymers is necessary.

The gelation of rod-like polymers poses a theoretical as well as practical problem. Upon reduction of solvent quality, a solution of rod-like polymers will form a thermoreversible gel. When the concentration of a solution of rod-like molecules is increased above a certain concentration, an ordered liquid crystalline (LC) state should exist. This has been theoretically predicted[7,8] and experimentally observed.[9-12] Unlike the liquid crystalline state, the gel state of a solution of rodlike polymers is not theoretically predicted. According to Flory,[8] upon solvent quality reduction, liquid-liquid phase separation occurs where an isotropic and a liquid crystalline phase should coexist. This discrepancy has been experimentally studied extensively by Miller and others.[13-16] It has been postulated that spinodal decomposition is the method of liquid-liquid phase separation occuring,[15] but this has never been proven or

disproven. Clearly, more studies are needed before a conclusive mechanism of phase separation can be identified.

The objective of this thesis is to understand the phase transition of lyotropic liquid crystalline polymers. Specifically, the system of Poly (γ-benzyl L-glutamate) (PBLG) in the helicogenic solvent benzyl alcohol (BA) is studied. Understanding the molecular origins and the dynamical processes that occur during gelation is a main goal of this study. In order to understand the process, light scattering and neutron scattering are used to study the conformation, *i.e.* radius of gyration and persistence length, of the polymer as the solution undergoes the isotropic to gel phase transition. From this conformational analysis, the intermolecular and intramolecular ordering processes that occur as the system undergoes gelation are monitored. By changing the temperature and concentration of this system, a better understanding of the molecular structure as the system approaches gelation is obtained. Small angle neutron scattering is also used to study the fractal dimension of gels formed from the isotropic phase for different molecular weight polymers and different annealing procedures. Many studies have been completed correlating the fractal dimension of an aggregated system to its kinetic method of aggregation. Therefore, determination of the fractal dimension may allow an identification of the kinetic mechanism of aggregation. Even if a mechanism is not definitely identified, the identification of a fundamental property such as the fractal dimension of the aggregated gel is paramount in understanding the formation of the gel.

Quasi-elastic neutron scattering experiments are also completed to elucidate the local dynamics of the gelation process. Backscattering experiments are performed on PBLG/BA systems as the cholesteric-gel phase transition is approached and passed to understand the dynamics of the polymer chain on a very local scale. (Characteristic length scale, ≈ 10 Å)

These experiments will help to increase the knowledge and understanding of the phenomenon of gelation, but this is a very complex system with many facets that are not well understood. When studying such a complex problem it is beneficial to simplify the problem by concentrating on one aspect of the problem in an attempt to understand that one aspect and determine its effect on the problem. As the initial gel that is formed upon solvent quality reduction can serve as an impedance to any further phase separation, the effect of impurities on the nematic to isotropic transition of a liquid crystal is studied. Using Monte Carlo simulation, the result of the introduction of impurities on the nematic to isotropic phase transition of a liquid crystal and on phase transitions and critical phenomena in general is studied.

Critical phenomena are fascinating. In 1869, Andrews first observed critical behavior while studying CO_2.[17] He observed the coexistence of the liquid and gas phase at the critical point and its continuous change from one phase to the other. Andrews' experiment began what is now called the "classical era" of critical phenomena study. The "modern" era of the study of critical phenomena began with Onsager's exact solution of the two dimensional Ising model in 1944.[18]

This mathematical triumph forced scientists to realize that an exact solution to more complex models would not be forthcoming soon. This led the way to the use of approximate methods in solving theoretical models. In the 1950's the idea of critical exponents became widely accepted as a method of characterizing phase transitions. In the 1960's the introduction of the scaling approach as a method to compare and contrast different transitions through critical exponents led the way to the adaptation of the renormalization group[19] (RG) technique in the 1970's as a method for approximating the solution of more complex theoretical models.

However, most theoretical work and analytical theories have centered on ideal homogeneous systems. Though analogous ideal homogeneous systems can be created in the laboratory to test these predictions, the step to everyday phenomena must include some heterogeneity. Every real system will contain some amount of heterogeneity due to the presence of surfaces, impurities, disclinations, grain boundaries, etc. In theoretical models, the easiest method to include heterogeneity or disorder is to randomly replace magnetic atoms with non-magnetic atoms. This method is called "dilution". The effect of dilution on a phase transition has been studied extensively for magnetic phase transitions (Ising, Heisenberg, X-Y model, etc...) using renormalization group,[20] expansion methods,[21-23] and Monte Carlo simulation,[24-27] but it has rarely been applied to a first order phase transition. Monte Carlo simulation will be used to quantitatively measure the effect of dilution on a fluid phase transition to understand phase transitions of real dilute systems.

The nematic to isotropic phase transition of a liquid crystal on a lattice is simulated using Monte Carlo methods. Dilution is effected by denoting random points on the lattice as occupied by impurities and therefore inaccessible to the liquid crystal. The only interaction between liquid crystal and impurity is steric, there is no repulsive or attractive interaction. A series of impurity concentrations, (1-p), are studied. The phase transition is monitored by calculating the heat capacity, C_v and the order parameter, $< S >$ as the system undergoes the order to disorder phase transition. C_v is defined as the fluctuation in the energy,

$$C_v = < E^2 > - < E >^2$$

and the order parameter is defined as

$$< S > = 1/2 [3f - 1].$$

where f is the fraction of lattice steps along the preferred axis of orientation and E is the total energy of the system. $< ... >$ denotes the ensemble average. Finite size analysis of the observed critical phenomena is used to determine the order of the phase transition for the pure and impure system.

As a simple experiment in conjunction with the computer experiment, the nematic to isotropic transition of a liquid crystal confined to a controlled pore glass (CPG) is monitored by differential scanning calorimetry (DSC). The CPG serves as the disorder for the liquid crystalline system undergoing a phase transition. The disorder takes the form of the surfaces and finite size of the CPG. An important parameter in this study is the ratio of the pore size to the molecular size, λ. If λ is

large then surface effects dominate, whereas if λ is small finite size is important. By varying the pore size, the ratio λ can be systematically changed and each type of disorder studied.

Literature Review

Gelation of Rod-Like Polymers

Original calculations by Onsager[7] demonstrated that a state of parallel order will be obtained from a solution of anisotropic molecules above a certain concentration due solely to steric interactions. Flory[8] used an extension of his lattice theory for random coil polymers to show that inflexibility of the polymer chain and steric interactions will create a liquid crystalline state. Flory calculated the effect of temperature as well as concentration on the phase diagram. His calculations showed transitions from the isotropic to liquid crystalline state with concentration and the transition with temperature from the liquid crystalline or isotropic phases into a biphasic region where isotropic and liquid crystalline phases should coexist. The phase diagram that Flory predicted for rod-like polymers from statistical mechanics is still used today as the basis for lyotropic liquid crystalline polymers. The problem is that Flory predicted the emergence of a biphasic region upon a decrease in solvent quality. Experimentally, if a solution of rod-like polymers is exposed to a sudden decrease in solvent quality due to temperature change or addition of non-solvent, reversible gelation occurs. Though this was experimentally observed almost 20 years ago,[9] there is still no theory to describe the process of gelation of rod-like polymers.

The first synthetic macromolecule to exhibit a phase diagram similar to the one predicted by Flory was poly (γ-benzyl L-glutamate). PBLG will molecularly disperse in polar solvents such as *n*-Dimethylformamide (DMF) whereas it will aggregate in less polar solvents such as benzene or dioxane.[28] Wee and Miller extensively studied the solution of PBLG in DMF and determined that its phase diagram closely resembles Flory's predicted phase diagram.[11,12] The transition from isotropic to liquid crystal is in good agreement with Flory's lattice theory, including the passage through a narrow biphasic region. When the temperature is reduced from either the isotropic or cholesteric phase, however, a gel that is a continuous polymer phase in a three dimensional network is formed.

In an attempt to explain this discrepancy, spinodal decomposition,[29,30] and then polymer immobility to prevent further ripening, has been proposed as the mechanism that occurs upon solvent quality reduction.[15,31] According to Cahn and Hilliard, when a system is suddenly brought into the thermodynamically unstable region, the system composition becomes bicontinuous with a characteristic periodicity. Further separation occurs as the components flow against the concentration gradient. It has been proposed that further flow does not occur in this system due to the fiber-like structure of the polymer rich phase.[15] This mechanism results in a bicontinuous interconnected structure for a system with approximately equal fractions of both components. As the amount of the minor component decreases, the bicontinuous connectivity is expected to disappear. Cahn[30] estimated that a decrease below 15% of the minor phase will result in the transition

from a continuous minor phase to isolated particles. Therefore, at concentrations below 15% PBLG, the spinodal decomposition mechanism should leave isolated particles, not a continuous phase. Miller[15] has suggested that due to molecular asymmetry the growth of the polymer phase may be anisotropic, and therefore an interconnected minor phase would result. The spinodal line for a system of hard rods in solution has been calculated for different axial ratios.[4,8,11,32] These calculations show that the spinodal line is very close to the binodal line for the cholesteric–gel phase transition, but a large gap exists between the binodal and the spinodal for the isotropic–gel phase transition. This indicates that the spinodal mechanism may contribute to the cholesteric–gel phase transition but any attempt to describe the isotropic–gel transition with spinodal decomposition is questionable at best. Experiments have been completed in an attempt to prove that spinodal decomposition occurs during the gelation of a solution of PBLG.[13,32] Unfortunately, the contribution of spinodal decomposition to the gelation of solutions of PBLG has not yet been proven or disproven.

Experimental study of the gel phase formed from the PBLG/DMF and PBLG/BA systems have been numerous in an effort to define the gel structure as well as understand the process of gelation. Experimental studies on the PBLG/BA study have centered on determination of the phase diagram and characterization of the gel. Differential scanning calorimetry (DSC),[16,32] x-ray scattering,[16,33] electron microscopy,[16] light scattering,[32] rheology,[14,16,32] and dynamic light scattering[32] are among the methods used on this system. Structural analysis of microcellular foams have been completed in an effort to understand the separation

mechanism from the final structure of the gel.[4,5] Methods used in examining these foams include electron microscopy, wide angle x-ray scattering, and modulus experiments. Nuclear magnetic resonance (NMR), polarized light microscopy, isopiestic, and hydrodynamic measurements were used by Miller *et. al.*[11,12] to determine the phase diagram of the PBLG/DMF system. Phase diagram determination, analysis of the resultant gel, and effect of addition of non-solvent have all been attempted to understand the process of gelation better.

The identification and description of the gel phase and its molecular origins is a fundamental problem in polymer physics today. A description of the dynamics of the formation of the gel as well as the gel itself is necessary in order to develop a theory describing the solutions of rod-like polymers in all phases.

If a sample of aggregated particles has a two point density correlation function $\rho(r)$ of a power law form,

$$\rho(r) \propto r^{-A}$$

for values of r between the particle size, a, and the cluster size, R, it is said to be self-similar over this length scale. One direct result of this is that the radius of gyration of the sample is related to the number (or mass) of the particles, M_a.

$$M_a \propto R_g^{D}$$

D=d-A where D is the Hausdorff[34] of fractal[35] dimension and d is the imbedding dimension. The structure factor S(q), which is measured in a scattering experiment, is the fourier transform of the two point

density correlation function. The power law dependence is manifested in a scattering experiment as a power law dependence, $S(q) \propto q^{-D}$ over the range $R^{-1} \leq q \leq a^{-1}$. The fractal dimension, D, is measured for the gels formed from the isotropic phase using SANS. D is physically a measure of the "compactness" of a system. The Hausdorff dimension of a rod equals 1.0, a random coil 2.0, and the fractal dimension of a self-avoiding walk in three dimensions according to mean field calculations is 1.667. Many studies linking the fractal dimension to a kinetic method of aggregation have been completed, including scattering experiments,[36-42] Monte Carlo simulations,[43-48] and analytical calculations.[49] The kinetic models that have been considered include the clustering of clusters, diffusion limited aggregation, percolation, and reaction limited aggregation. As each of the above kinetic models present a possible growth mechanism, identification of the fractal dimension, and therefore possibly the kinetic mechanism of growth, will lead to a better understanding of the molecular origin of the process of gelation.

A polymer molecule in solution is constantly undergoing dynamic motion due to the interaction of the polymer with the solvent, other polymer chains and within the polymer chain itself. The energy ΔE associated with these dynamics depends on the frequency, ω, of the motion through the equation, $\Delta E = \frac{h\omega}{2\pi}$ where h is Planck's constant. One method to detect the dynamics of a polymer solution is to impinge a beam of incident radiation on the solution and measure the energy transferred between the solution and the radiation.[50,51] This energy identifies the frequency of the dynamics. Different types of radiation will study different length scales and frequencies. Using light scattering, the

diffusive nature of the complete polymer chain can be measured with a length scale of ~ 100 Å and a time scale of 10^{-4} s, with the neutron spin echo technique the dynamics along the polymer chain can be determined with a length scale of ~ 40 Å and a time scale of 10^{-7} s, and using neutron backscattering the local dynamics, *i.e.* rotation of 1 to 2 bonds, can be studied on a length scale of ~ 5 – 10 Å and a time scale of 10^{-10} s. Therefore quasi-elastic neutron scattering can be used to study the local dynamics of a polymer in solution. The incoherent quasi-elastic scattering, $S_{inc}(q,\omega)$, is the quantity measured in scattering experiments. This quantity is related to the space time self correlation function and therefore contains information about the dynamics of the polymer in solution. The rotational motion scattering, $S_{rot}(q,\omega)$, can be separated out of $S_{inc}(q,\omega)$. The incoherent rotational scattering is given as a sum of a purely elastic component and a quasi-elastic component.[52]

$$S_{rot}(q,\omega) = A_o(q)\delta(\omega) + S_{rot}^{qel}(q,\omega)$$

The intensity of the elastic portion, the elastic incoherent structure factor (EISF) is a measure of the time averaged spatial distribution of the protons. It's variation with q gives information of the geometry of the rotational motion. The quasielastic portion describes the time frame, *i.e.* the frequency, of the rotation. In its most general form $S_{rot}^{qel}(q,\omega)$ is a summation of Lorentzians. The full width at half maximum (HW) of a given Lorentzian is inversely proportional to the residence time of that motion. The change with q of the EISF and HW has been calculated for some simple motions.[53] For example a dumbbell motion has an EISF that decays from 1.0 at q=0.0 to an equilibrium value of 0.5 at large q and its HW will not change with q. For rotation on a sphere, the EISF will

decay from 1.0 at q=0 to 0.0 at large q and the HW will be dependent on q. The rate of decay will give the characteristic size of the motion. The measured change in the EISF and HW with q can be compared with model results in order to determine the motions present in the polymer solution. In this way one is able to visualize the dynamical motion of the hydrogen atoms, and therefore the polymer chain in solution.

Monte Carlo Simulations and Phase Transitions with Disorder

Monte Carlo simulations have been used extensively to study the thermodynamics of model systems.[54] Computer simulations are similar to experiments in that an average quantity is found with incorporation of as little bias as possible. The difference is the average in computer simulations is found from the creation of many different ensembles consecutively, whereas experiments measure the average of many different ensembles that occur simultaneously. Starting from initial statistical mechanics and fundamental microscopic interactions, the "experiment" is carried out and final properties are calculated from ensemble averages. In this way, simulations serve as a link between theory and experiment. As in experiments, non-trivial conclusions can be drawn that can not be inferred from the theoretical description of the model, yet this experiment incorporates only the microscopic interactions of the model. This link serves to make Monte Carlo simulations an invaluable tool to observe subtle and otherwise neglected relations in physics as well as to assess basic assumptions and predictions of analytical theories.

Monte Carlo simulation has become a common method to solve problems in statistical mechanics. The Monte Carlo method can be envisaged as an integration technique from which a thermodynamic average, <A>, can be calculated by recursively sampling points in phase space, calculating A for each point, and averaging over all phase points. There exist many difficulties to accurately implementing this procedure including ergodicity, microscopic reversibility, and the vastness of phase space. With a correct algorithm these difficulties can be eliminated or minimized as the following detailed description will elucidate.

In a canonical ensemble a system is defined that contains $\underline{N}$ particles at a temperature $\underline{T}$ in a volume $\underline{V}$. Each particle in this system has associated with it a set of dynamic variables $\{ \rho_i \}$ that describe the configurational state of the particle. The set $\left[\{\rho_1\} \{\rho_2\} \ldots \right]$ then defines the point in phase space, ñ, that the system occupies. An observable thermodynamic property <A> can then be found for this system by averaging this property over phase space.

$$<A> = \frac{\int_{\Omega} d\tilde{n}\, A(\tilde{n}) \exp\left[-\mathcal{H}_{\underline{N}}(\tilde{n})/kt\right]}{\int_{\Omega} d\tilde{n} \exp\left[-\mathcal{H}_{\underline{N}}(\tilde{n})/kt\right]} \qquad (1)$$

where $\mathcal{H}_{\underline{N}}(\tilde{n})$ is the hamiltonian of the system and describes the inter- and intraparticle interactions and Ω denotes that the integral is done over the phase space volume Ω. This integral can be approximated as a

sum over randomly selected points in phase space according to a uniform distribution.

$$\langle A \rangle \approx \frac{\sum_{i=1}^{M} A(\tilde{n}) \exp\left[-\mathcal{H}_{\underline{N}}(\tilde{n})/kt\right]}{\sum_{i=1}^{M} \exp\left[-\mathcal{H}_{\underline{N}}(\tilde{n})/kt\right]} \qquad (2)$$

Unfortunately, for statistical mechanical problems of interest, the configurations of the system occur with nonrandom probability and much time is wasted sampling configurations that contribute little to the average.

This problem was overcome when Metropolis *et al.*[55] introduced *importance sampling*. In this algorithm the points in phase space are not selected randomly but are picked according to an occurrence probability, $P(\tilde{n})$. In this case equation 2 becomes

$$\langle A \rangle \approx \frac{\sum_{i=1}^{M} A(\tilde{n})\, P^{-1}(\tilde{n}) \exp\left[-\mathcal{H}_{\underline{N}}(\tilde{n})/kt\right]}{\sum_{i=1}^{M} P^{-1}(\tilde{n}) \exp\left[-\mathcal{H}_{\underline{N}}(\tilde{n})/kt\right]} \qquad (3)$$

If $P(\tilde{n})$ is chosen to be $P(\tilde{n}_i) = \exp\left[-\mathcal{H}_{\underline{N}}(\tilde{n}_i)/kt\right]$ then (3) becomes

$$\langle A \rangle = \frac{1}{M} \sum_{i=1}^{M} A(\tilde{n}_i) \qquad (4)$$

A second feature of the Metropolis method is that the system walk through phase space is a random process known as a Markov chain.

Each successive configuration in the Markov process is accepted or rejected into the chain based on the probability of the transition from the starting configuration to the successive configuration. This transition probability $W(\tilde{n}_i \rightarrow \tilde{n}_j)$ is chosen so that other requirements of a Markov process are fulfilled. These requirements are that the moves must satisfy ergodicity and microscopic reversibility. Ergodicity states that configuration $\tilde{n}_i$ can be reached from configuration $\tilde{n}_j$ through a finite number of steps of the random walk. In other words, that all positions in phase space are accessible to the system from all others. The concept of microscopic reversibility states that the transition probability of moving from $\tilde{n}_i \rightarrow \tilde{n}_j$ is equal to the transition probability of moving from $\tilde{n}_j \rightarrow \tilde{n}_i$ *times* the ratio of the occurrence probabilities of state j and state i.

There are many choices for $W(\tilde{n}_i \rightarrow \tilde{n}_j)$ that satisfy these conditions but one common choice, and the method used in our simulation, is

$$W(\tilde{n}_i \rightarrow \tilde{n}_j) = \begin{cases} \frac{1}{\tau_s} \exp(-\delta H/kt) & \delta H > 0 \\ \frac{1}{\tau_s} & \text{Otherwise} \end{cases}$$

Where $\delta H = \mathcal{H}(\tilde{n}_j) - \mathcal{H}(\tilde{n}_i)$ and τ_s is an arbitrary number and is usually set to one.

Therefore, using Monte Carlo methods, thermodynamic quantities can be found for a given [N,V,T] of a system with defined molecular interactions. This is done by defining a system with N particles whose dynamic variables $\{ \rho_i \}$ are known. Phase space is then sampled using the Metropolis algorithm and the thermodynamic quantity is averaged over this phase space. In the Metropolis algorithm the configuration

$\{ \tilde{n}_i \}$ of the system is perturbed into configuration $\{\tilde{n}_j\}$. If the transition $(\tilde{n}_i \rightarrow \tilde{n}_j)$ is allowed according to the transition probability $W(\tilde{n}_i \rightarrow \tilde{n}_j)$ then $\{ \tilde{n}_j \}$ is accepted and entered into the ensemble average. If $\tilde{n}_j$ is not allowed, $\tilde{n}_i$ is recounted in the average. In this way phase space is efficiently sampled and the thermodynamic average is correct for the given set of conditions.

One area where Monte Carlo simulation has been extensively used is the study of phase transition and critical phenomena.[56] The order-disorder transition of many systems have been studied by Monte Carlo simulations including magnetic and fluid systems. These models typically assume homogeneity. However, since pure ideal systems do not occur in nature, the study of systems with disorder deserves attention.[57] There are many methods to simulate disorder in a theoretical model. These mechanisms include adding non-magnetic atoms to a lattice of magnetic atoms, called "dilution"; imposing a random magnetic field to a model system, called "random field"; or denoting the interatomic interactions as random, called "random bond". The easiest of these mechanisms to implement is dilution.

Since the order-disorder transition temperature (the Curie temperature for magnetic systems) is proportional to the total intermolecular interaction, the introduction of isolated random impurities will decrease the total intermolecular interaction, and therefore the transition temperature, T_c. However, long range order can only be attained if there exists sufficient pathways through which interactions can correlate. Above a certain impurity concentration, $1\text{-}p_c$, (p_c is the percolation threshold) these pathways cease to exist, *i.e.*

separate domains exist, and no transition can occur. Therefore, the transition temperature should decrease linearly with impurity concentration, 1-p, in the dilute limit and continue to decrease to zero at the percolation threshold. Our study will concentrate on the dilute limit, p = 0.925 – 1.00. The slope of the initial decrease, ($\Sigma = T_c^{-1}\, dT_c/dp$) has been calculated by Monte Carlo simulation and other methods for many magnetic systems including the three dimensional Heisenberg model[24] ($\Sigma = 1.3 \pm 0.2$), the two dimensional Ising model[25,27] ($\Sigma = 1.5$), and the three dimensional Ising model[26] ($\Sigma = 1.1$). More important than the initial slope of the change of T_c with impurity concentration is the nature of the phase transition in the presence of dilute impurities. Harris[22] has postulated that, for a second order phase transition, if the specific heat exponent, α, is negative a dilute system will exhibit a sharp transition with the same critical exponents as the pure system. If α is positive, however, a sharp transition is predicted with critical exponents different than the pure system. For a system with α=0, the dilute system is expected to undergo a sharp phase transition similar to the pure system with logarithmic corrections. This is known as the Harris criterion. The only "experiment" available to test these prediction (*i.e.* insure an exact impurity concentration) is Monte Carlo simulation. Unfortunately, attempts to obtain conclusive results of a change in critical exponents with dilution have been unsuccessful. Two dimensional[25,27] (α=0) and three dimensional[26] ($\alpha \approx 1/8$) Ising models are among the models that have been studied, but results have not been precise enough to detect a change in the critical point exponent and therefore test the validity of the Harris criterion.

Imry and Wortis[58] were the first to study the effect of disorder on a first order phase transition. Using a heuristic argument, they showed that the presence of quenched impurities will smear the phase transition. The extent of rounding was shown to depend on the extent of the fluctuations in the impurity density as well as the interfacial energy between competing phases. More recently Hui and Berker[59] and separately Aizenmann and Wehr[60] have shown that a two dimensional system with quenched impurities can not undergo a first order phase transition. Extending this[61], It was shown that a first order phase transition will be suppressed to a second order phase transition with the introduction of infinitesimal bond randomness below a threshold dimension $\underline{d}$. The value of $\underline{d}$ depends on the symmetry of the system. It was also shown that above $\underline{d}$, a threshold amount of bond randomness is needed to suppress the discontinuity in the phase transition, but the suppression occurs nonetheless. The object of this study is to use Monte Carlo simulation to study the effect of the introduction of disorder on the the nematic to isotropic phase transition of a liquid crystal. In doing this we hope to understand the mesophase transitions of liquid crystals and their response to external perturbations as well as to extend the research on the response of first order phase transitions to quenched impurities.

Disorder Effects of the Nematic-Isotropic Transition of Liquid Crystals

Disorder in real systems can take many different forms, including surfaces, grain boundaries, impurities, disclinations, or the finite size of the system. Usually, these forces are negligible, but for systems with a characteristic length scale less than 1 μm, these forces become very

important. Because liquid crystals are soft, *i.e.* the energy responsible for long range order is small,[62] disorder will dramatically affect their thermodynamic properties. Studies of these effects on liquid crystals therefore deserve attention. Both the solid to nematic (S–N) and nematic to isotropic (N–I) transitions have been experimentally studied in finite systems.[63-66] Thin films[63] ($d \approx 1\text{-}1000\ \mu$) and cylindrical pores[64-66] ($R \approx 50 - 2000$ Å) have been used as model systems. In all cases, a decrease in the S–N transition temperature with a decrease in characteristic size was observed. The effect of surfaces and size on the N–I transition is less well understood. Some studies[63,65,67-70] show a decrease in the N–I transition temperature with decreasing characteristic size, while others show an increase.[64,66,71] Model finite systems in these studies include porous media[64-69], thin films[63,71], and polymer dispersed liquid crystalline droplets[70].

The effect of a surface on the nematic to isotropic transition (N-I) of a liquid crystal has been extensively studied theoretically[72,73] and experimentally.[65,66,70,71,74] The first theoretical work of surface effects on the phase transitions of a liquid crystal was done by Sheng.[73] In this work, the N-I transition of a thin liquid crystalline film was studied. Using the Landau-DeGennes theory[63,75] for the free energy density of a liquid crystal, the effect of the thickness of surface aligned thin films was calculated for the N-I transition. By adding a surface potential to the free energy, Sheng showed that the N-I transition temperature will increase as the film thickness decreases until a critical thickness, D_c, is reached. For thicknesses below D_c, the first order N-I phase transition should become continuous. One assumption of this calculation is that the liquid

crystal is strongly anchored at the surface wall. Sheng has extended this work[72] by varying the substrate-liquid crystal interaction parameter, g, to include strong and weak surface anchoring. Sheng showed that three regimes exist, each depending on the strength of the interaction parameter, g. It was found that certain values of g can cause not only a boundary layer with an order parameter different from the bulk, but a boundary layer phase transition separate and at a higher temperature than the bulk transition. Below a certain value, g_o, the entire system, boundary layer and bulk, will undergo a normal first order phase transition at the bulk transition temperature. For values $g_o < g < g_c$, there is a boundary layer phase transition, separate from the bulk phase transition, which occurs at a higher temperature than the bulk transition. For values $g > g_c$, both the boundary layer and bulk phase transitions coincide and undergo a first order transition at a temperature above the bulk transition temperature. The previously described critical thickness, D_c, is also found to vary with the strength of the interaction parameter, g. Due to the finite interaction g, the liquid crystal will always exhibit a degree of surface induced order. This permanent order leads to the high temperature phase being termed "paranematic", analogous to the "paramagnetic" phase for magnetic phenomena. Therefore, theory predicts that a three dimensional, g-D-T, phase diagram exists with transitions between the nematic, isotropic, and paranematic phases. The existence of a separate boundary layer phase transition has been experimentally verified.[71]

The effect of finite size and impurities in the N-I transition of a liquid crystal has been less studied. Many experimental studies have

been completed on liquid crystals in confined spaces, but no attempt has been made to separate the different type of disorder. Sheng *et. al.*[76] have studied the effect of finite size on the melting transition. Using positional disorder theory, it was shown that the specific heat of a small, finite cluster of molecules will peak at a temperature lower than the bulk transition temperature and the peak will be broadened. Their calculations served to explain experimental results of a variety of adsorbate systems such as H_2O in porous Al_2O_3. As both transitions involve a first order transition where poorly correlated domains exist, it is expected that there will be similar finite size effects on the N-I transition of a liquid crystal confined to a controlled glass.

In order to understand the effect of disorder on the N-I transition, an experimental study of N-I transition of a liquid crystal in a controlled pore glass (CPG) is studied. Using differential scanning calorimetry (DSC), the nematic-isotropic transition of a small molecule liquid crystal in a CPG is monitored. The ratio of pore size to liquid crystal, $\lambda=R_p/R_g$, is used to determine the type of disorder that affects the system. It is expected that at large λ, the surface should strongly affect the transition whereas at small λ finite size effects should dominate. This is best understood by visualizing the liquid crystal in the pore. At large λ a small portion of liquid crystal will experience an alignment due to the pore wall. The rest of the system will not experience anything different from the pure state. If λ is small however, all of the liquid crystal experiences the confinement of the walls and most correlations can only occur axially. Each pore will define a domain that contains liquid crystal that cannot correlate with other domains (pores). Therefore, clusters

exist that are not correlated. Different pore sizes are used to determine the response of the liquid crystalline system to different types of disorder.

References

1. E. W. Choe and S. N. Kim, Macromolecules **14**, 920 (1981).

2. W. Huh and Y. C. L. Charles, Polym. Mater. Sci. Eng. **60**, 861 (1989).

3. C. L. Jackson, E. T. Samulski, and M. T. Shaw, Polym. Mater. Sci. Eng. **57**, 107 (1987).

4. C. L. Jackson and M. T. Shaw, Polymer **31**, 1070 (1990).

5. M. Mustafa and P. S. Russo, Polym. Mater. Sci. Eng. **59**, 1053 (1989).

6. J. H. Aubert and R. L. Clough, Polymer **26**, 2047 (1985).

7. L. Onsager, Ann. N.Y. Acad. Sci. **51**, 627 (1949).

8. P. J. Flory, Proc. Roy. Soc. (London) **A234**, 73 (1956).

9. W.G. Miller, C.C. Chuan, E.L. Wee, G.L. Santee, J.H. Rai, and K.G. Goebel, Pure Appl. Chem. **38**, 37 (1974).

10. A. Nakajima, T. Hayashi, and M. Ohmori, Biopolymers **6**, 973 (1968).

11. E. L. Wee and W. G. Miller, J. Phys. Chem. **75**, 1446 (1971).

12. W. G. Miller, J. H. Rai, and E. L. Wee, in *Liquid Crystals and Ordered Fluids*, edited by R. Porter and J. Johnston (Plenum, New York, 1974).

13. P. S Russo, P. Magestro, and W. G. Miller in *Reversible Polymeric Gels and Related Systems, ACS Symposium Series* #350 edited by P.S. Russo, (American Chemical Society, Washington D.C., 1987).

14. A. K. Murthy and M. Muthukumar, Macromolecules **20**, 564 (1987).

15. W. G. Miller, L. Kou, K. Tohyama, and V. Voltagio, Journ. Poly. Sci.: Polym. Symp. **65**, 91 (1978).

16. S. Sasaki, M. Hikata, C. Shiraki, and I. Uematsu, Polym. Journ. **14**, 205 (1982).

17. T. Andrews, Phil. Trans. Soc. **159**, 575 (1869).

18. L. Onsager, Phys. Rev. **65**, 117 (1944).

19. K. G. Wilson and J. Kogut, J. Phys. Rep. **12**, 75 (1974).

20. U. Krey, Z. Physik. B **26**, 355 (1977).

21. C. Domb, J. Phys. C: Solid State Phys. **5**, 1399 (1972).

22. A. B. Harris, J. Phys. C: Solid State Phys. **7**, 1671 (1974).

23. D. E. Khmel'nitskii, Sov. Phys.–JETP **41**, 981 (1976).

24. V. Wildpaner, H. Rauch, and K. Binder, J. Phys. Chem. Solids **34**, 925 (1973).

25. E. Stoll and T. Schneider, J. Phys. A: Math. Gen. **9**, L67 (1976).

26. D. P. Landau, Physica B **86-88**, 731 (1977).

27. W. Y. Ching and D. L. Huber, Phys. Rev. B **13**, 2962 (1976).

28. R. Sakamoto and M. Watanabe, Cont. Topics in Polym. Sci. **4**, 259 (1984).

29. J. Cahn and J. Hilliard, J. Chem. Phys. **31**, 688 (1959).

30. J. Cahn, J. Chem. Phys. **42**, 93 (1965).

31. K. Tohyama and W. G. Miller, Nature **289**, 813 (1981).

32. P. Shukla, Ph.D. Dissertation, Univerity of Massachusetts, (1989).

33. S. Sasaki, K. Tokuma, and I. Uematsu, Polym. Bull. **10**, 539 (1983).

34. F. Hausdorff, Math. Ann. **79**, 157 (1919).

35. B. Mandelbrot, *Fractals, Form, Chance, and Dimension* (Freeman, San Francisco, 1977).

36. D. W. Schaefer, J. E. Martin, P. Wiltzius, and D. S. Cannell, Phys. Rev. Lett. **52**, 2371 (1984).

37. J. Marignan, C. Guizard, and A. Larbot, Europhys. Lett. **8**, 691 (1989).

38. C. Quellet, H. F. Eicke, R. Gehrke, and W. Sager, Europhys. Lett. **9**, 293 (1989).

39. T. Ogawa, S. Miyashita, and H. Miyaji, J. Chem. Phys. **90**, 2063 (1989).

40. W.-L. Wu, B. Bauer, and W. Su, Polymer **30**, 1384 (1989).

41. Ph. Mangin, B. Rodmacq, and A. Chamberod, Phys. Rev. Lett. **55**, 2899 (1985).

42. C. Aubert and D. S. Cannell, Phys. Rev. Lett. **56**, 738 (1986).

43. M. Kolb, J. Phys. A: Math. Gen. **19**, L263 (1986).

44. D. W. Heermann and W. Klein, Phys. Rev. Lett. **50**, 1062 (1983).

45. P. Meakin, Phys. Rev. A **27**, 604 (1983).

46. T. A. Witten, Jr. and L. M. Sander, Phys. Rev. Lett. **47**, 1400 (1981).

47. P. Meakin, Phys. Rev. Lett. **51**, 1119 (1983).

48. M. Kolb, R. Botet, and R. Jullien, Phys. Rev. Lett. **51**, 1123 (1983).

49. M. Muthukumar, Phys. Rev. Lett. **50**, 839 (1983).

50. B.J. Berne and R. Pecora, Dynamic Light Scattering (John Wiley and Sons, New York, 1976).

51. L.K. Nicholson, J.S. Higgins, and J.B. Hayter, Macromolecules **14**, 836 (1981).

52. A.J. Leadbetter and R.E. Lechner in *The Plastically Crystalline State*, edited by J.N. Sherwood (Wiley, New York, 1979).

53. J.A. Janik and T.Riste in *Methods in Experimental Physics, Vol 23B*, edited by K. Sköld and D.L. Rice (Academic Press, Boston, 1986).

54. K. Binder in *Monte Carlo Methods in Statistical Physics*, edited by K. Binder (Springer–Verlag, New York, 1974).

55. N. Metropolis, A.N. Rosenbluth, M.N. Rosenbluth, A.H. Teller, and E. Teller, J. Chem. Phys. **21**, 1087 (1953).

56. O.G. Mouritsen, *Computer Studies of Phase Transitions and Critical Phenomena* (Springer–Verlag, New York, 1984).

57. K. Binder and D. Stauffer in *Monte Carlo Methods in Statistical Physics*, edited by K. Binder (Springer–Verlag, New York, 1974).

58. Y. Imry and M. Wortis, Phys Rev. B **19**, 3580 (1979).

59. K. Hui and A.N. Berker, Phys. Rev. Lett. **62**, 2506 (1989).

60. M. Aizenmann and J. Wehr, Phys. Rev. Lett. **62**, 2503 (1989).

61. A.N. Berker, Bull. Am. Phys. Soc. **14**, 1990 (1990).

62. P. G. DeGennes, *The Physics of Liquid Crystals* (Oxford University Press, Oxford, 1974).

63. M.V. Kurik, Sov. Phys. Solid State **19**, 1081 (1977).

64. F.M. Aliev and M.N. Breganov, Sov. Phys. JETP **68**, 70 (1989).

65. D. Armitage and F.P. Price, Chem Phys. Lett. **44**, 305 (1976).

66. F.M. Aliev, Sov. Phys. Crystallogr. **33**, 573 (1988).

67. D. Armitage and F.P. Price, Mol. Cryst. Liq. Cryst. **44**, 33 (1978).

68. D. Armitage and F.P. Price, J. Polym. Sci. Polym. Symp. **63**, 95 (1978).

69. M. Kuzma and M.M. Labes, Mol. Cryst. Liq. Cryst. **100**, 103 (1983).

70. A. Golemme, S. Zumer, D.W. Allender, and J.W. Doane, Phys. Rev. Lett **61**, 2937 (1988).

71. Y. IImura, H. Mada, and S. Kobayashi, Phys Lett. **103A**, 342 (1984).

72. P. Sheng, Phys. Rev. A **26**, 1610 (1982).

73. P. Sheng, Phys. Rev. Lett. **37**, 1059 (1976).

74. A. Poniewierski and T. J. Slukin, Mol. Cryst. Liq. Cryst. **111**, 373 (1984).

75. P. G. DeGennes, Mol. Cryst. Liq. Cryst. **12**, 193 (1971).

76. P. Sheng, R. W. Cohen, and J. R. Schrieffer, J. Phys. C: Solid State Phys. **14**, L565 (1981).

CHAPTER 2

MATERIALS AND EXPERIMENTAL TECHNIQUES

Materials

The primary investigations reported in this thesis concern the lyotropic liquid crystal poly (γ-benzyl l-glutamate) (PBLG) which has the chemical structure

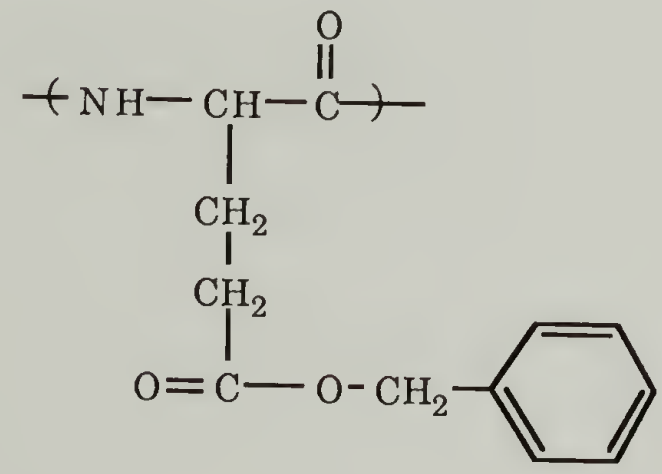

Poly (γ-benzyl l-glutamate)

This molecule was the first synthetic polymer to exhibit lyotropic behavior as predicted by Flory[1] in 1956.

In the solvent benzyl alcohol (BA), PBLG is known to take an α-helix configuration.[2] The molecule therefore simulates a rod-like molecule in this solvent and is a perfect candidate for lyotropic behavior. The PBLG/BA system does indeed exhibit lyotropic behavior with an isotropic state in the high temperature, low concentration regime, a

cholesteric phase in the high temperature, high concentration regime, and a gel phase in the low temperature regime. The transition from the isotropic to the gel phase is between 30 °C and 40 °C dependent upon concentration and molecular weight of the PBLG, the transition from the cholesteric phase to the gel is between 40 °C and 50 °C again dependent upon concentration and molecular weight of the polymer, and the isotropic to cholesteric transition occurs at approximately 7 to 10 wt % PBLG dependent upon the temperature and the molecular weight of PBLG. The temperature and concentration ranges of the various transitions make them easily accessible. The fact that the PBLG/BA system forms a gel phase at low temperatures instead of the predicted biphasic state is of primary interest to our studies. The molecular weights used in our studies are 20,000, 70,000, and 238,000.

In studying the effect of disorder on the nematic to isotropic (N-I) phase transition of liquid crystals, we have examined the N-I transition of a small molecule liquid crystal that has been confined to a porous media. This small molecule liquid crystal is *p*-azoxyanisole

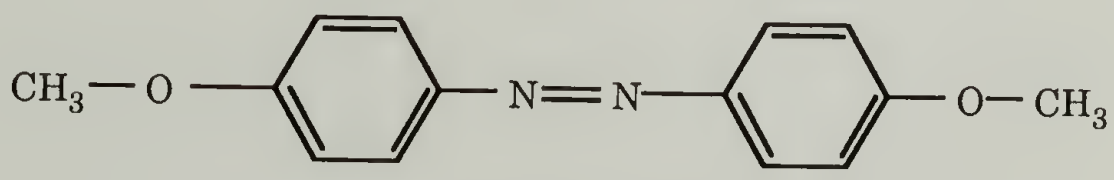

p - azoxyanisole

The nematic to isotropic transition of this molecule is well characterized with T_{NI} = 136 °C and ΔH_{NI} = 0.67 cal/gm. An important parameter in this study is the ratio of the pore size to the molecular size, $\lambda = R_p / R_g$. Therefore, an average size of the molecule is needed. We will calculate an approximate radius of gyration to be used as the

characteristic size of the molecule. Assuming the molecule is rodlike with a length of 14 Å, the radius of gyration can be calculated to be approximately 16 Å. As we desire a rough estimate of the size of the molecule, this figure has been further approximated to R_g = 15 Å.

Techniques

Small Angle Neutron Scattering

The small angle neutron scattering (SANS) experiments were completed at the instruments KWS I and II at the Institut für Festkörperforschung at the Kernforschungsanlage (KFA), Jülich, Germany, instrument D11 at the Institut Laue-Langevin (ILL) in Grenoble, France, and at the 8 meter scattering instrument at the National Institute of Standards and Technology (NIST) in Gaithersburg, Maryland. All three small angle instruments are similar scattering instruments with pinhole collimation and located at high flux research reactors. They can all be described with the following diagram, Figure 2.1

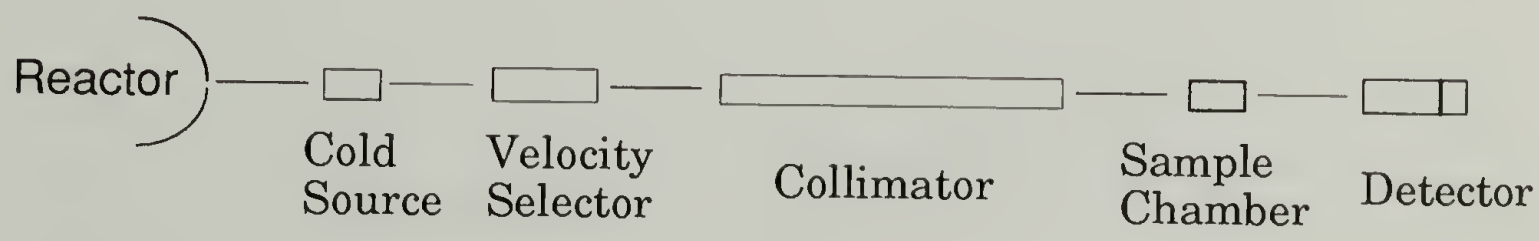

Figure 2.1 Schematic diagram of small angle neutron scattering instruments

As described in this diagram, the reactor produces a multichromatic beam of neutrons that are sent through a cold source that cools the beam and slows the neutrons. After this the beam of neutrons passes through a velocity selector that results in a monochromatic beam of neutrons. Typical wavelengths accessible are 5 Å - 15 Å. This monochromatic beam then passes through a collimator into the sample chamber and impinges on the sample. The sample scatters the neutrons and the detector records the scattering pattern of the sample. Differences in the three instruments include neutron flux from the reactor, the method of velocity selection, length of collimation, sample to detector distance, and detector type. The only difference that manifests itself in the results is the difference in the sample to detector distance. KWS I and KWS II have a 20 meter maximum that can also be set at 1, 2, 4, 8, and 14 meters, D11 has a 40 meter maximum and is also adjustable, and the instrument at NIST is a fixed 8 meter maximum. This results in momentum transfer vectors, $q = 2\pi/\lambda \sin\theta$, of $10^{-3} \leq q \leq 10^{-1}$ for KWS I, KWS II, and D11 and $8 \times 10^{-3} \leq q \leq 10^{-1}$ for the 8 meter instrument at NIST.

Quasi-Elastic Neutron Scattering

The quasi-elastic neutron scattering experiments were performed on the Pi backscattering instrument at the Institut für Festkörperforschung at the Kernforschungsanlage (KFA) in Jülich, Germany. The principle of backscattering that is employed in the Pi instrument at Jülich is straightforward. A beam of cold neutrons is collimated to strike a monochromating crystal, the beam is reflected off

the crystal at an angle close to 90° and collimated again, it strikes the target and is scattered to an analyzing crystal where it is reflected off the analyzing crystal at an angle close to 90° onto a detector. This is schematically shown in figure 2.2

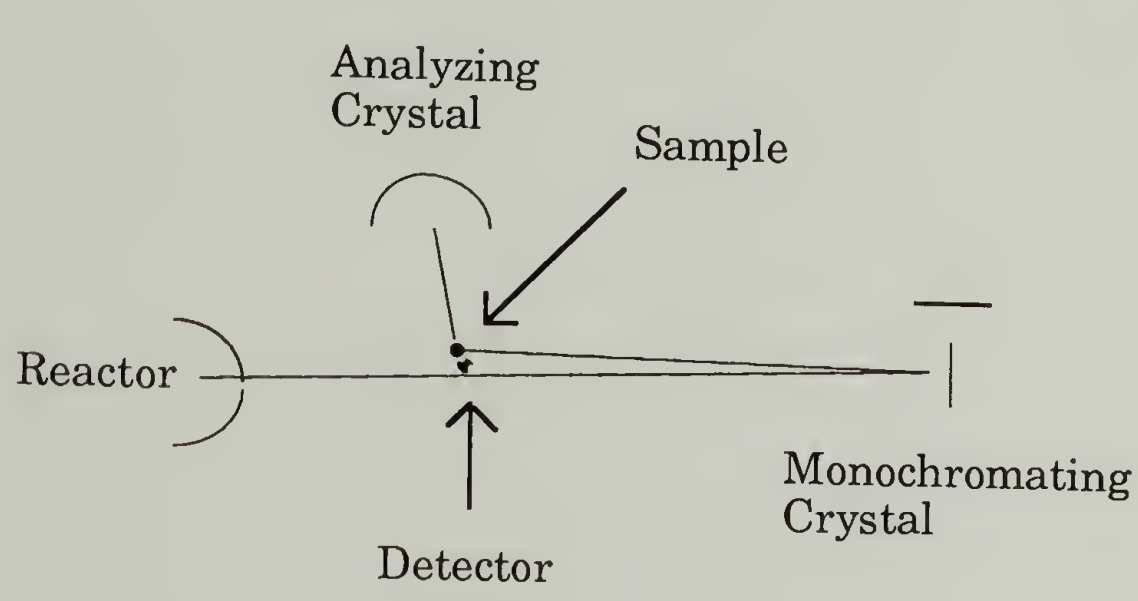

Figure 2.2 Schematic diagram of a backscattering spectrometer.

The analyzing crystal is usually an array of small crystals in a spherical arrangement with the detector at their focus. Both the monochromating and analyzing crystals are identical so that only elastically scattered neutrons reach the detector if the monochromating crystal is stationary. The advantage of reflecting the beam of neutrons at 90° is that a very monochromatic beam is produced. The energy resolution, $\frac{\Delta E}{E}$, has no angle dependent part and is only limited by the mosaic spread within the

monochromating crystal, which is on the order of 10^{-4} to 10^{-5}. In operation, the energy of the incoming neutron is precisely regulated by oscillating the monchromating crystal on a doppler drive. Therefore the energy of the neutron beam that strikes the sample varies sinusoidally about a fixed energy that is required to reflect off the analyzer crystal to reach the detector. At anytime the sample can inelastically scatter the incoming neutron beam to cancel the energy of the doppler drive to allow the scattering to be counted. This is summarized in equation 1.

$$E_m \pm E_d + E_{is} = E_A \qquad (1)$$

$E_A = E_M$ is the energy of the fixed monochromator or analyzer crystal.

E_d is the variation in the energy due to the doppler drive.

E_{is} is the variation in the energy due to inelastic scattering of the sample

With this precision in energy determination it is possible to study molecular motions on the length scale of 5 - 10 Å and a time scale of 10^{-10} s. This corresponds to the rotation of a few bonds.

Low Angle Light Scattering

The low angle light scattering experiments were completed using an Otsuka electronics DLS 700 dynamic and low angle light scattering instrument. The instrument is a self-contained light scattering apparatus. Within the device a helium-neon laser emits a monochromatic beam of light which is focused with a pair of lenses onto the test tube that contains the solution. In the static mode, the intensity

of the scattered light is then detected with a photomultiplier tube. The angle of detection is changed with a movable goniometer to allow the measurement at a series of angles. The entire sample chamber is maintained at a given temperature with a circulating temperature bath. The precision of the temperature bath is ± 0.1 °C.

Differential Scanning Calorimetry.

Analysis of the small molecule liquid crystal confined to a porous glass was completed on a Perkin Elmer DSC-4 differential scanning calorimeter. The analysis consisted of obtaining the thermogram of the sample as it was heated at a rate of 5 K/minute in a nitrogen atmosphere. The temperature and transition enthalpies on the calorimeter were calibrated with an indium standard. The peak maximum and the heat of transition were used to characterize the transition.

Sample Preparation

The poly (γ-benzyl l-glutamate) was purchased from Sigma Chemical Company and used as received. The molecular weights as reported from the manufacturer are listed in table 2.1. The deuterated benzyl alcohol was purchased from MSD isotopes in the United States and The Medgenix Group in Europe. Benzyl alcohol was purchased from Aldrich Chemical Company. The *p*-azoxyanisole was obtained from Aldrich and used as received.

Table 2.1

Molecular Weights of PBLG Used in Studies

Sample Name	Molecular Weight
PBLG20	20,000
PBLG70	70,000
PBLG238	238,000

Small Angle Neutron Scattering

The preparation of the small angle neutron scattering samples were similar for all the experiments completed at the three scattering stations. In Jülich, Hellma quartz cuvettes with a path length of 1 or 2 mm were used as sample containers for room temperature measurements and measurements where some temperature uncertainty was tolerable. ($\Delta T = \pm 2$ °C) The measurements performed at Grenoble also utilized the Hellma cuvettes with a 2 mm path length. For precise temperature studies in Jülich, a sample holder made at Jülich was used to fit with the oven that allowed precise temperature control ($\pm$ 0.05 °C). This holder consists of a circular niobium back, an O-ring, a circular quartz window, and an annular retaining ring. For the SANS studies performed at NIST, quartz cells from NSE Precision Cells, Inc. with a path length of 2 mm were used. In all cases the solutions were made by adding the PBLG and deuterated benzyl alcohol

to the cell and annealing at a temperature well into the isotropic range (≈ 70 – 80 °C) for 8 – 72 hours.

Quasi-Elastic Neutron Scattering

Sample preparation for the quasi-elastic neutron scattering experiments were similar to the preparation of the small angle neutron scattering experiments. The sample holder was an aluminum cell made in Jülich that conforms to the temperature controller in the Pi backscattering instrument at the KFA in Jülich. The poly (γ-benzyl l-glutamate) and the deuterated benzyl alcohol were added to the cell and then allowed to anneal at approximately 75 °C for 12 hours.

Low Angle Light Scattering

The most important aspect of the preparation of the sample for the dilute solution low angle light scattering is the purification of the solution. It is imperative that there exist no dust or impurities on the sample that would also scatter light and invalidate the results. Reliable and reproducible results can only be found if the only particle that scatters light is the solute.

The procedure to prepare the samples for the low angle light scattering experiments are as follows. The PBLG was weighed and placed in a 10 ml volumetric flask. Benzyl alcohol was purified by syringing it through a 0.2 micron filter. The purified benzyl alcohol was added to the flask and the system was allowed to anneal at ≈ 70 °C for five days. The test tubes used to hold the light scattering solution were washed with liquid detergent until water did not wet the surface. The

test tube was then rinsed ten times with ultra pure water and dried with dust free acetone. The solvent and light scattering solutions were then filtered into the dust free test tube with a syringe and a 0.5 μm filter. This rinsing/filtering procedure was repeated 6 to 10 times for each light scattering sample. In this manner pure PBLG/benzyl alcohol solutions were prepared for the light scattering experiments

Differential Scanning Calorimetry

For the differential scanning calorimetry experiments, the samples were weighed in aluminum pans to contain approximately equal weights of *p*-azoxyanisole and porous glass. The exact amounts of PAA and Controlled pore glass (CPG) in the samples used are listed in table 2.2 The system was then annealed at elevated temperatures to allow the liquid crystal to penetrate the pores. For two of the three systems studied, it was sufficient to anneal the sample in the nematic range, but for the system with the smallest pore size, CPG3, it was necessary to anneal the sample in the isotropic regime to allow the liquid crystal to penetrate the pores.

Table 2.2

DSC Experiment Sample Characteristics

Sample	CPG	PAA
CPG1	6.73 mg	6.09 mg
CPG2	6.10 mg	6.40 mg
CPG3	5.20 mg	6.00 mg

References

1. P. J. Flory, Proc. Roy. Soc. (London) **A234**, 73 (1956).

2. H. Block, *Poly (γ-benzyl l-glutamate) and Other Glutamic Acid Containing Polymers*, (Gordon & Breach Science Publishers, New York, 1983).

CHAPTER 3

THE GELATION OF POLY (γ-BENZYL l-GLUTAMATE)

Introduction

The gelation of anisotropic polymer molecules is a perplexing phenomenon. This phenomenon is commonly utilized in the processing of rod-like polymers. Yet it is neither well understood nor theoretically predicted. In 1956, using a statistical mechanical theory that is similar to his lattice theory for random coil polymers, Flory[1] predicted the temperature-concentration phase diagram of a solution of rod-like polymers using a lattice theory. Some of his predictions included an isotropic phase in the high temperature low concentration regime, a liquid crystalline region that occurs at high temperature and high concentration, a narrow biphasic region between the isotropic and liquid crystalline phases, and a phase separated biphasic (liquid crystalline and isotropic) regime at low temperature. He also predicted that the molecule must have a length to diameter ratio of 6.7 in order to observe a liquid crystalline phase.

It was not until almost 20 years later that the complete temperature-concentration phase diagram of a synthetic polymer molecule was found to follow the behavior predicted by Flory. Using nuclear magnetic resonance and polarizing light microscopy, Miller and

coworkers[2] found that poly (γ-benzyl l-glutamate) in dimethyl formamide (DMF) has a phase diagram that is very similar to that predicted by Flory over a limited temperature-concentration region. This includes isotropic and liquid crystalline phases and a narrow biphasic region between the two at high temperature. This partial phase diagram was extended[3] to the complete temperature-concentration range using isopiestic and hydrodynamic measurements. The overlap agreement between the experimental and theoretical phase diagrams was excellent. But, upon further investigation[4], it was found that the low temperature phase is not biphasic but a gel that is a three dimensional self supporting polymer rich network. In an attempt to explain this unpredictable result, Miller[4] *et al.* suggested that the gel is a result of kinetic phenomena. Spinodal decomposition and polymer immobility were purported to be the mechanisms responsible for the formation of the gel upon solvent quality reduction. The role of spinodal decomposition in the process of gelation has been studied,[5,6] but its contribution to gelation has not been proven nor disproven. Further studies of PBLG discovered other solvent systems that also result in a polymeric gel upon solvent quality reduction,[7] including benzyl alcohol.[8]

Many investigations have been completed in an attempt to determine the driving force behind the creation of this network or gel, as well as to describe the gel itself. Nuclear magnetic resonance (NMR), isopiestic measurements, polarized light microscopy, and hydrodynamic measurements were used by Miller *et al.*[2,3] to determine the phase diagram of the PBLG/DMF system. Dynamic light scattering,[6] light scattering,[6] x-ray scattering,[9,10] differential scanning calorimetry,[9,11,12]

rheology, [9,13] NMR,[11] and polarizing optical microscopy[14] have all been used to study the PBLG/BA system and the resultant gel in hopes of obtaining better understanding of the gelation phenomena.

The identification and description of the gel phase and its molecular origins is a fundamental problem of polymer physics today. In order to optimize the use of the gelation phenomena in polymer processing, a theory that describes the solutions of rod-like polymers in all phases is necessary. A description of the dynamics on the molecular level as gelation is approached must also be studied in order to understand the gelation process fully.

The goal of the present work is to investigate the polymer molecule in solution as the system approaches and undergoes gelation. Low angle light scattering, small angle neutron scattering, and quasi-elastic neutron scattering are used to examine the polymer molecule as the system approaches and passes through the gelation threshold. Using low angle light scattering (LALS), the radius of gyration of the polymer molecule in dilute solution is measured as the temperature of the solution is lowered to the gelation transition. Quasi-elastic neutron scattering (QENS) is used to determine the local dynamics of the polymer molecule as the temperature of the system is lowered and the system passes from the liquid crystalline to the gel phase. This allows the knowledge of the local (5 – 10 Å) structure and dynamics of the side chain of the polymer as it passes from the liquid crystalline to the gel phase to be obtained. Small angle neutron scattering (SANS) is used to study the configuration, *i.e.* persistence length and radius of gyration, of the polymer molecule as the polymer solution goes from the isotropic to

gel phase. SANS is also used to determine the fractal dimension of the gel on the length scale of 20 – 500 Å. The fractal dimension of the gel formed from the isotropic phase for different molecular weights and different annealing procedures of PBLG is measured. The description of a fundamental property such as the fractal dimension will allow a better understanding of the resultant gel on a very local length scale and possibly the gelation process.

Experimental

Low Angle Light Scattering

The samples for low angle light scattering (LALS) were prepared as described in the previous chapter. The molecular weight of the PBLG used for the LALS studies is 70,000 as reported by the manufacturer. In order to determine the radius of gyration of a macromolecule in solution using light scattering, the solution must be dilute enough so that only single molecules scatter light. This is only achieved if the solution is sufficiently less than the overlap concentration, c*. The overlap concentration is defined as the concentration at which the total volume of all the molecules will just fill the volume of solution if the volume of a single molecule were equal to that of a sphere with a radius that is equal to the radius of gyration of the molecule in solution. The overlap concentration was calculated to be 3.1×10^{-3} g/cm^3 ≡ 3.1 mg/ml. In order to insure that single molecule statistics are achieved, concentrations of less than c*/10 were used. Exact concentrations of samples used are listed in table 3.1.

Table 3.1

Concentrations of Samples for LALS Experiments

Sample Name	Concentration mg/ml
LALS1	0.121
LALS2	0.197
LALS3	0.288

The scattering intensity at a series of angles was measured for each sample at approximately 50 °C, 40 °C, 30 °C, and room temperature. The supporting software uses the scattered intensity to calculate the Rayleigh Ratio at each angle. The Rayleigh ratio, $R(\theta)$, is defined as

$$R(\theta) = \frac{r^2 I(\theta)}{V(\theta) - I_o}$$

Where θ is the scattering angle, $V(\theta)$ is the scattering volume, r is the distance from the scattering center to the detector, $I(\theta)$ is the scattering intensity, and I_o is the intensity of the incident light. Taking into account the angular effect on the scattering volume and the sensitivity of the photomultiplier tube, $R(\theta)$ can be written as

$$R(\theta) = \Psi\, n_s^2\, (I(\theta) / I_o) \sin \theta$$

where Ψ is a constant that is instrument dependent and is easily determined. Therefore, $R(\theta)$ can be calculated for each sample at each

angle with knowledge of the scattered intensity, the refractive index of the solution, and the incident intensity.

For a dilute solution, the Rayleigh ratio can be expressed as a series as the concentration goes to zero

$$\frac{K\,C}{R(\theta)} = \frac{1}{M_w}\left(1 + \frac{1}{3} < S^2 > q^2 \ldots\right)$$

where $< S^2 >$ is the radius of gyration of the scattering particle, C is the concentration, q is the momentum transfer vector, $\frac{4\pi}{\lambda} \sin\left(\frac{\theta}{2}\right)$, and K is the optical constant defined as

$$K = \frac{4\,\pi^2\,n_o^2}{N_A\,\lambda_o^{\,4}}\left(\frac{dn}{dc}\right)^2$$

where N_A is Avogadro's number, λ_o is the wavelength of the incident light, n_o is the refractive index of the solution and $\frac{dn}{dc}$ is the change in the refractive index with concentration. The value of $\frac{dn}{dc}$ for the system of poly (γ-benzyl l-glutamate) in benzyl alcohol was measured simultaneously with the LALS experiments. A value of $\frac{dn}{dc} = 0.777\ \frac{ml}{g}$ was found.

Therefore, a plot of $\frac{K\,C}{R(\theta)}$ vs. q^2 will have a slope that is proportional to $< S^2 >$, the radius of gyration of the scattering particle. $< S^2 >$ is found for each sample in this way.

Small Angle Neutron Scattering

The initial goal of the proposed small angle neutron scattering experiments was to characterize the phase diagram and the fluctuations upon the approach of a phase transition of the system. The method of accomplishing this was to use the random phase approximation (RPA) to determine the interaction parameter, χ. In order to use RPA theory, however, the structure factor of both constituents of the solution must be known. It was decided that the structure factor of a single PBLG molecule must be found. A series of dilute solution measurements of three molecular weights were made. This was done to try to fit the measured structure factor to theoretical models of a semi-flexible polymer molecule.

It was found to be very difficult to obtain the structure factor of a single polymer chain in dilute solution using small angle neutron scattering. This was due mainly to the low intensity of the scattering of a very dilute solution. There were other complications, however, including a very strong and varying background intensity. The background is minimal for strong scattering samples, but for the dilute solutions that were measured, these factors were considerable. It is believed that good statistics could be achieved, but extremely careful attention to the background and its fluctuations must be considered.

When the difficulty in obtaining the single chain structure factor with small angle neutron scattering was realized a separate series of experiments were proposed in order to understand the isotropic–gel phase transition using small angle neutron scattering. These

experiments were a study of the radius of gyration, R_g, and the persistence length, l, as a function of concentration and temperature in the isotropic phase, a study of the fractal dimension, D_f, of the gel that is formed from the isotropic phase for different size polymers and annealing procedures, and a study of the role of spinodal decomposition in the cholesteric to gel transition.

The study of the change in the configuration with concentration and temperature and the study of the fractal dimension of the gel were completed, but the study of the role of spinodal decomposition was not successful. It was hoped that by measuring the structure factor at q=0, that either fluctuations could be seen and a spinodal point found or no fluctuations could be seen and therefore the mechanism of spinodal decomposition would be disproven. Unfortunately, due to the large forward scattering in the cholesteric phase, it was impossible to measure S(q=0) using small angle neutron scattering.

For both the configurational study and the fractal dimension study, the neutron scattering pattern of the PBLG solution was recorded and then calibrated to an absolute intensity, I(q), in cm^{-1}. A water standard was used for the conversion of the measurements completed at the ILL and NIST, while a lupolen standard was used for the measurements completed in Jülich. To determine the radius of gyration, persistence length, and fractal dimension from the measured scattering pattern, the following schemes were followed. For the radius of gyration, a plot of q^2 vs. 1/I(q) was made (Zimm plot). Figure 3.1 is an example of this plot. It is a Zimm plot for a 1% solution of PBLG in DBA at 83 °C. The radius of gyration is taken to be

$$R_g = (3 \times \text{slope} / \text{intercept})^{1/2}.$$

To determine the persistence length of a molecule in solution, a plot of q vs. $q^2I(q)$ was made (Kratky plot). Figure 3.2 is an example of this plot. This is a Kratky plot for a 3% solution of PBLG in DBA at 46 °C. The persistence length of the scattering chain can be determined from the point where the function $q^2I(q)$ differs from that for the Debye function, the ideal scattering curve of a chain that is modeled as a self-avoiding walk. A Kratky plot of the Debye function will level off to a finite value at large q. However, for a real chain, as seen in figure 3.2, the function $q^2I(q)$ will level off for q values $R_g^{-1} < q < l^{-1}$ and then continues to increase linearly with q for $q > l^{-1}$. Therefore, the point, q*, where the function $q^2I(q)$ changes from being independent of q to linear with q is inversely proportional to the persistence length. More specifically,

$$l = \frac{q^* \pi}{6}.$$

As was described in the introduction, a structure that is self-similar will have a power law scattering pattern, $I(q) \propto q^{-D}$ where D is the fractal dimension of the structure. Therefore a plot of ln(q) vs. ln(I(q)) will have a slope that is equal to the fractal dimension. The fractal dimension of the examined gels was determined in this way. Figure 3.3 is an example, showing the scattering pattern of a gel formed from a 1% solution of PBLG in DBA through a step quench procedure.

Quasi-Elastic Neutron Scattering

The quasi-elastic neutron scattering experiments (QENS) were completed at the Pi backscattering instrument in the Kernforschungsanlage (KFA) in Jülich, Germany. The samples were prepared as described in chapter 2. The molecular weight of the PBLG used on the QENS studies was 238,000. The exact concentrations of the two samples are listed in table 3.2.

Table 3.2

Concentrations of Samples for QENS Experiments

Sample Name	Concentration (wt %)
QENS10	9.68 %
QENS14	14.0 %

When a monochromatic beam of neutrons is scattered by a sample and the energy of the scattered beam is analyzed, the result will be a strong central peak with some broadening. The neutrons contributing to the center peak are elastically scattered, however some neutrons undergo small energy shifts due to interaction with molecular vibrations and rotations. These molecules contribute to the broadening of the peak.

Analysis of the peak height and half-width can give information concerning residence time and spatial extent of molecular reorientations. For high energy resolution (full width at half maximum of peak ≤ 10 μEV) and not large momentum transfer vector ($q \leq 2$ Å^{-1}), vibrational motion is negligible and the measurements only concern the rotational motion of the protons. As these conditions are satisfied for the present experiment, only the rotational scattering function is measured. As described in the introduction, The rotational scattering function (RSF) is given as a sum of a purely elastic component and a quasi-elastic component.[15]

$$S_{rot}(q,\omega) = A_o(q)\delta(\omega) + S_{rot}^{qel}(q,\omega) \qquad (1)$$

The intensity of the elastic portion, $A_o(q)$, known as the elastic incoherent structure factor (EISF) is a measure of the time averaged spatial distribution of the protons. It's variation with q gives information of the geometry of the rotational motion. The quasielastic portion, $S_{rot}^{qel}(q,\omega)$, describes the time frame, *i.e.* the frequency, of the rotation. In it's most general form $S_{rot}^{qel}(q,\omega)$ is a summation of Lorentzians. The full width at half maximum (HW) of a given Lorentzian is inversely proportional to the residence time of that motion.

An example of the observed quasi-elastic neutron scattering pattern of a solution of PBLG in DBA is shown in figure 3.4. This is the observed scattering pattern for a 9% solution of PBLG in DBA at 315 K and $q=0.56$ Å^{-1}. This scattering pattern can be fit to the sum of two lorentzians. Therefore, according to equation 1, both $A_o(q)$ and $S_{rot}^{qel}(q,\omega)$ are approximated to single lorentzians. In the fitting

procedure the full width at half maximum (HW) of $A_o(q)$ is fixed at a small value ($\cong 0.01$) while the HW of $S_{rot}^{qel}(q,\omega)$ remains variable.

From this fit the intensity of the elastic portion, the EISF, and the HW of the lorentzian fit of $S_{rot}^{qel}(q,\omega)$ can be found. The EISF is calculated as

$$EISF = \frac{H1}{H1 + H2}.$$

where H1 is the intensity of the lorentzian that approximates the elastic scattering and H2 is the intensity of the lorentzian that approximates the quasi-elastic scattering. These variables in turn provide information on the geometry and time scale of local motions. The EISF and HW are found at the given set of angles for each concentration and temperature.

Results

Our first experiment is a study of the change in the radius of gyration (R_g) of the PBLG molecule in dilute solution with temperature using low angle light scattering. Our results are shown in table 3.3 on page 55. The concentrations of the samples in table 3.3 are as follows. The concentration of sample 1 is 0.1208 mg/ml, sample 2 is 0.1973 mg/ml, and sample 3 is 0.2877 mg/ml. The values for samples 1 and 2 are informative, but they should only be taken qualitatively, not quantitatively. This is because the measured values of R_g do not satisfy the necessary condition that $q_{min}R_g < 1$.

Our second experiment was a set of small angle neutron scattering runs to examine the change in the radius of gyration and

persistence length of the polymer as a function of concentration and temperature as the isotropic to gelation transition is approached, as well as a study of the fractal dimension of the gel that is formed from the isotropic phase for different molecular weights. As the definition of the gel itself is elusive, the definition of a primary characteristic such as the fractal dimension will contribute to the description and understanding of the resultant gel. The results of the study of the radius of gyration, R_g, and persistence length, l, with temperature and concentration can be seen in figures 3.1 and 3.2 Figure 3.1 shows the calculated radius of gyration for 1%, 3%, 5%, and 7% solutions versus temperature, while figure 3.2 shows the change in the persistence length with temperature for the 1% and 3% samples.

The results of the study of the fractal dimension of the gel formed from different molecular weights and annealing procedure are shown in tables 3.4 and 3.5 (pages 56 and 57). The molecular weight of the polymer used in the results that are reported on table 3.4 is 238,000, while the molecular weight of the polymer of the results in table 3.5 is 70,000.

Table 3.3

Radius of Gyration (in Å) as a Function of Temperature

Temperature (°C)	1	2	3
47	1.56×10^{3}	1.60×10^{3}	1.64×10^{3}
39	4.02×10^{3}	2.61×10^{3}	2.24×10^{3}
29	2.86×10^{3}	7.23×10^{3}	2.32×10^{3}
24	**	3.73×10^{3}	1.48×10^{3}

** not measurable.

Table 3.4

Fractal Dimension of PBLG238 Sample

Concentration	Fractal Dimension Step Quench	Fractal Dimension Sudden Quench
1%	1.84	1.68
3%	1.83	1.78
5%	1.80	1.74
7%	2.62	1.52

Molecular Weight = 238,000

Table 3.5

Fractal Dimension of PBLG70 Sample

Concentration	Fractal Dimension Step Quench
0.35 %	*
0.75%	2.36 (a)
2%	1.72 (b)
4%	1.66 (b)

Molecular Weight = 70,000

* Did not show fractal behavior.

(a), (b) denotes step quench method, see text.

The step quench method listed in table 3.4 consisted of a series of 10 °C temperature steps from 80 °C to 30 °C with an equilibration time at each temperature of 7 to 8 hours. There are two annealing protocols for the samples listed in table 3.5. The first, denoted by (a), is a series of 20 °C temperature steps from 60 °C to 20 °C with an annealing time of about 24 hours at each temperature. The second procedure, denoted by (b), is a series of 10 °C from 70 °C to 50 °C with an equilibration time of 8 to 10 hours per temperature and then a quench to 25 °C. The fractal

dimension of the 7% solution of table 3.4 for the step quench method shows a marked difference from all other values. It should be noted that the 7% solution showed phase separation at the end of the step quench sequence. The scattering cell contained a lower half that was turbid and an upper half which was fairly clear with a clear line delineating the two. This is evidently caused by the passage through the narrow isotropic-cholesteric biphasic region of the phase diagram. The two phases and, therefore, the interface between the two phases were within the scattering window. This leads to a very complex scattering window, one that is difficult to interpret readily. Therefore the reported fractal dimension does not accurately describe the local structure of the gel and can be discarded.

Our results of the quasi-elastic neutron scattering experiments are shown as the change in the EISF and HW with q in figures 3.3-3.6 Figure 3.3 shows a plot of the change in the EISF with q at 338 K, 315 K, and 280 K for the 14% solution. For these two solutions, 338 K is well into the cholesteric phase, 315 K is just below the cholesteric–gel phase transition, and 280 is deep into the gel phase. The change in the HW with q for these temperatures and this sample are shown in figure 3.4 Figures 3.5 and 3.6 show the data for the same conditions for the 9.8% solution. The q dependence of the EISF and HW were calculated for eight temperatures, but these results are typical of the observed trends that the limiting value of the EISF at large q is 0.0 at high temperature and increases to 0.3–0.4 as the temperature is decreased until it reaches 0.5 well into the gel phase. The HW is also dependent on q at all temperatures. In order to evaluate this data, they must be compared to

the q dependence of the EISF and HW of simple motions. Figure 3.7 and 3.8 show the q dependence of the EISF of a continuous motion on a sphere and a jump-like reorientation between two points, respectively.

Discussion

In order to evaluate the results of the study of the temperature dependence of the radius of gyration, it is important to first obtain a theoretical value for the radius of gyration to which the measured values can be compared. Assuming that the polymer is a perfect α-helix, each monomer translates 1.5 Å. The molecular weight as reported by the manufacturer of the polymer used is 70,000 as measured by low angle light scattering and 86,000 as measured by viscometry. For a PBLG molecule of molecular weight 70,000, the degree of polymerization is 320. Therefore

$$L = 320 \text{ monomers} \times \frac{1.5 \text{ Å}}{\text{monomer}} = 480 \text{ Å}$$

The radius of gyration of a rod is given by $R_g^2 = \frac{L^2}{12} \Rightarrow R_g = 138$ Å. For a PBLG molecule with a molecular weight of 86,000, the calculated R_g will be 170 Å.

Kim and Ree[16] have calculated the radius of gyration of a model rod-like molecule that contains 2-4 'coil-like sections'. This model is unique because it takes into account the experimentally observed characteristic that the distance translated per monomer is greater than 1.5 Å for small chains. This results in the astonishing result that the

calculated radius of gyration using this model is greater than the radius of gyration of a perfect α-helix for small chains ($M_w \leq 100{,}000$). However, in this way, the model simulates an actual molecule better than a simple broken rod model. The calculated value for the R_g of a PBLG molecule with molecular weight of 70,000 using this model is R_g = 196 Å and for a molecular weight of 86,000, R_g = 235 Å.

Upon comparison of the theoretical values to the measured values it is seen that the measured values are 6 to 12 times the theoretical values. This can not be attributed to experimental precision or solvent expansion of the molecule. It must indicate that there exists an aggregation of molecules at all temperatures measured, even in the isotropic phase. Therefore these experiments demonstrate that the particle that is scattering light in the isotropic phase is an aggregation of PBLG molecules. It also shows that the aggregate particle changes little as the gelation temperature is approached. The response of the system as the gelation threshold is crossed seems to show that the scattering particle changes very little in size. This could be because further aggregation is inhibited due to the extent of dilution of these samples.

The results of the study of the radius of gyration as a function of concentration and temperature by small angle neutron scattering as shown in figure 3.1 shows that the polymer stays at a fairly constant size (≈ 700 Å) up until the gelation temperature is reached. Upon gelation the measured R_g increases substantially. The calculated value for R_g in the gel phase can only be taken qualitatively, not quantitatively, as $q_{min}R_g > 1$. Figure 3.2 shows the change in the persistence length with temperature for the 1% and 3% samples. Here a small increase in the

persistence length is seen as the temperature is decreased for these solutions. The scattering patterns of the 5% and 7% solutions did not allow an accurate measurement of l throughout the temperature span, but for the temperatures where l was determined, the results showed the same trend.

As was described in the light scattering results, a theoretical value for the R_g of a molecule that is modeled as a rod-like α-helix can be calculated as well as for a molecule that is described by the model of Kim and Ree. These values for PBLG molecule of the size used in these experiments are R_g (Kim and Ree) = 385 Å and R_g (α-helix) = 472 Å, while the measured R_g is approximately 730 Å. This again shows that there exists some aggregation in the isotropic phase up to 80 °C. At the same time, the persistence length changed little as the gelation threshold is approached. This seems to suggest that the system changes little while approaching the gelation threshold, but changes dramatically as gelation conditions are met.

The radius of gyration increases greatly as the gelation threshold is passed, indicating a larger aggregate. These results could indicate, as has been predicted before,[6] that gelation from the isotropic phase occurs via a clustering of clusters method. This aggregation method occurs as its name indicates. Clusters form through aggregation and further coalescence occurs when these cluster come together to aggregate. Theory and computer simulation predict that a system that is formed through the method of clustering of clusters will have a fractal dimension of 1.72 ± 0.04, independent of the size of the aggregating particles. Therefore a study of the fractal dimension of the gel formed

from different molecular weights should all be 1.72 ± 0.04 if the gel is formed via the clustering of clusters method.

The results of the study of the fractal dimension of the resultant gel of different size polymers and various annealing protocols elucidate the nature of the local structure of the gel that is formed from the isotropic phase. For a sudden quench or an annealing protocol of 10 °C temperature steps with an equilibration time of 7–10 hours per temperature, the system, on the length scale of 20–500 Å, is as approximately compact as a self avoiding walk (D_f = 1.667), regardless of the size of the polymer. The observed fractal dimension is also close to that which is found in aggregated systems that are formed through the clustering of cluster mechanism (D_f = 1.72). However, the fractal dimension of the 0.75% sample in table 3.5 is substantially larger than that for all other samples, 2.36 vs. 1.7. This signifies that, on this length scale, a more compact structure is formed. This suggests that the longer equilibration time of this sample allows the system to rearrange or relax into a more compact structure. Therefore, the thermal history and annealing protocol of the sample in the isotropic phase is an important parameter in determining the local structure of the resultant gel. The size of the PBLG molecule does not influence the local structure of the resultant gel for a sudden quench or an annealing procedure that includes an equilibration time of 7–10 hours per temperature. If the process of gelation included a relaxation or rearrangement of the aggregating polymers on this time scale, the rearrangement of the smaller particles would occur much quicker than the larger molecules and a more compact structure would result for the smaller molecular

weight polymer. Therefore, the similarity of the fractal dimension of the gels formed from polymers whose size differ by a factor of 3 indicates that the process of gelation does not include a rearrangement of the aggregating particles on the time scale of ≤ 10 hours for these molecular weights. However this is not true for an annealing procedure of 24 hours per temperature. This procedure produces a more compact structure, indicating that rearrangement of the relatively small molecules can occur on this time scale.

For the QENS result, both concentrations show the same trend. At high temperature, the EISF decays from 1.0 at q=0 to 0.0 at large q, while as the temperature is lowered the large q values of the EISF increase, to 0.3 at 315 K and 0.5 at 280 K. The HW depends on q for all temperatures.

An EISF that decays to zero denotes a continuous motion, while a non-zero value at large q denotes a jump-like reorientation. From this, it can be seen that the hydrogen molecules undergo a continuous rotational motion in the high temperature liquid crystalline phase, but as the temperature is lowered the motions become less fluid and more jump-like. First the motions resemble jumps between 3 or 4 sites at 315 K and finally jumps between 2 sites (dumbbell motion) at 280 K. An ideal situation would be to be able to fit the observed EISF dependence to that of a simple motion. This would allow the extraction of the geometry and time scale of the motions. This has been attempted and failed at most temperatures. The problem is that there exist 13 hydrogens on a single PBLG monomer. Out of these 13 there are 8 dynamically different sets of hydrogens; the backbone methine hydrogen, the α-methylene protons, the β-methylene protons, the benzyl protons, the meta phenyl hydrogens,

the ortho phenyl hydrogens, the para phenyl hydrogen, and the amido hydrogen. Fitting the observed values to a single motion assumes that all these protons are dynamically equivalent. This is false. Clearly the observed scattering function is the average of the scattering functions of the dynamically different protons. This means that the calculated EISFs and HWs are averages of the different motions of the different hydrogens on the polymer chain.

Unfortunately, the system is too complex to deconvolute easily and no exact time and length scales or specific molecular motions can be definitively identified. Therefore, the only conclusion that can be drawn from these results is that the dynamics of the protons, and therefore the polymer side chain, undergoes a fluid continuous rotational motion at high temperature in the liquid crystalline phase, while lowering the temperature confines the rotation of the hydrogens to jump-like reorientational motions, until in the gel phase the motion resemble that of a dumbbell, a jump-like motion between two points.

Conclusion

The following conclusions can be drawn from our experimental studies of the PBLG/BA system:

1. The observed size of the scattering particle is between 2 and 12 times greater than the expected size of a single molecule. This indicates that an aggregation of PBLG molecules exists in the isotropic phase in benzyl alcohol up to 80 °C. The size of the particle changes little as the gelation threshold is approached for the time scales that we measured (2–8

hours/temperature). As gelation occurs, the size of the scattering particle increases an order of magnitude for concentrations that form gels.

2. For a sudden quench from the isotropic to gel phase in benzyl alcohol or a step quench procedure with annealing times of 7–10 hours, the local structure, on a length scale of 20–500 Å, of the gel that is formed is about as open as aggregates that are formed through the clustering of clusters method regardless of the size of the polymer. However, a step quench procedure that includes longer annealing times (24 hours) produced a more compact structure. This indicates a rearrangement or relaxation of the structure. Therefore, the thermal history of the system in the isotropic phase will influence the final structure of the resultant gel, with shorter annealing times (0–10 hours) resulting in an open, clustering of clusters like structure and longer annealing times producing a denser structure.

3. The dynamics of the protons, and therefore the polymer side chain, undergoes a fluid continuous rotational motion at high temperature in the liquid crystalline phase, while lowering the temperature confines the rotation of the hydrogens to jump-like reorientational motions, until in the gel phase the motion resemble that of a dumbbell, a jump-like motion between two points.

Figure 3.1 Zimm plot of a 1% solution of PBLG in DBA at 83 °C. The radius of gyration of the PBLG molecule in solution can be determined from this plot.

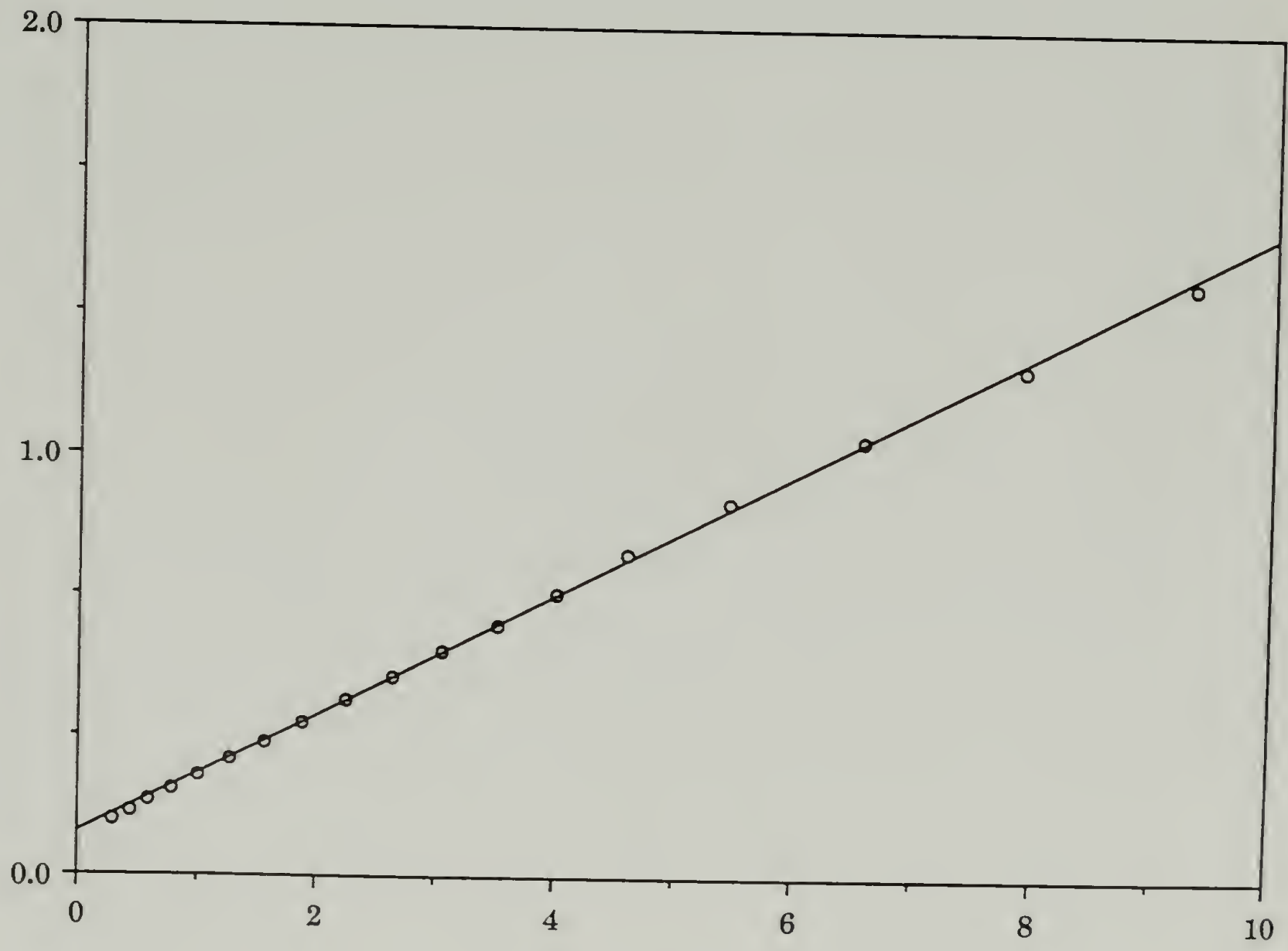
$\frac{1}{I(q)}$
2.0
1.0
0.0
0
2
4
6
8
10
$q^2 \times 10^6$

Figure 3.2 Kratky plot of a 3% solution of PBLG in DBA at 46 °C. The persistence length of the PBLG molecule in solution can be determined from this plot.

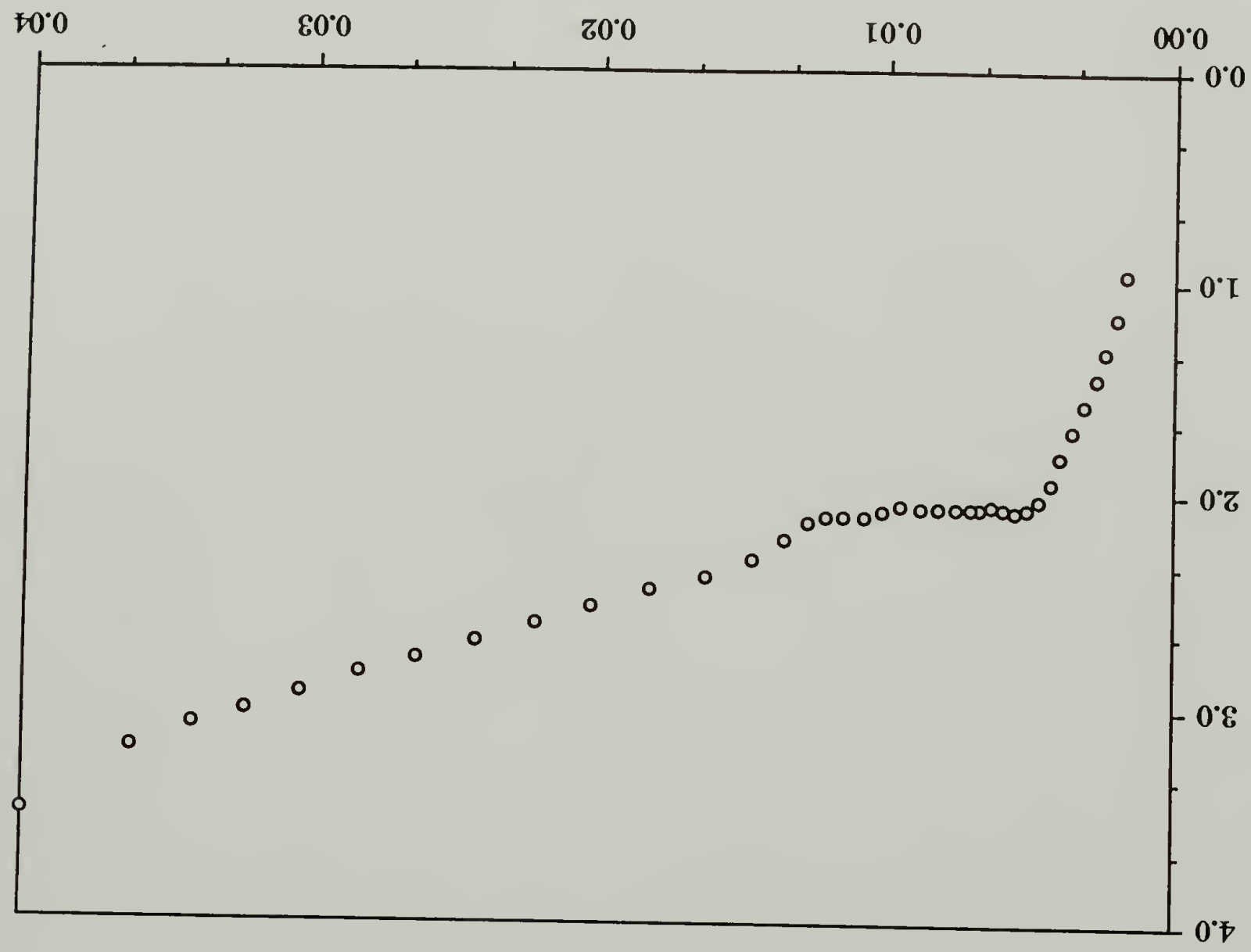

8

Figure 3.3 Porod plot of a gel formed from a 1% solution through a step quench annealing procedure. The fractal dimension of the gel can be determined from this plot.

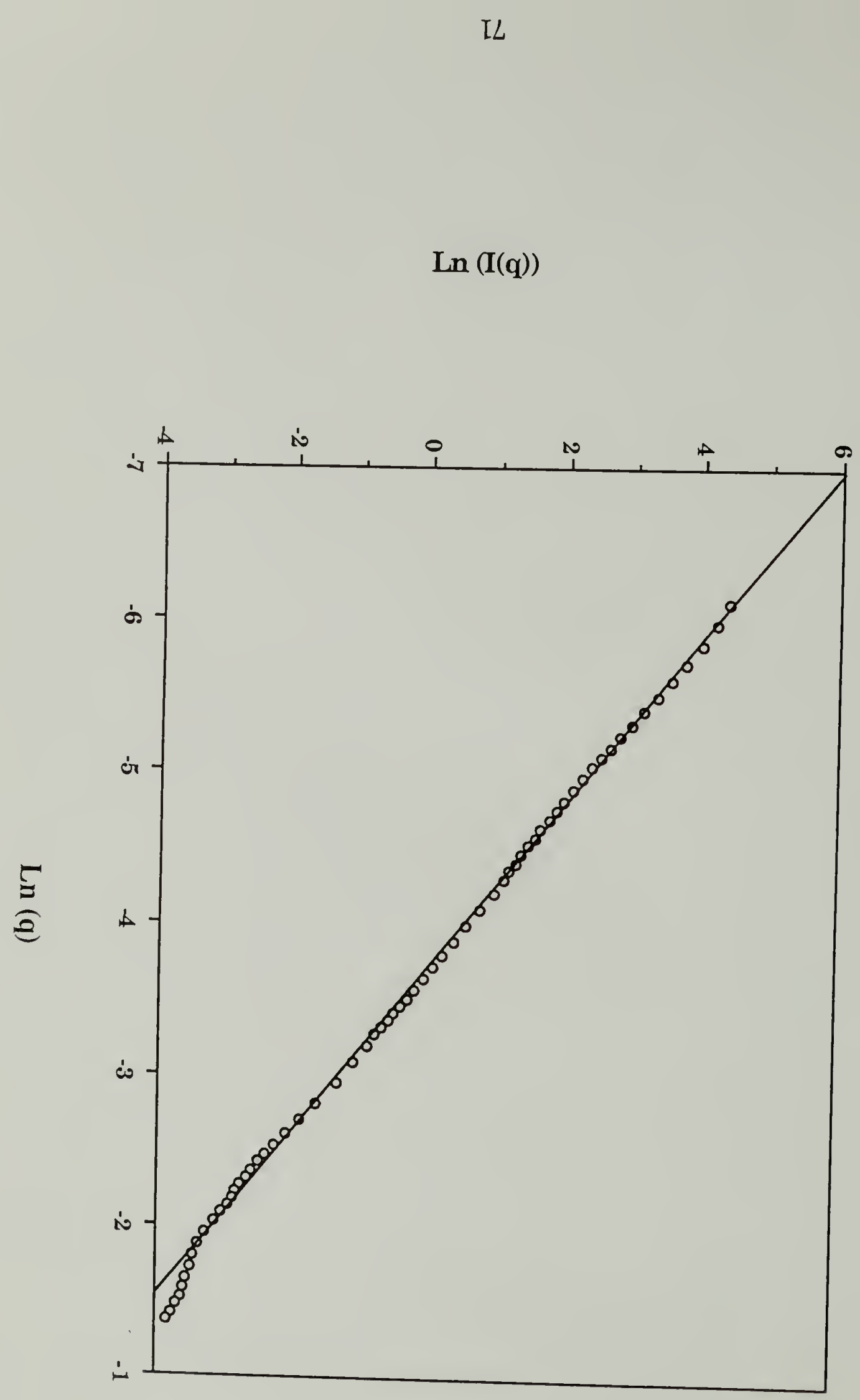
Ln (I(q))
Ln (q)
-4
-2
0
2
4
6
-7
-6
-5
-4
-3
-2
-1

Figure 3.4 The quasi-elastic scattering pattern of a 9% solution of PBLG in DBA at 315 K and q=0.56 $Å^{-1}$.

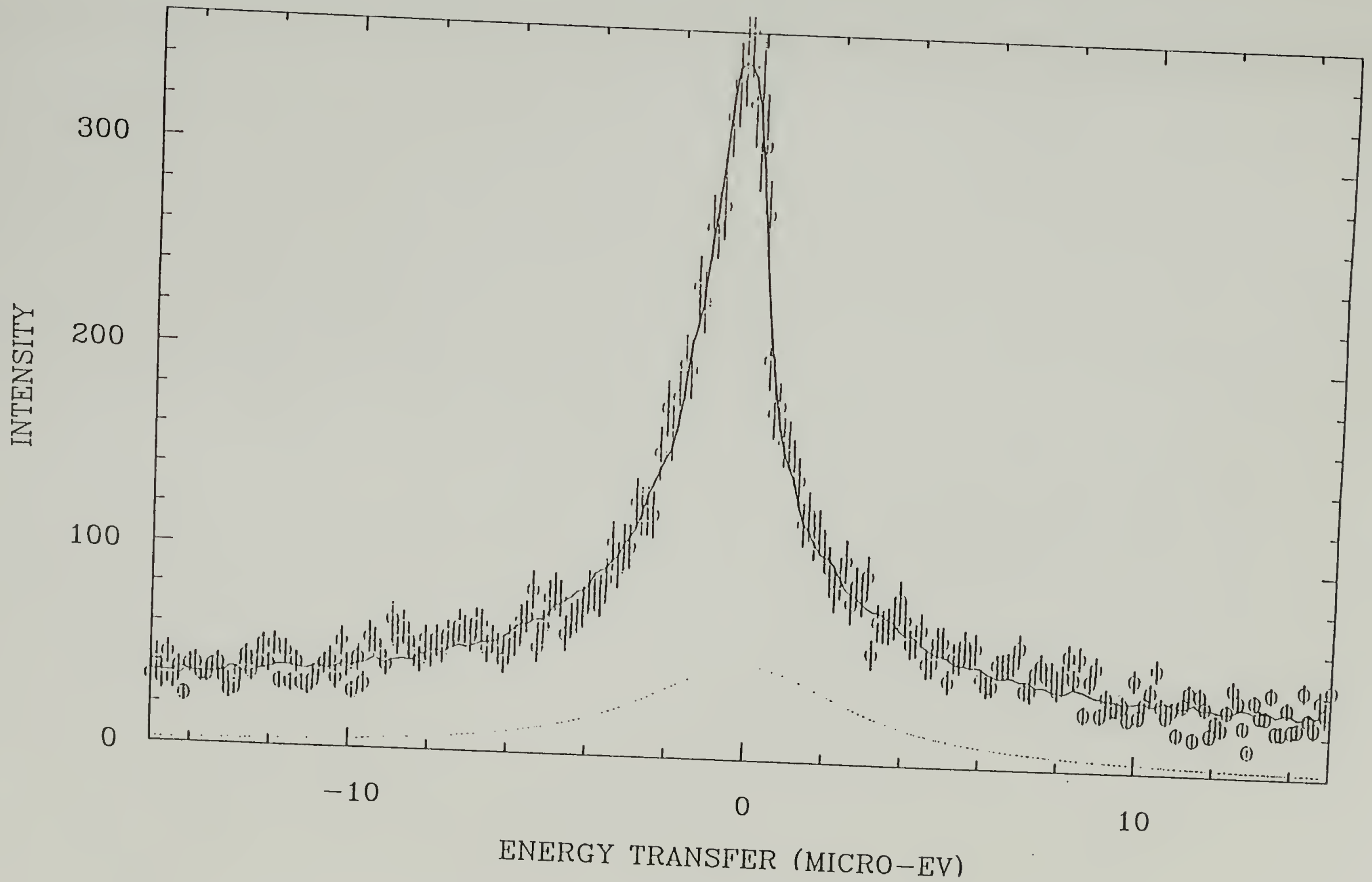
INTENSITY
300
200
100
0
−10
0
10
ENERGY TRANSFER (MICRO−EV)

Figure 3.5 The temperature dependence of the radius of gyration of a PBLG molecule in the isotropic phase in benzyl alcohol.

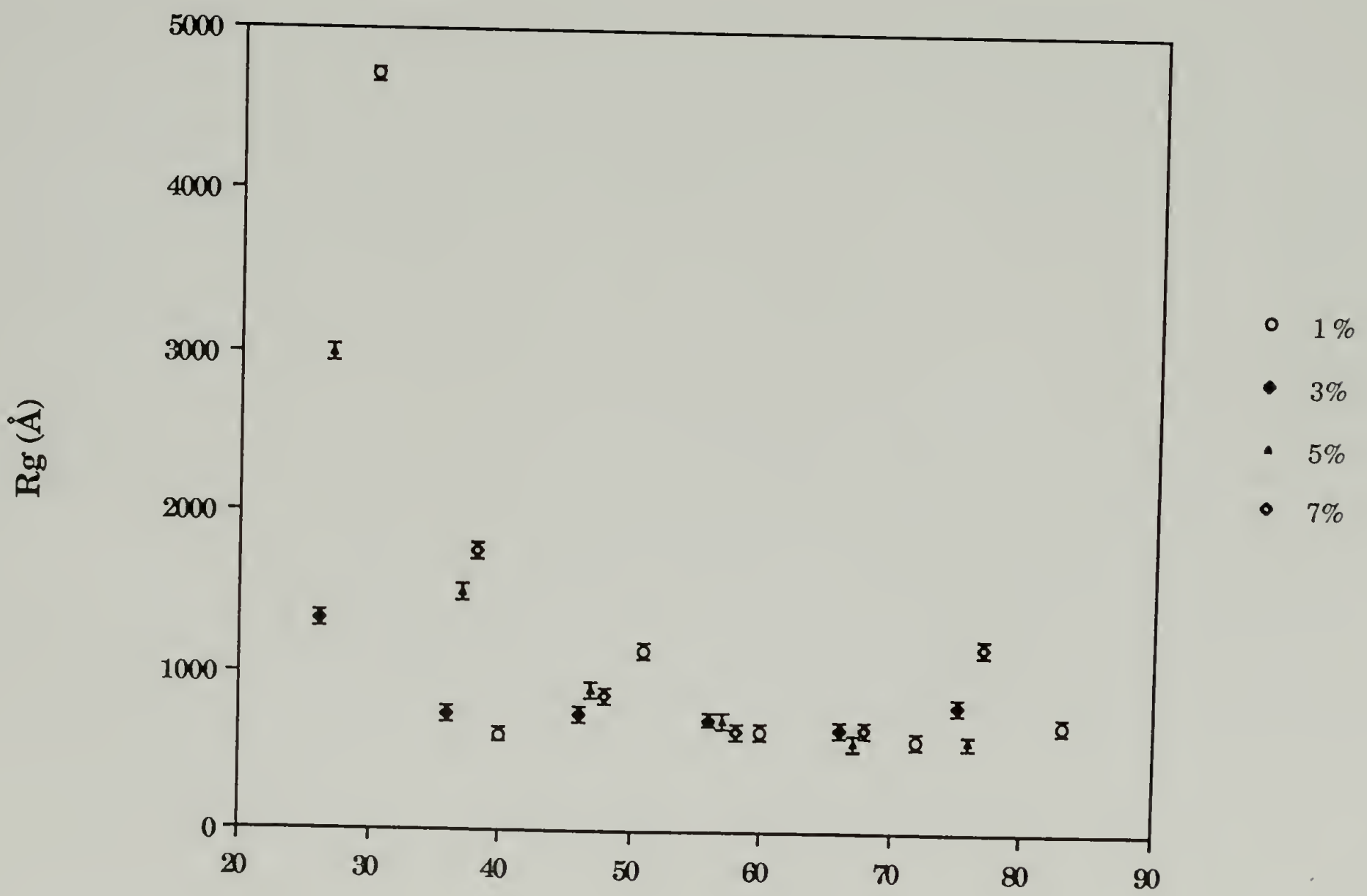
Rg (Å)
5000
4000
3000
2000
1000
0
20
30
40
50
60
70
80
90
Temperature (°C)
1%
3%
5%
7%

Figure 3.6 The change in the persistence length of a PBLG molecule with temperature in the isotropic phase in benzyl alcohol.

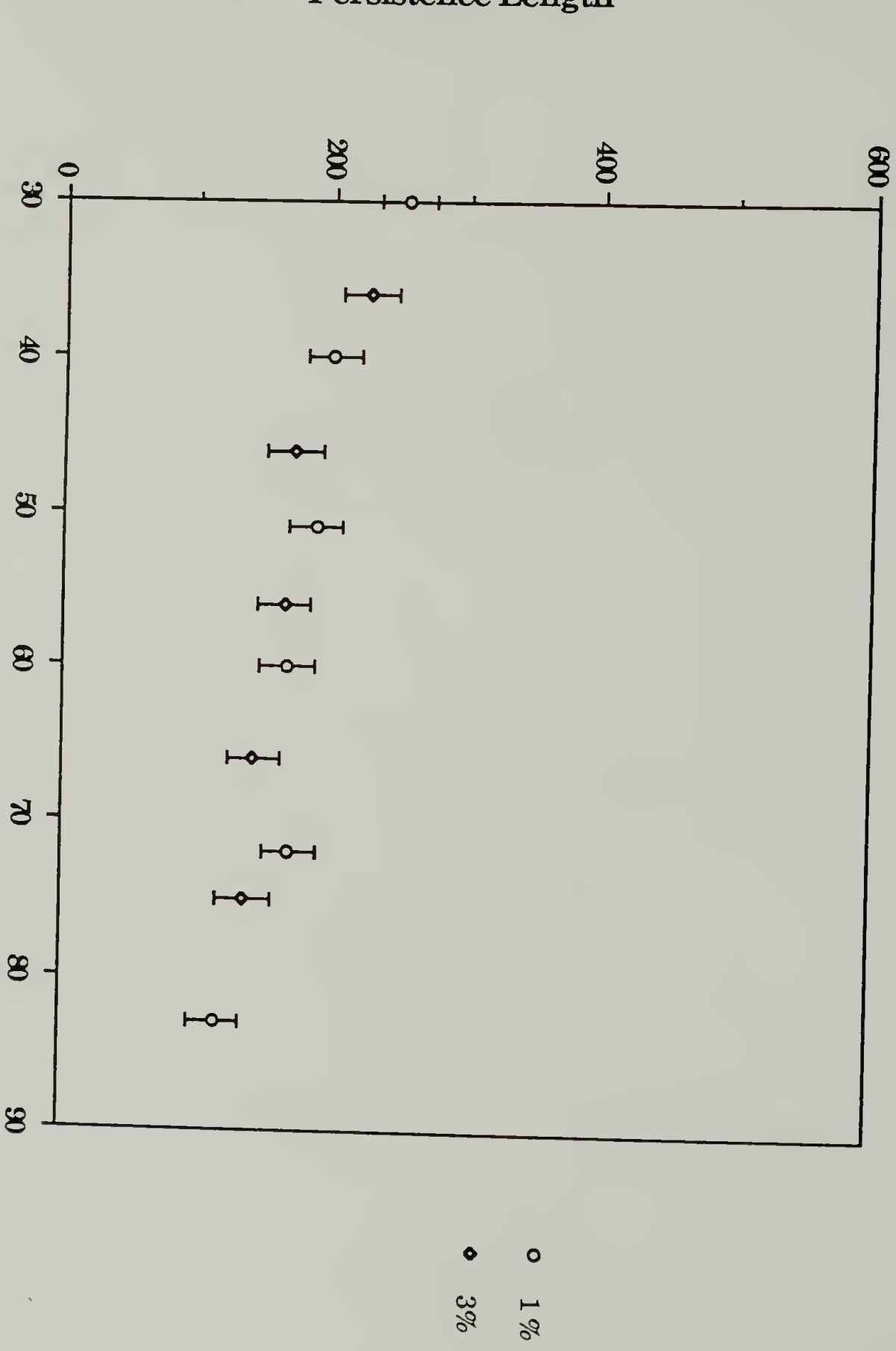
Persistence Length
0
200
400
600
Temperature
30
40
50
60
70
80
90
1%
3%

Figure 3.7 The change in the EISF with q for a 14% solution of PBLG in benzyl alcohol for different temperatures. A.) 338 K, B.) 315 K, and C.) 280 K.

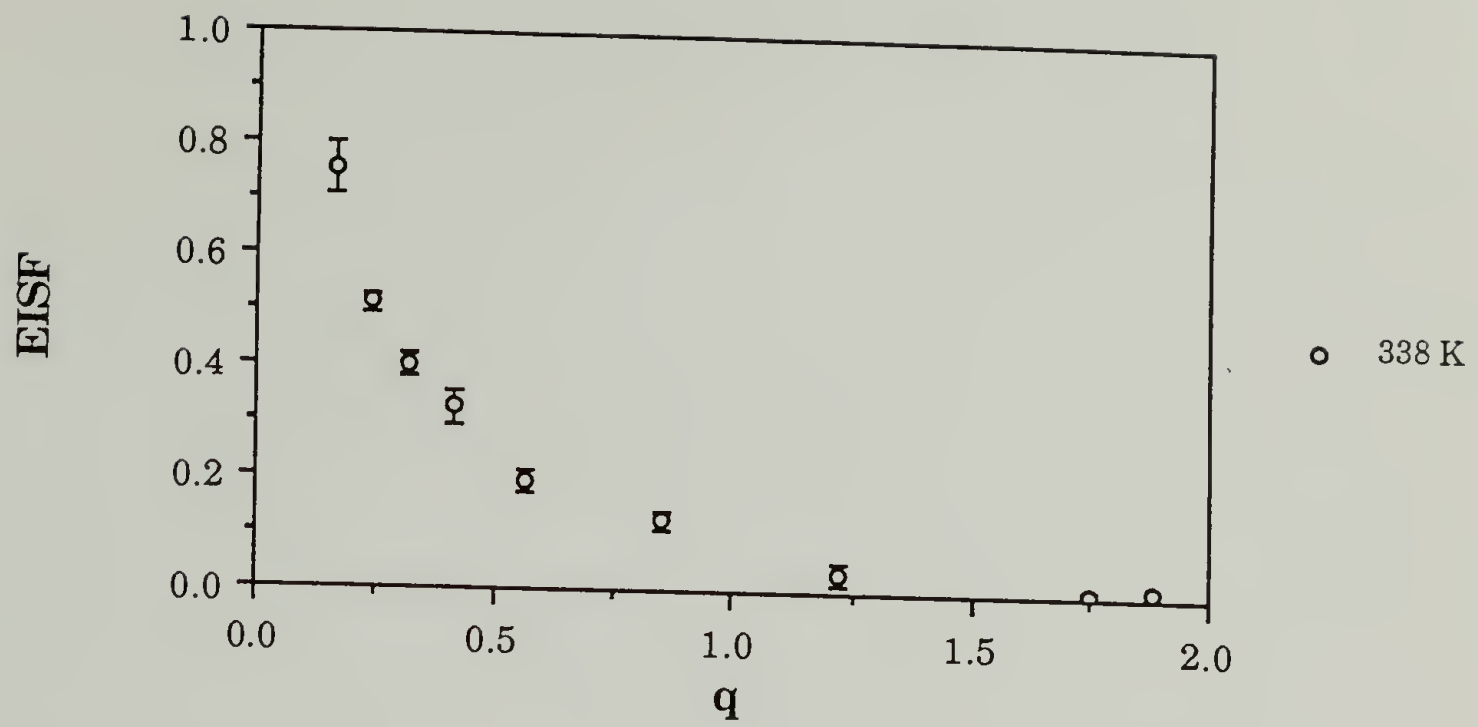
EISF
1.0
0.8
0.6
0.4
0.2
0.0
0.0
0.5
1.0
1.5
2.0
q
338 K

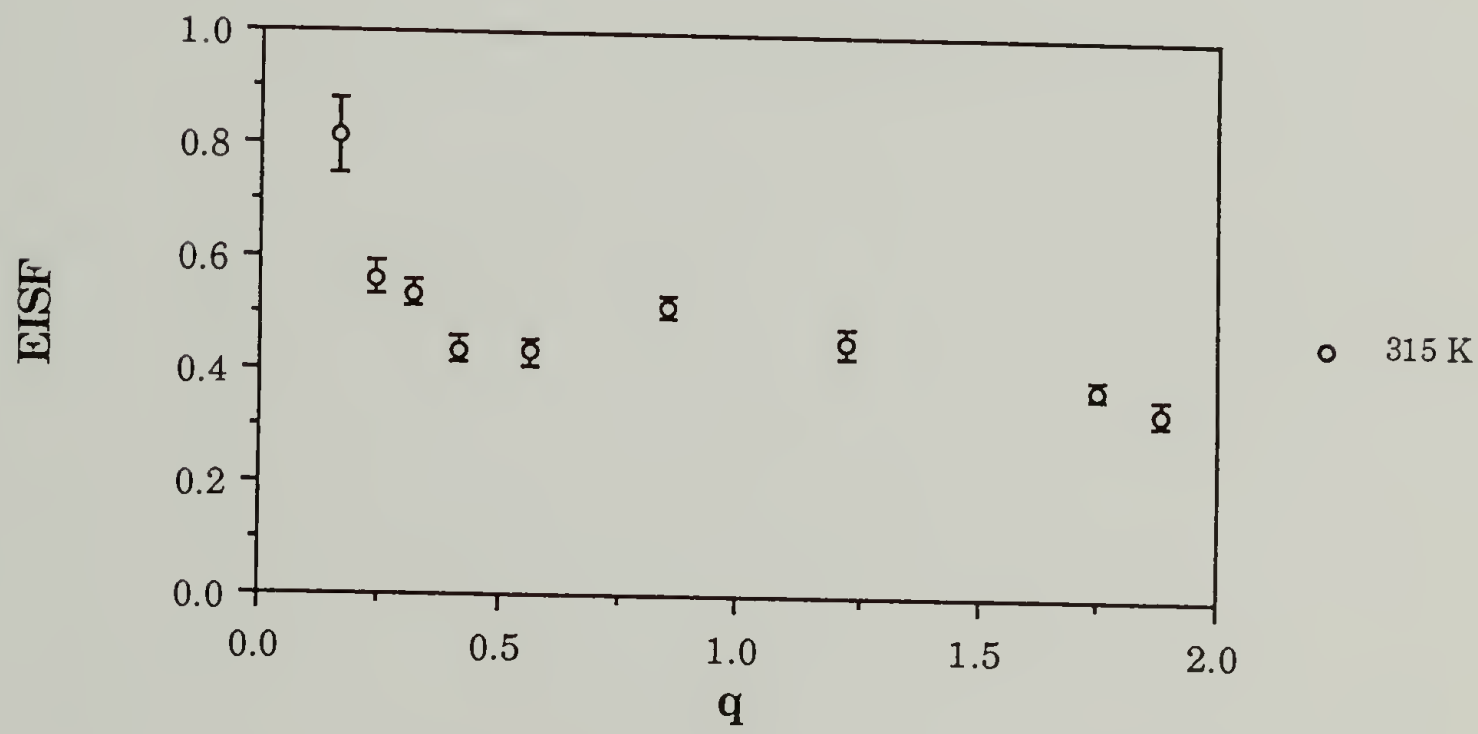
EISF
1.0
0.8
0.6
0.4
0.2
0.0
0.0
0.5
1.0
1.5
2.0
q
315 K

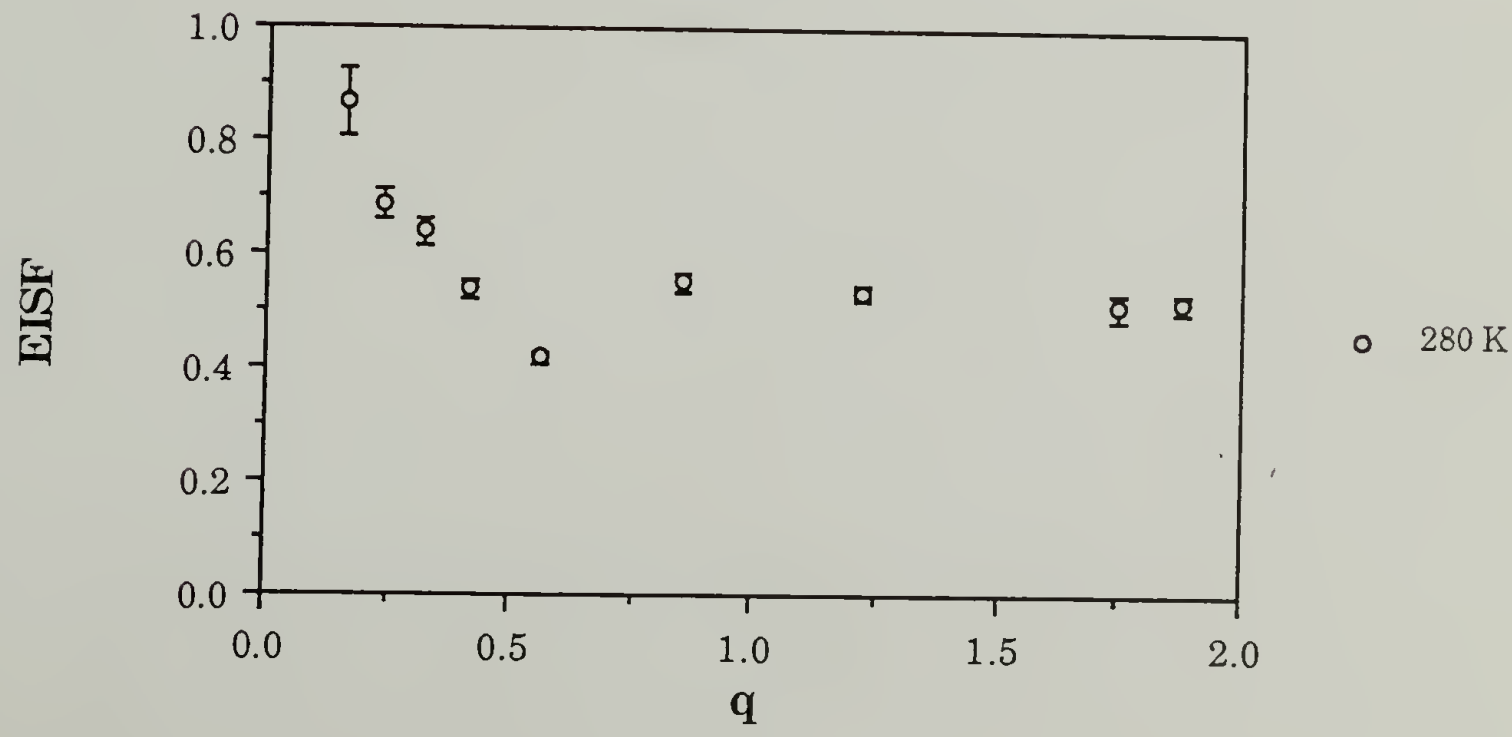
EISF
1.0
0.8
0.6
0.4
0.2
0.0
0.0
0.5
1.0
1.5
2.0
q
280 K

Figure 3.8 The change in the HW with q for a 14% solution of PBLG in benzyl alcohol for different temperatures. A.) 338 K, B.) 315 K, and C.) 280 K.

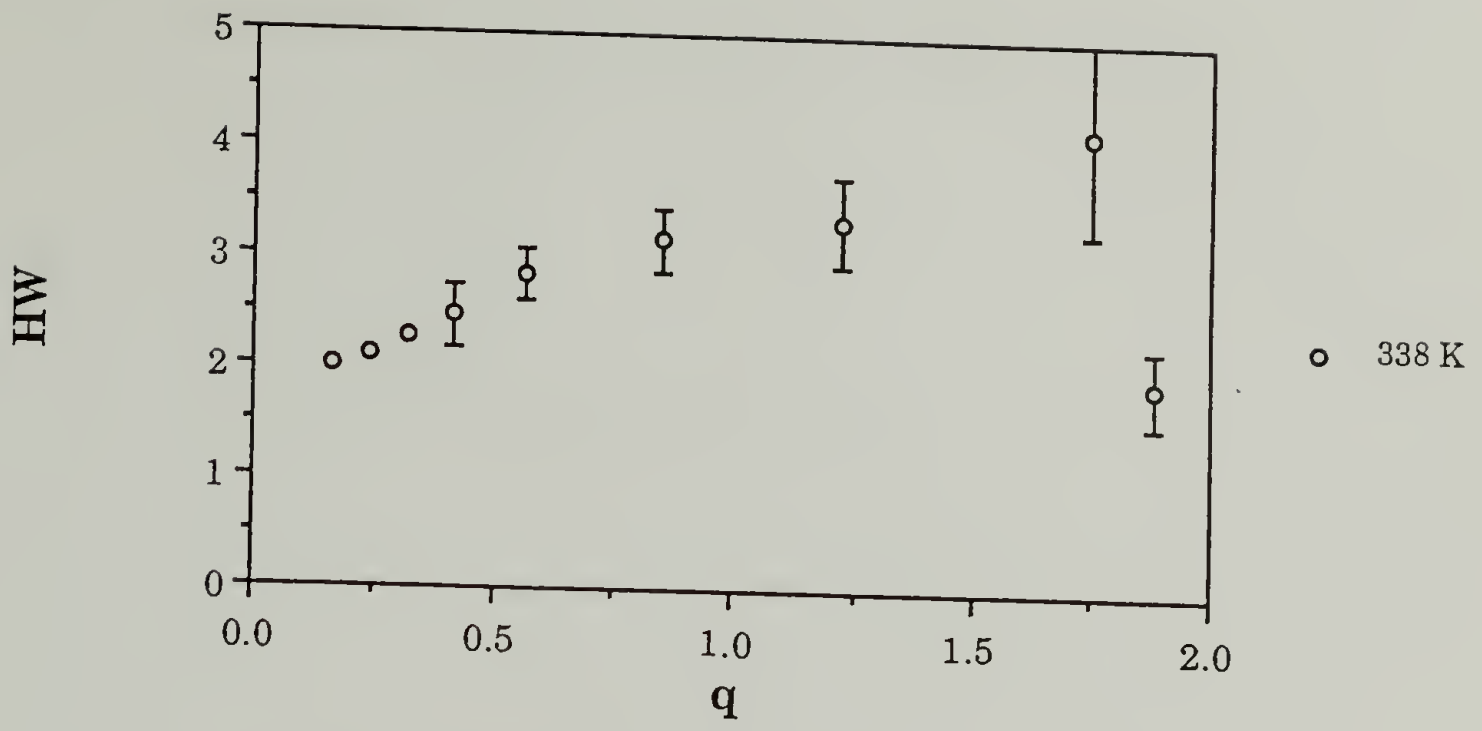
HW
5
4
3
2
1
0
0.0
0.5
1.0
1.5
2.0
q
338 K

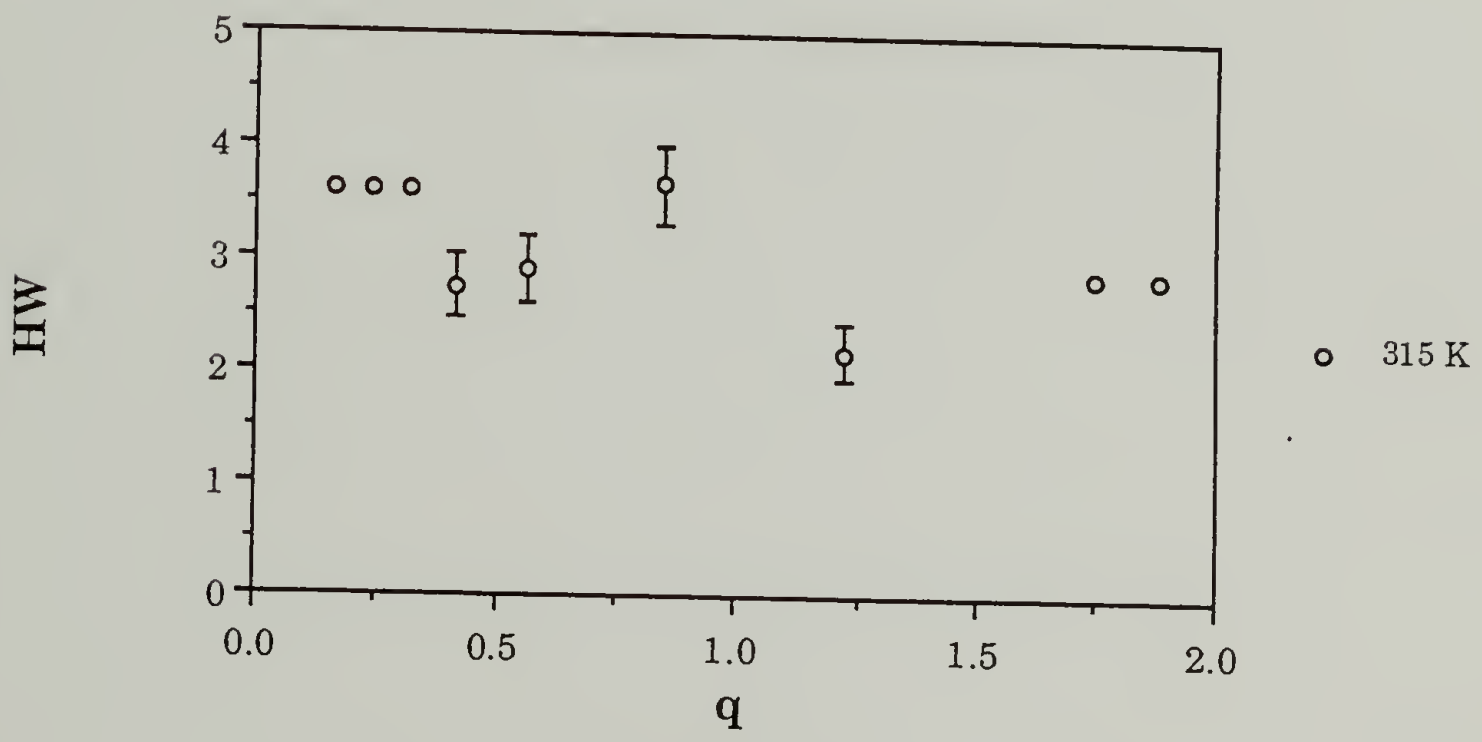
HW
5
4
3
2
1
0
0.0
0.5
1.0
1.5
2.0
q
315 K

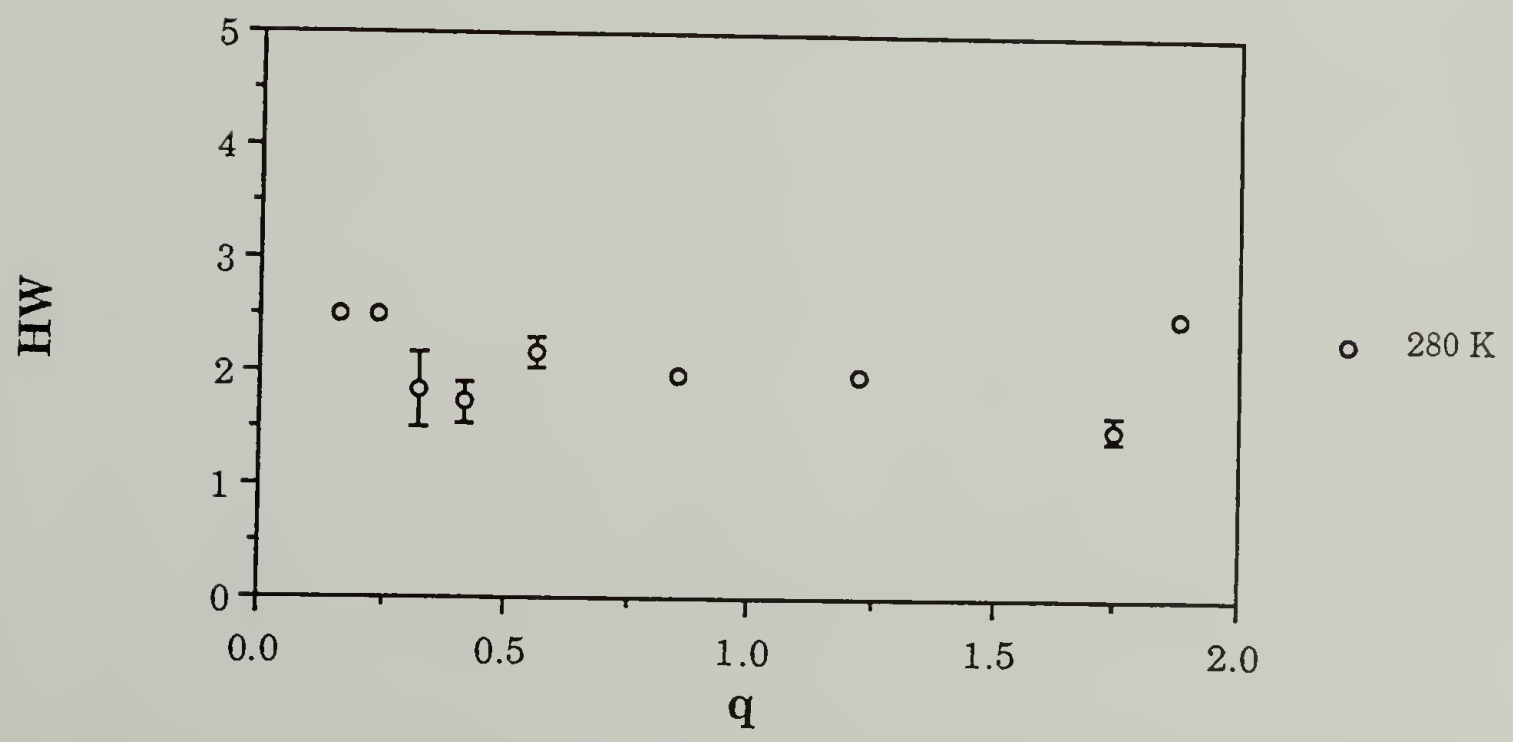
HW
5
4
3
2
1
0
0.0
0.5
1.0
1.5
2.0
q
280 K

Figure 3.9 The change in the EISF with q for a 9% solution of PBLG in benzyl alcohol for different temperatures. A.) 338 K, B.) 315 K, and C.) 280 K.

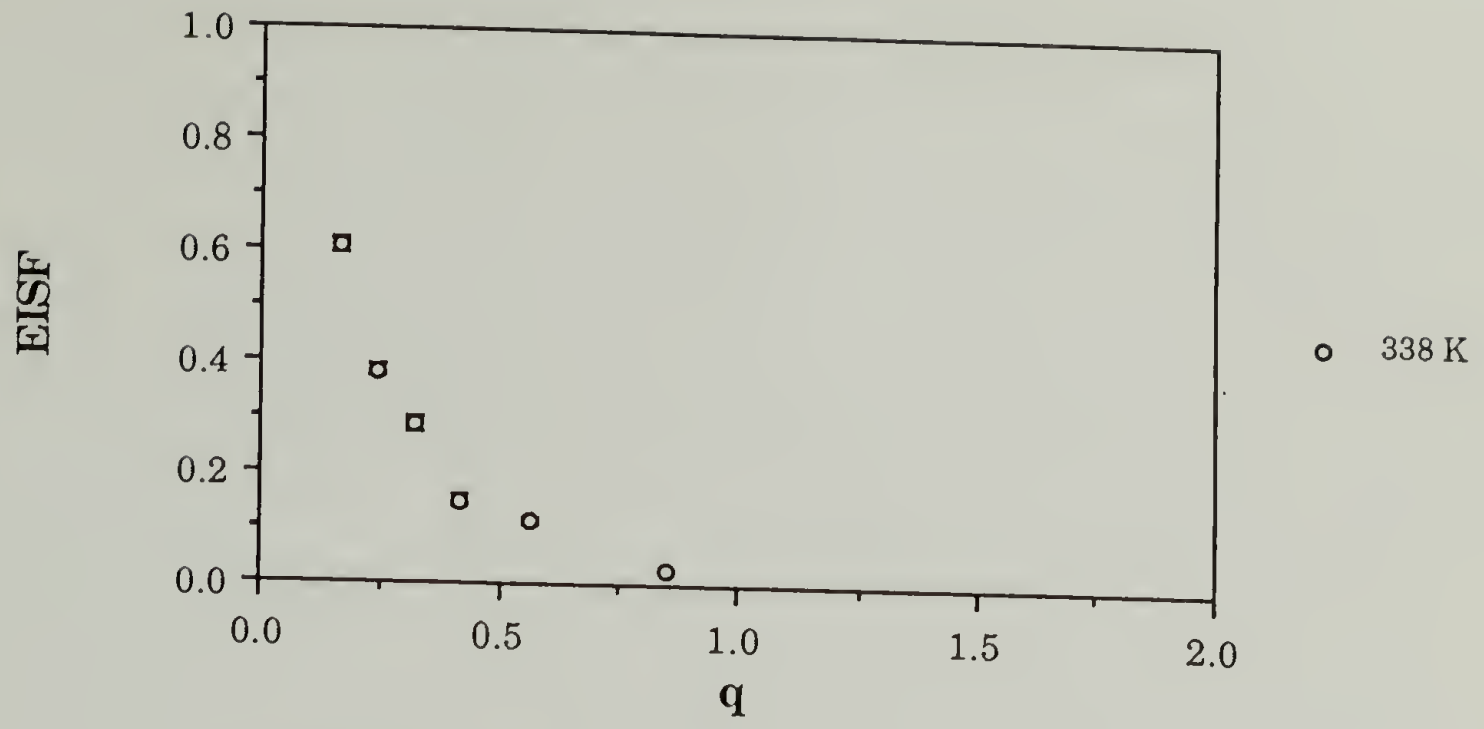
EISF
1.0
0.8
0.6
0.4
0.2
0.0
0.0
0.5
1.0
1.5
2.0
q
338 K

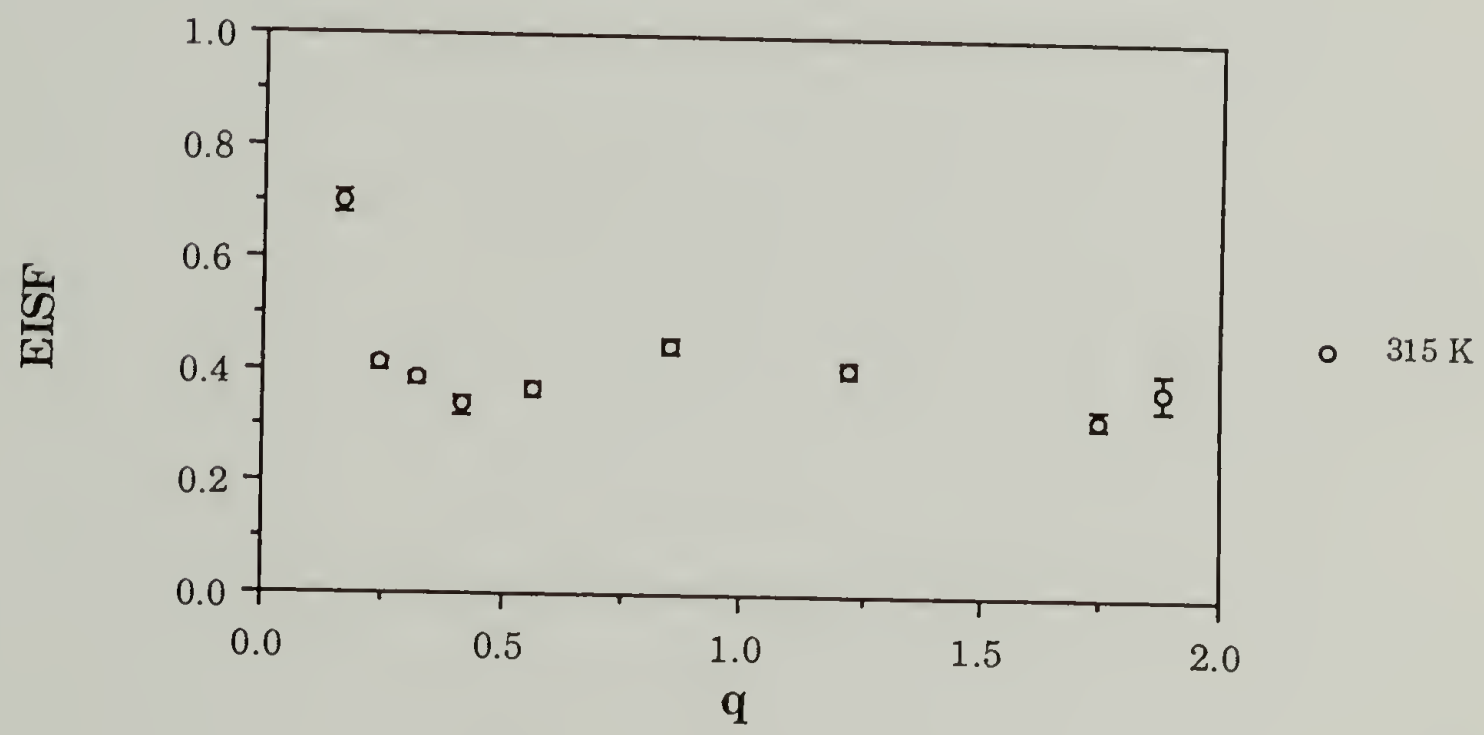
EISF
1.0
0.8
0.6
0.4
0.2
0.0
0.0
0.5
1.0
1.5
2.0
q
315 K

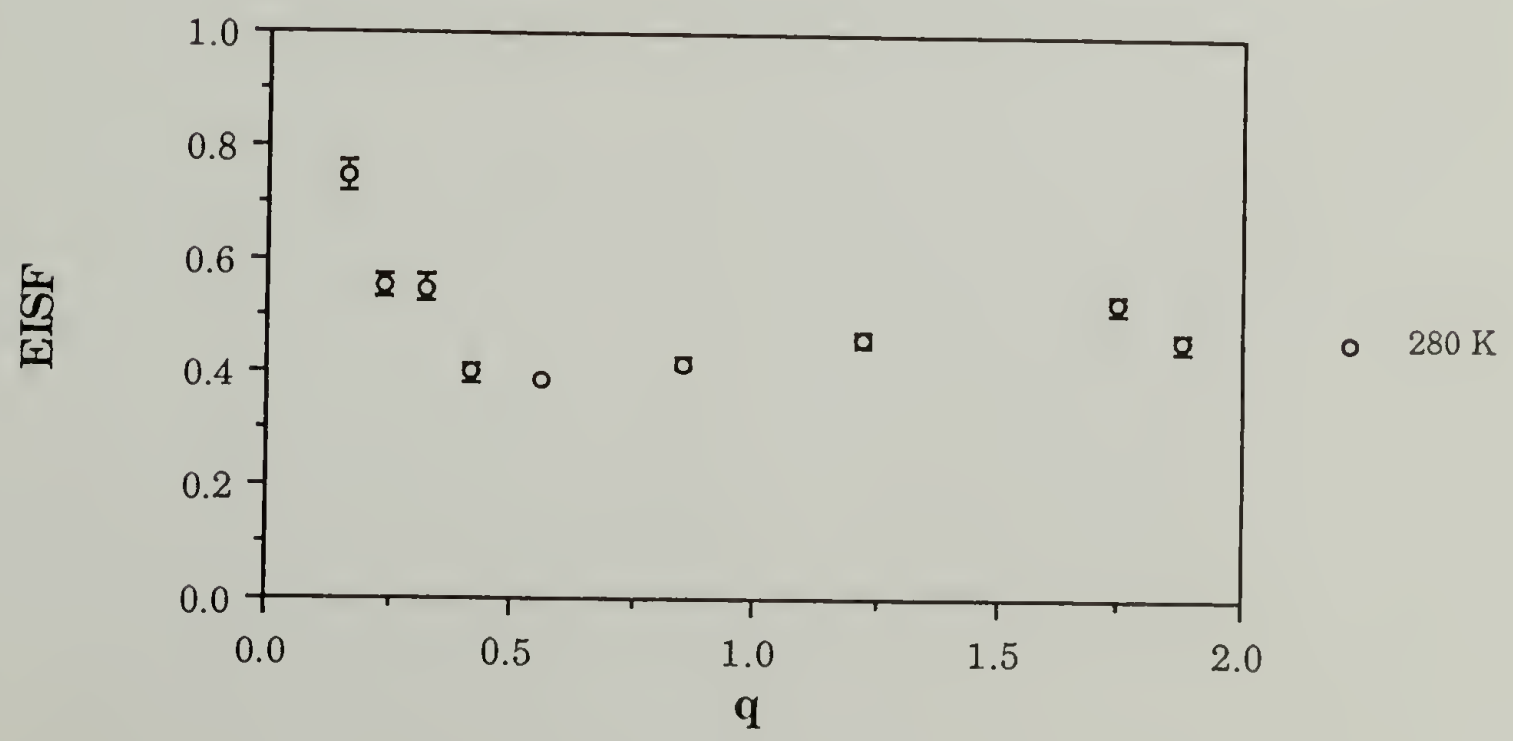
EISF
1.0
0.8
0.6
0.4
0.2
0.0
0.0
0.5
1.0
1.5
2.0
q
280 K

Figure 3.10 The change in the HW with q for a 9% solution of PBLG in benzyl alcohol for different temperatures. A.) 338 K, B.) 315 K, and C.) 280 K.

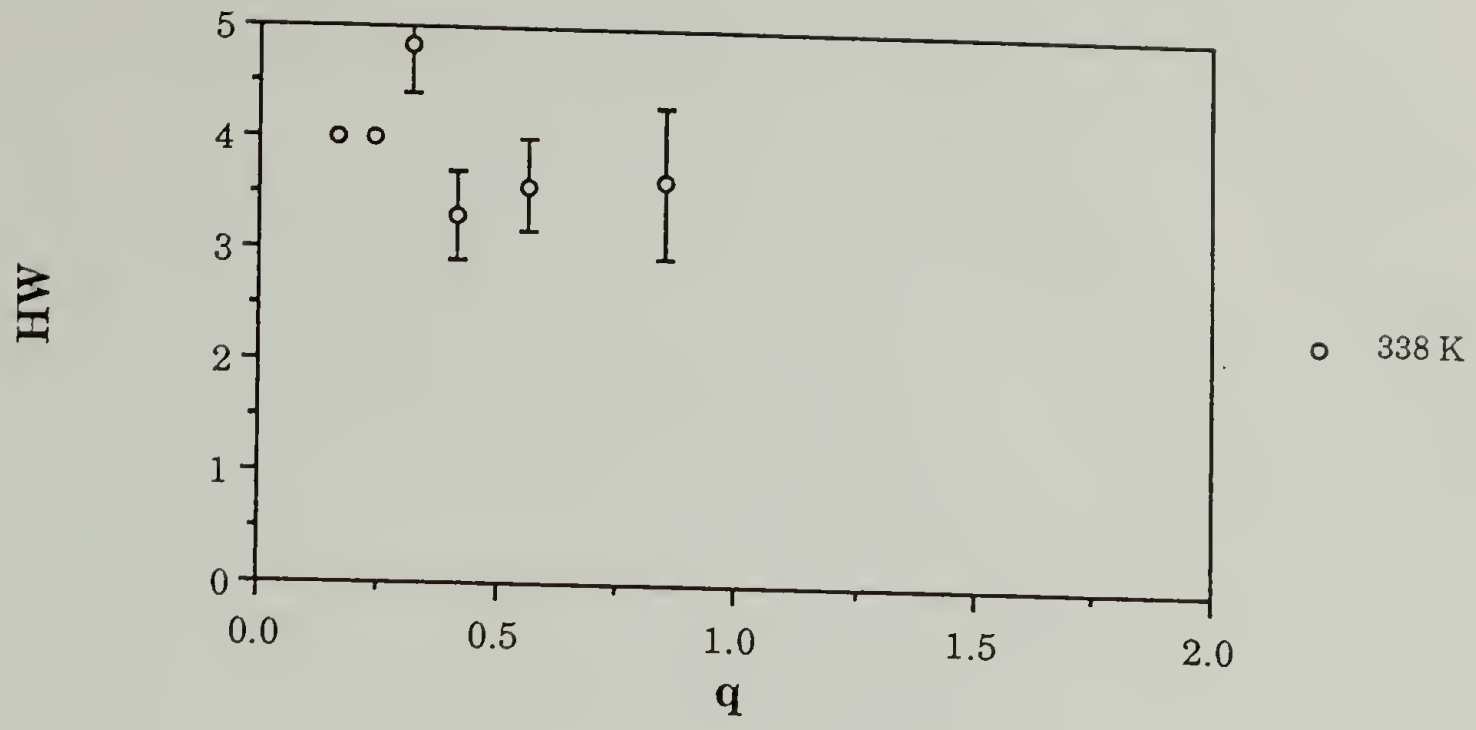
HW
5
4
3
2
1
0
0.0
0.5
1.0
1.5
2.0
q
338 K

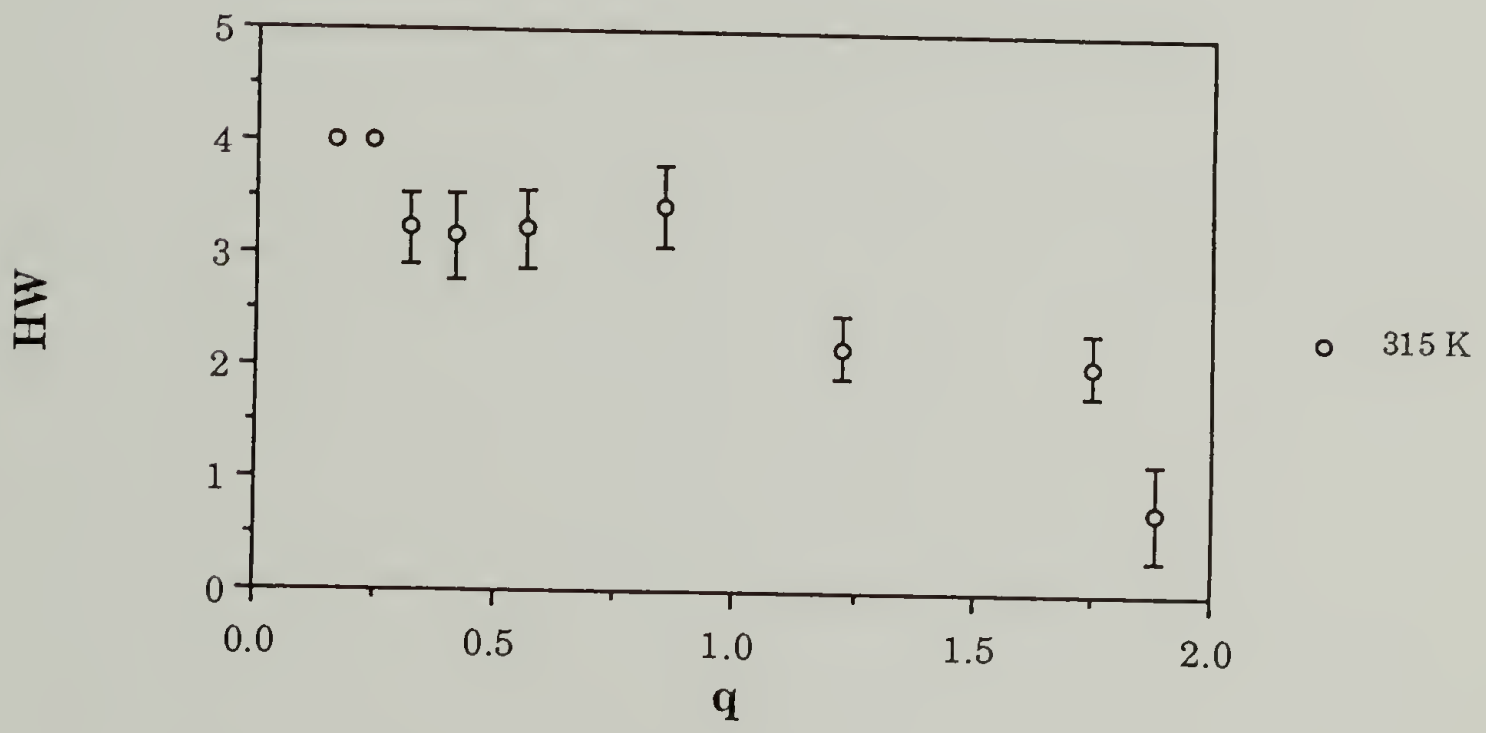
HW
5
4
3
2
1
0
0.0
0.5
1.0
1.5
2.0
q
315 K

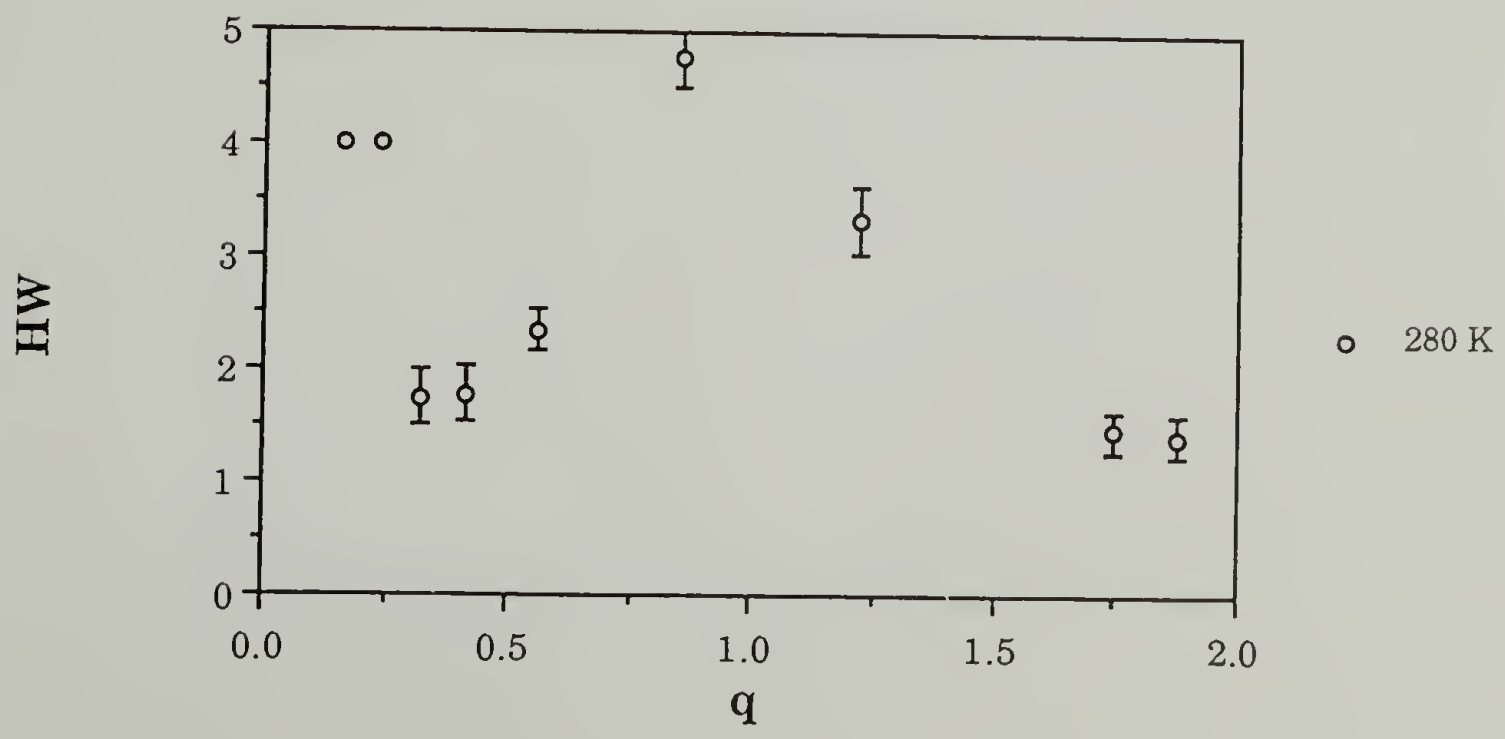
HW
5
4
3
2
1
0
0.0
0.5
1.0
1.5
2.0
q
280 K

Figure 3.11 The change in the EISF with q for a continuous motion on a sphere of radius 5 Å.

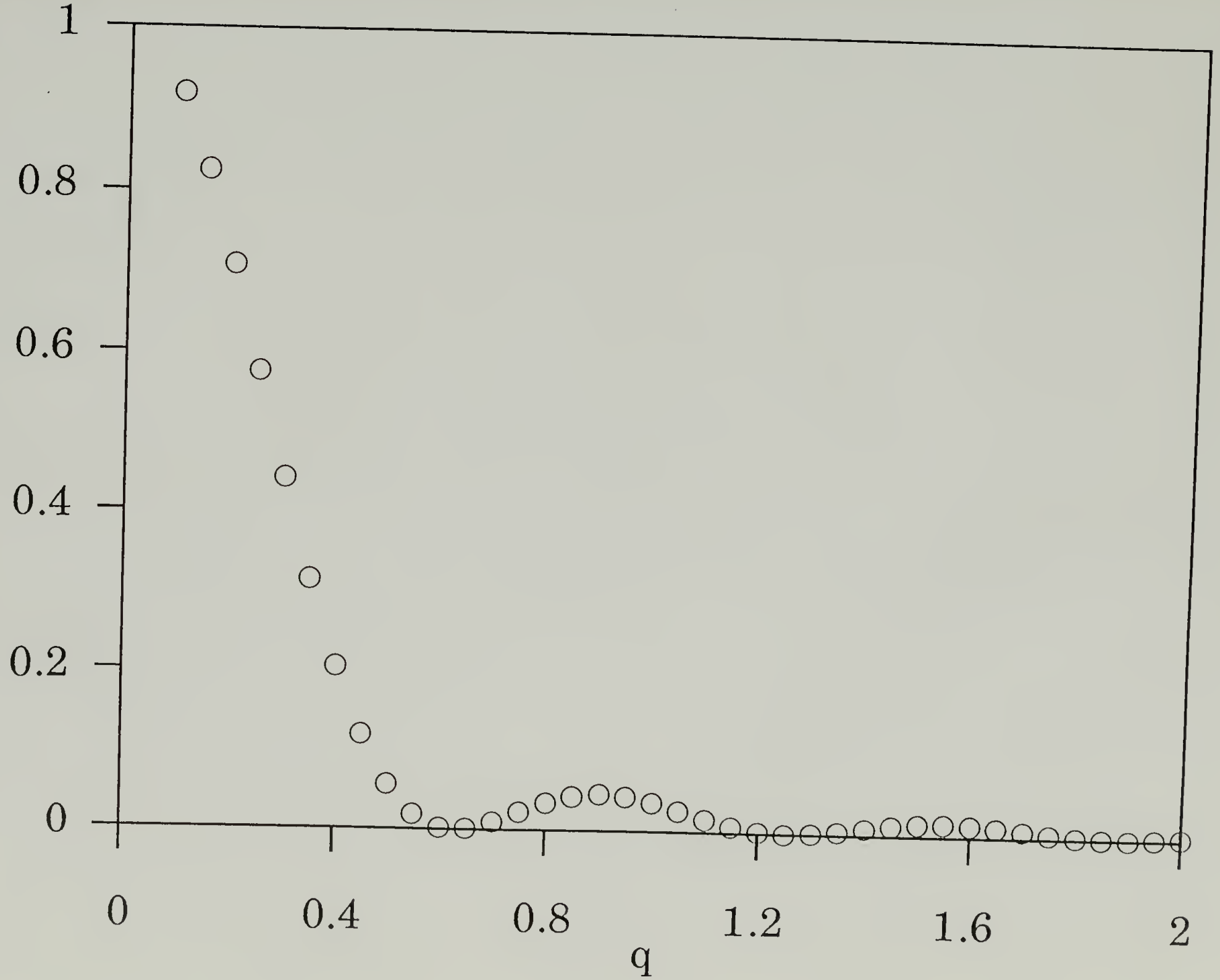
EISF
1
0.8
0.6
0.4
0.2
0
0
0.4
0.8
1.2
1.6
2
q

Figure 3.12 The change in the EISF with q for a jump-like reorientational motion between two points separated by 5 Å.

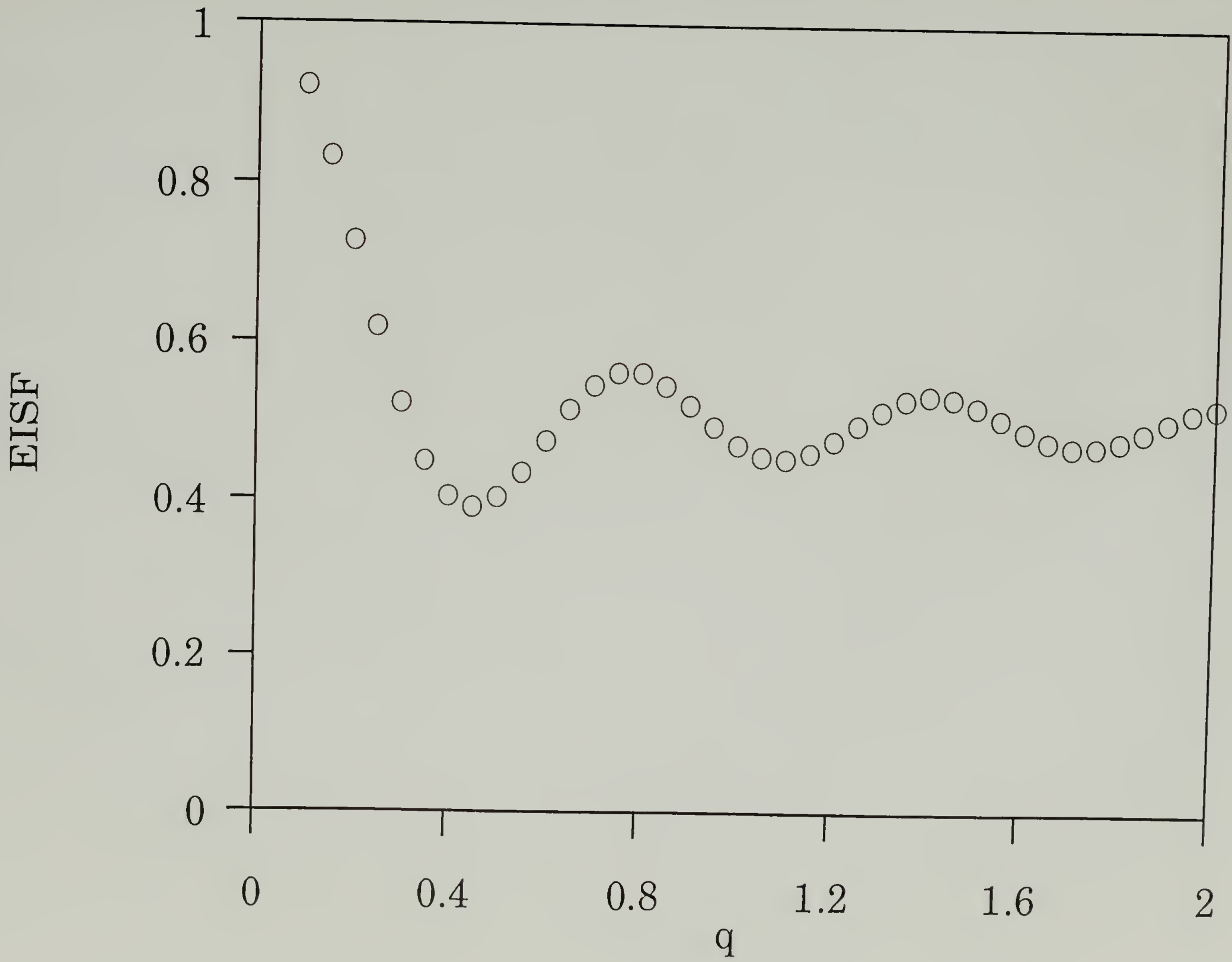
EISF
1
0.8
0.6
0.4
0.2
0
0
0.4
0.8
1.2
1.6
2
q

References

1. P. J. Flory, Proc. Roy. Soc. (London) **A234**, 73 (1956).

2. E. L. Wee and W. G. Miller, J. Phys. Chem. **75**, 1446 (1971).

3. W. G. Miller, J. H. Rai, and E. L. Wee, in *Liquid Crystals and Ordered Fluids*, edited by R. Porter and J. Johnston (Plenum, New York, 1974).

4. W. G. Miller, L. Kou, K. Tohyama, and V. Voltagio, Journ. Poly. Sci.: Polym. Symp. **65**, 91 (1978).

5. P. S Russo, P. Magestro, and W. G. Miller in *Reversible Polymeric Gels and Related Systems, ACS Symposium Series* #350 edited by P.S. Russo, (American Chemical Society, Washington D.C., 1987).

6. P. Shukla, Ph.D. Dissertation, University of Massachusetts, (1989).

7. H. Block, *Poly (γ-benzyl l-glutamate) and Other Glutamic Acid Containing Polymers*, (Gordon & Breach Science Publishers, New York, 1983).

8. S. Sasaki, M. Hikata, C. Shiraki, and I. Uematsu, Polym. Journ. **14**, 205 (1982).

9. S. Sasaki, M. Hikata, C. Shiraki, and I. Uematsu, Polym. Journ. **14**, 205 (1982).

10. S. Sasaki, K. Tokuma, and I. Uematsu, Polym. Bull. **10**, 539 (1983).

11. J.G.L. Pluyter and E.T. Samulski, ACS Polymer Preprints **32**, 140 (1991).

12. A. Hill and A.M. Donald, Polymer **29**, 1426 (1988).

13. A. K. Murthy and M. Muthukumar, Macromolecules **20**, 564 (1987).

14. A. Hill and A.M. Donald, Liq. Cryst. **6**, 93 (1989).

15. A.J. Leadbetter and R.E. Lechner in *The Plastically Crystalline State*, edited by J.N. Sherwood (Wiley, New York, 1979).

16. J. R. Kim and T. Ree, J. Poly. Sci.; Polym. Chem. **23**, 215 (1985).

CHAPTER 4

THE RESPONSE OF SEMI-FLEXIBLE LIQUID CRYSTALS TO QUENCHED RANDOM DISORDER

Introduction

Liquid crystals are known to form several mesophases. Because of their technological importance, many theoretical and experimental investigations of the mesophase transitions have been completed. These mesophases include the smectic, nematic, and cholesteric phases. One of the variables describing the extent of ordering is the order parameter, S.

$$S = \langle 3 \cos^2(\phi) - 1 \rangle / 2$$

where ‹...› denotes spatial averaging and ø is the angle between the anisotropic axis of the molecule and the local director. The local director is a unit vector along the 'macroscopic' axis of symmetry. Macroscopic here denotes a scale larger than the molecular size. S equals one in the fully ordered state and zero in the isotropic state.

Original calculations due to Flory [1] and Onsager [2] demonstrated that a state of parallel order can be obtained due solely to the anisotropy of the molecule and steric interactions. Intermolecular interactions were of secondary importance. On the other hand, calculations by Maier and

Saupe [3] show a phase transition from the disordered (isotropic) to ordered state (nematic) due solely to orientational (intermolecular) interactions between molecules with anisotropic polarizabilities. The realistic case is probably a combination of the two effects.

To date, most theoretical and analytical calculations have centered on ideal homogeneous systems. In general the experimental systems studied contain defects rising from surfaces, impurities, and other foreign species. Liquid crystalline polymer systems are some of the most impure systems due to disclinations, dust, and extraneous initiator and monomer from the polymerization. Even the polydispersity of the polymer sample is a degree of disorder, albeit characterizable. As liquid crystals are 'soft', *i.e.* the energy responsible for long range order is small,[4] disorder will have a significant effect on their thermodynamic properties. This makes liquid crystals an ideal system to study the effect of disorder on fluid phase transitions. And due to their technological importance, we are interested in how the mesophase transition responds to the introduction of disorder.

There are three common methods to incorporate disorder into a model system. These mechanisms include adding quenched non magnetic atoms to a lattice of magnetic atoms, called dilution[5]; imposing a random magnetic field to a model system, called random field[6,7,8]; and denoting the intermolecular interactions as random, called random bond[9,10]. The easiest of these to implement is dilution.

The effect of dilution on a phase transition has been studied extensively for magnetic systems (Ising, Heisenberg, X-Y model, etc...)

using renormalization group,[11] expansion methods,[12,13,14] and Monte Carlo simulation.[15,16,17,18] Since the order-disorder transition temperature (the Curie temperature in magnetic systems) is proportional to the total intermolecular interaction, the introduction of isolated random impurities will decrease the total intermolecular interaction and therefore the transition temperature, T_c. Earlier studies have shown that the depression of T_c is proportional to the impurity density, I, if the latter is low. However, long range order can only be attained if there exist sufficient pathways through which interactions can correlate. Above a certain impurity concentration, $1\text{-}p_c$, where p_c is the porosity at the percolation threshold, these pathways cease to exist, *i.e.* separate domains exist, and no transition can occur. Therefore, the transition temperature should decrease linearly with impurity concentration in the dilute limit and continue to decrease to zero at the percolation threshold [5,19,20] as in figure 4.1 The linear decrease in the dilute limit has been seen in studies of magnetic systems.[15-18]

The effect of disorder on first order phase transitions was first examined by Imry and Wortis[21]. Using a heuristic argument, they showed that quenched impurities can round the phase transition. The existence and extent of rounding depends upon the fluctuation in the impurity density and the interfacial energy between the competing phases. Imry and Wortis did not attempt to describe the transition itself, unable to determine if the discontinuity will be reduced or eliminated. Recently Hui and Berker[11] and, separately Aizenmann and Wehr[22,23], have shown that a system with quenched randomness will not undergo a first order phase transition in two dimensions. These calculations were

then extended[24] to show that discontinuities can be suppressed in all dimensions, dependent upon the symmetry of the system and the strength of the random field.

The aim of the present work is to use Monte Carlo simulations to elucidate the effect of dilution on the isotropic to nematic phase transition of a model semiflexible polymer. In so doing, we hope to understand the mesophase transitions of liquid crystals and their response to external perturbations as well as to extend the research on the response of first order phase transitions to quenched impurities. The polymer chains are simulated as trimers. This is the same model system studied by Baumgärtner[25,26] for the pure system. Dilution has been effected by denoting random points on the lattice as occupied by impurities and therefore inaccessible to the liquid crystal. The interactions between the impurities and the lattice chains are purely excluded volume and there is no attractive interaction.

The dilute limit is the region of interest in this study. Systems containing impurity concentrations of 0.00%, 2.50%, 5.01%, and 7.51% have been studied. The task of pinpointing and characterizing the transition was accomplished by monitoring the specific heat of the system as it passed through the phase transition.

Model and Simulation Technique

The model system in this study consists of a set of chains of length N beads (N-1 bonds) confined to a cubic lattice. All chains in this study are trimers, *i.e.*, N=3. To simulate a set of finite chains in an infinite box, the system is approximated as a set of infinitely many identical cells

of length L with periodic boundary conditions. The density, ρ, of the system is defined as the fraction of trimers which occupy the lattice, $\rho = N_p N/L^3$ where N_p is the number of trimers and L^3 is the volume of the lattice.

In order to simulate the isotropic-nematic transition it is necessary to include both inter- and intra-molecular interactions.[25] The intramolecular energy of two adjacent bonded segments is $\varepsilon_b < 0$ if they are collinear and zero otherwise. The intermolecular energy between two neighboring nonbonded segments is $\varepsilon_s < 0$ if they are parallel and zero otherwise. In our model ε_s and ε_b are equal. This definition of intermolecular orientation differs from the Maier-Saupe interaction in that this model shows a local dependence whereas the Maier-Saupe interaction is between the two entire macromolecules. The steric interactions are considered as excluded volume; double occupancy of a given lattice site is forbidden.

The initial configuration of the system is created as follows. The impurities are placed randomly in the lattice via the percolation method. Each impurity is a forbidden site on the lattice; there is no attractive or additional repulsive interaction between the trimers and the impurity. The trimers are then added to the lattice in a totally ordered state. Different chain configurations are created by a modified reptation technique.[25,26] In this modified reptation technique, a void (*i.e.*, a point on the lattice where there is no polymer or impurity) is selected at random. If one of the randomly selected nearest neighboring lattice points is the end of a trimer then the trimer is moved into the void and the other end is vacated, thereby displacing the void and creating the new

configuration for the chain. The new configuration is accepted according to the Metropolis[27] sampling technique. The system is characterized at each temperature by the heat capacity, C_v;

$$C_v = \langle E^2 \rangle - \langle E \rangle^2$$

where E is the total normalized energy of the system defined as

$$E = (1 - N_b/(N_p (N-2))) + (N_s/4N_p)$$

N_s is the number of parallel pairs of segments and N_b is the number of bends in the system. ‹ ... › denotes the ensemble average.

First, the order of the transition as seen in the pure system was determined using finite size analysis. The effect of disorder on the nature of the phase transition was then systematically studied by monitoring the specific heat of systems containing 2.50%, 5.01%, and 7.51% impurities as they undergo the order-disorder phase transition. Finally, the order of the phase transition of the impure system was determined by completing finite size analysis on systems with 5.0 ± 0.007% impurities.

Results

The isotropic-nematic phase transition of a thermotropic liquid crystal is known to be first order.[4] The isotropic-nematic phase transition as simulated by Baumgärtner seemed to be first order in three dimensions. It was necessary to verify this.

In a theoretical infinite system a first order phase transition is characterized by a discontinuity in the first derivative of the free energy.

This results in a δ function singularity in the heat capacity, the second derivative of the free energy. This divergence is a consequence of the coexistence of two phases.[28,29] The system does not anticipate the transition and there is no critical region or critical exponents. In second order phase transitions, there is a power law divergence in the heat capacity, but this divergence is a consequence of the correlation length becoming infinite.[29] The system anticipates the transition and a critical region and critical exponents are found. In real finite systems this divergence does not occur. Finite size effects cause the divergence to become a finite peak. There are two effects, a rounding of the peak with decreasing lattice size and a shifting of the peak with a change in lattice size. In second order phase transitions the shift of heat capacity peak is due to the limitation of the correlation length to the lattice size, L. Scaling theory therefore[30,31] predicts that the heat capacity maximum, C_v^{max} will diverge as $L^{\alpha/\upsilon}$ while the transition temperature will shift as

$$T_c - T_c^* / T_c^* \sim L^{1/\upsilon}$$

where T_c is the transition temperature of the finite system and T_c^* is the transition temperature of the infinite system.

In first order phase transitions the lattice size dependence is in the form of the volume, L^d. The finite size of the system affects the transition only when the coexisting phases reach the extent of the volume of the lattice. Scaling theory [28,32] then predicts that C_v^{max} will diverge as L^d while the transition temperature will shift as

$$T_c - T_c^* / T_c^* \sim L^{-d}.$$

Therefore, one way to determine the order of a phase transition is to perform finite size analysis on the system and determine how the heat capacity peak and the transition temperature change with lattice size. Objections to using finite size analysis to determine the order of a transition include[28,33] the problems of long relaxation times of metastable states near a first order phase transition and critical slowing down near a continuous phase transition, as well as error inherent to the Monte Carlo method and smearing of discontinuities not attributable to finite size effects. Unfortunately, it is impossible to discount completely the possibility of a first order transition in an observed 'continuous' transition. In laboratory experiments, it is possible that phases coexist below the resolution of the equipment. In the same manner, observed metastability that signals a first order phase transition may be non-equilibrium effects of a continuous transition. Therefore, as definitive determination of the order of a phase transition is a deficiency of both computer simulation and laboratory experiments, all properties must be meticulously studied and compared to known phase transitions in order to make the best judgement possible.

With this in mind, a finite size analysis was completed on the pure system. Careful determination of effects other than finite size on the phase transition such as initial equilibration, trimer density, and long relaxation time near T_c were completed in order to minimize their effect. To insure that the systems studied were valid in finite size analysis, the order parameter, S, which is defined as $S = < 3 f - 1 > / 2$ where f is the number of bonds that are in the preferred direction and $< ... >$ denotes the ensemble average, was determined as each system passed through the

phase transition. Figure 4.2 shows the squared order parameter, S^2, for the pure systems of size L = 10, 13, and 16 in 4.2(a), 4.2(b), and 4.2(c) respectively. These plots show that the transition is sharp and, therefore, the use of finite size analysis is valid.

The results show that the system undergoes a first order order-to-disorder phase transition. Figures 4.3, 4.4, and 4.5 exemplify this. Figure 4.3 is a plot of the heat capacity vs. reduced temperature, Tau = k_BT/ε_b, for three different lattice sizes. This shows the effect of finite size on this phase transition. From the smallest lattice size, 10, up to the largest lattice size, 16, there is a continuous increase in the height and temperature of the maximum as well as a decrease in the roundedness of the peak. For a first order phase transition, the transition temperature T_c should depend upon the lattice size as $T_c \sim L^{-d}$ while the heat capacity maximum, $C_v^{max} \sim L^d$. Figures 4.4 and 4.5 are plots of C_v^{max} vs. L^d and T_c vs L^{-d} respectively. The observed linearity of both plots leads to the conclusion that the system undergoes a first order phase transition. It should be noted here that the dependence of C_v^{max} on lattice size is a more reliable sentinel variable for the finite size analysis. The transition temperature T_c is determined by changing the temperature in discrete increments whereas the heat capacity is calculated from an average of many Monte Carlo runs. Therefore, the error in C_v^{max} can be minimized while the error in T_c depends upon the rounding of the peak as well as the size of the discrete increments. The error due to rounding is minimal for large lattice sizes and the pure system, but becomes important for the impure system, especially for the smallest lattice size.

With the knowledge that the first order order to disorder phase transition was successfully simulated, the effect of the addition of impurities to the phase transition has been studied. The standard Monte Carlo methods[34] are used to simulate the order-disorder phase transition of a semi-flexible polymer chain on a cubic lattice in the presence of impurities. A $13 \times 13 \times 13$ lattice with periodic boundary conditions is used. The density of the system is ρ= 81.25 % trimers. Impurity concentrations are 0.00%, 2.50%, 5.01%, and 7.51%. The simulation was performed on an IBM 3090-600J supercomputer with vector and parallel processing located at the Cornell National Supercomputer Facility and an Alliant FX/40-4 mini supercomputer with vector processing at the Polymer Research Institute at the University of Massachusetts.

The change in the specific heat with temperature of the pure system as well as the 2.50%, 5.01%, and 7.51% impure systems are shown in figure 4.6 Inspection of these plots shows that as the impurity concentration increases, the transition temperature T_c decreases. There is also a decrease in the specific heat maximum as well as a rounding of the specific heat peak as the impurity concentration increases. Figure 4.7 shows the squared order parameter, S^2, as the impure systems undergo the phase transition. These plots show the order parameter for the systems with 2.5%, 5.0% and 7.5% impurities in 4.7(a), 4.7(b) and 4.7(c) respectively. Inspection of the plots shows that as the impurity concentration is increased, the discontinuity in the order parameter is decreased. Is the discontinuity partially decreased or entirely eliminated? This is difficult to determine from the diagrams, but, as described in the introduction, it is expected that the transition

temperature of a system with quenched impurities will decrease linearly with impurity concentration. To check this, Figure 4.8 is a plot of T_c vs. the porosity. The porosity, p is related to the impurity concentration, I as p = 1 - I. The expected linearity is not found here. Instead it is seen that the transition temperature changes linearly with the impurity concentration only in the impure region.

This suggests that the presence of impurities does change the nature of the phase transition. To investigate this further, a finite size analysis has been performed on an impure system, 5.01± 0.007 %. The specific heat was monitored on 5% impure systems with lattice sizes of L=10, L=13, and L=16. The change in specific heat with reduced temperature for the three systems is shown in figure 4.9 while figure 4.10 shows the change in C_v^{max} with L^d and figure 4.11 is a plot of T_c vs. L^{-d}. Both figures 4.10 and 4.11 are highly non-linear showing that this transition is not first order. Therefore, the addition of impurities to a system of semiflexible chains changes the order of the order-to-disorder transition. A comparison of figure 4.9 with figure 4.3 is also interesting. Figure 4.9 is a representation of the change in the specific heat with reduced temperature for the impure system, while figure 4.3 is the equivalent plot for the pure system. Both plots have the same abscissa and ordinate axes. As seen in figure 4.3, the heat capacity peak becomes much more rounded while the peak maximum and the transition temperature decrease noticeably as the lattice size decreases for the pure system. Comparison to figure 4.9 shows that the impure system does not undergo a drastic change with varying size as the pure system does. This is especially true of the specific heat maxima. This exemplifies the

differences between the pure and impure systems and shows that there is less finite size effect for the impure system.

Discussion and Conclusion

Disorder can take many different forms in real systems; disclinations, grain boundaries, finite size, surfaces, random fields, random bonds, or impurities. The result of this disorder on phase transitions and critical phenomena has been an intense, and yet still not well understood, field of study for the past two decades. The effect of disorder on a continuous transition is better understood theoretically than for a first order transition. Harris[10] used a self-consistent scaling argument to determine if the addition of impurities will change the nature (*i.e.* the critical exponents) of a continuous phase transition. The result, known as the Harris criterion, states that if α, the specific heat exponent for the pure system, is less than zero, the transition is not changed but if $\alpha > 0$, the transition is altered. Renormalization group calculations[14,35,36] later verified this result.

First order transitions with quenched impurities have been less studied. Imry and Wortis[21] extended Harris argument to first order transitions to argue that quenched impurities may cause a smearing of the discontinuity associated with the transition. Though they studied the result of quenched randomness on a first order phase transition, Imry and Wortis did not address the question of the nature of this phase transition. Hui and Berker[9] and Aizenmann and Wehr[22,23] have shown that a system with quenched disorder will not exhibit the discontinuity associated with a first order transition in two dimensions. These

calculations have been extended[24] to show that a system with continuous symmetry will not undergo a first order phase transition for $d \leq 4$ regardless of the strength of the disorder. Berker has shown that the discontinuity associated with any transition can be eliminated due to quenched disorder in any dimension, though a minimum strength of the random field may be necessary.

The argument of Imry and Wortis is a generalization of that of Harris for the effect of quenched impurities on a continuous phase transition. Starting with the coherence length, ξ, which remains finite at the transition, they examine the coherence volume ξ^d. The number of impurities in the coherence volume is $p\ \xi^d$ where p is the probability that a site is occupied by an impurity. The fluctuation in the impurity density within a coherence volume is

$$\Delta p \sim [\ p\ (p\text{-}1) / \xi^d\ ]^{1/2}$$

Therefore within a coherence volume the number of impurities will be $(p \pm \Delta p)\ \xi^d$. Since the transition temperature for each coherence volume depends explicitly on the number of impurities, this will lead to a spread or rounding of the transition temperature that is

$$\Delta T_c = |\ dT_c / dp\ |\ \Delta p$$

As argued by Imry and Wortis, it is incorrect to assume that each coherence volume will undergo a separate transition, as the presence of a 'new' phase in a coherence volume will create an interface between the 'new' phase and its surrounding coherence volumes that are still in the 'old' phase. Therefore there is a competition between the increase in the

free energy due to the creation of a new interface and the lowering of the free energy due to the phase change. This competition between surface and volume free energies determines the temperature range of the rounding and the spatial scale of the presence of each phase at a given temperature. Summarily, at a given temperature near $T_c(p)$, there will be coherence volumes that are in the 'other' phase. To what extent this occurs depends upon the interfacial energy, C, and the impurity density fluctuation, Δp.

Imry and Wortis did not address the question of the nature of the transition. They attempt to explain how, why, and to what extent the impurities smear the transition, but not how the system undergoes the phase transition. Is it still first order? Is the order changed? Do the 'wrong' phase coherence volumes aggregate together to minimize surface area and the system undergo a phase transition through the percolation of 'wrong' phases? Or does the system undergo a first order phase transition where the singularities are weakened but not obliterated?

We have attempted to answer this question for the specific transition of the nematic to isotropic transition of a model polymeric liquid crystal. We have found that the introduction of quenched impurities to a liquid crystalline system will

1.) Lower the transition temperature

2.) Round and lower the heat capacity peak

3.) Change the order of the transition.

These results are in agreement with the theoretical work of Imry and Wortis and extend their results to show that the introduction of impurities can change the order of the transition as well as round the singularity peak. This is in agreement of Hui and Berker who have shown that the introduction of quenched disorder can eliminate the discontinuity of a first order transition.

It should be noted that the destruction of the first order transition occurs below 2.5% impurities for the model system studied here. Further work is needed to determine whether the transition occurs at very low porosity, *i.e.* weak disorder, or at a porosity somewhere between 0.0 % and 2.5 %. The exact nature of the transition of the impure system has also not been determined. Whether the system exhibits critical behavior, the order of the transition of the impure system, and to what extent the discontinuity associated with a first order transition is eliminated are interesting questions and warrant further study.

The nematic to isotropic transition of a liquid crystal has been described as 'weakly first order', 'soft', or 'nearly second order' because the latent heat and volume changes are small at the transition and the energy required to sustain long range order is small. It should be noted that many experimental investigations that have been completed to study the effect of quenched disorder on first order phase transitions, such as the structural transitions of $RbCaF_3$,[37] $SrTiO_3$,[38] and $KMnF_3$,[39] are described as 'weakly first order'. Theoretical calculations,[24] however, indicate that "even strongly first order" transitions can be converted to second order with the introduction of quenched disorder. Clearly, a more

thorough understanding of the effect of disorder on first order phase transitions will only be found when a wider variety of phase transitions are studied.

The fact that the nematic-isotropic transition is soft seems to be an important point in the response of the system to the addition of disorder. Because the energy to sustain long range order is small, it seems reasonable that the presence of fluctuations can affect the state of the low temperature ordered phase, the high temperature disordered phase, and the transition between the two. It has been shown in this study that this indeed occurs; the fluctuations introduced into the system via the presence of defects not only shifts and rounds the discontinuity peak of the transition, but also results in a change in the order of the transition. Therefore, the mesophase transitions of liquid crystals will be susceptible to fluctuations and this must be considered when experimentally or theoretically studying the phase transitions of liquid crystals.

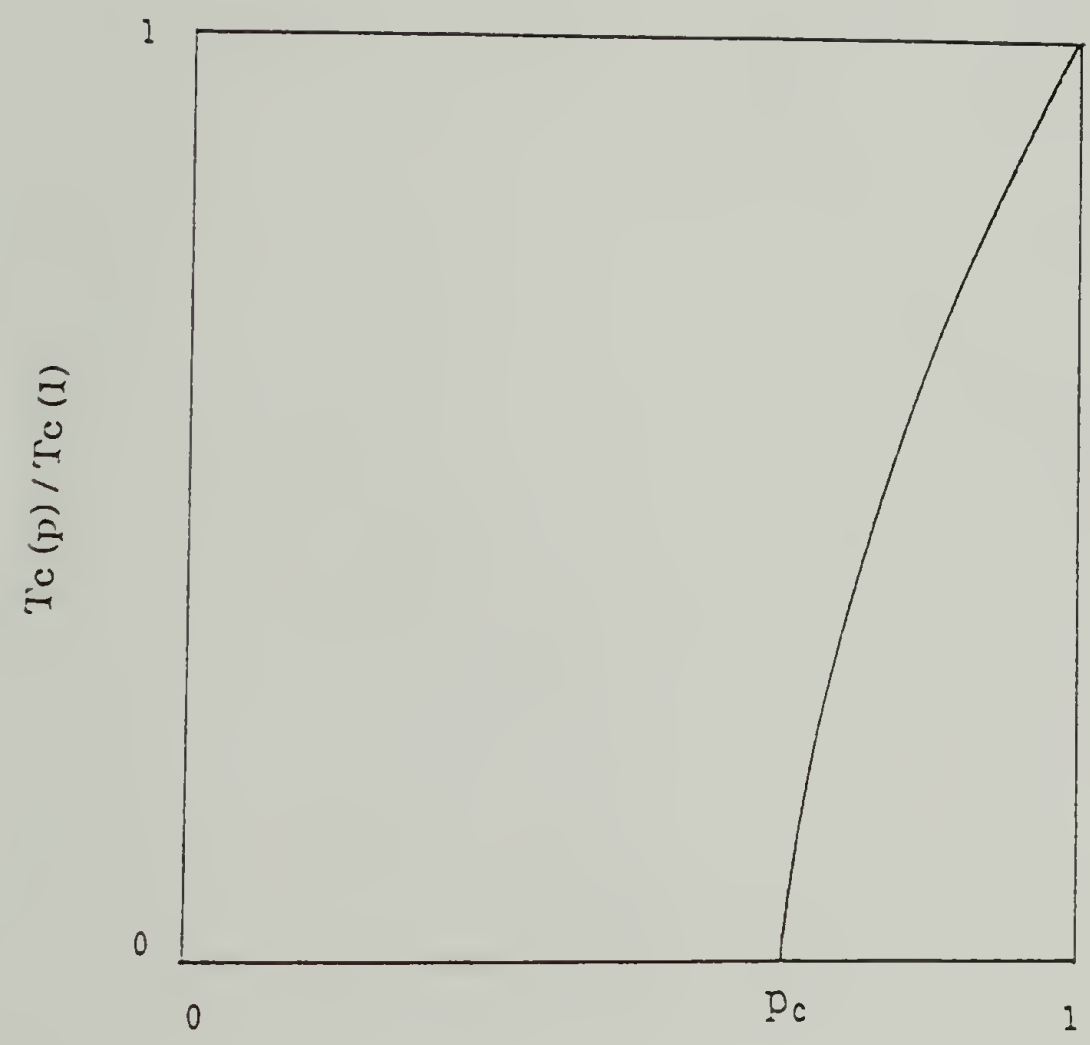

Figure 4.1 A schematic phase diagram of a magnet diluted with non magnetic atoms. The porosity is equal to one minus the impurity concentration.

Figure 4.2 The squared order parameter, S^2, as the pure system passes through the phase transition for varying sizes. **A.)** L=10 **B.)** L=13 **C.)** L=16. Tau is the reduced temperature and is defined as Tau = k_BT/e_b.

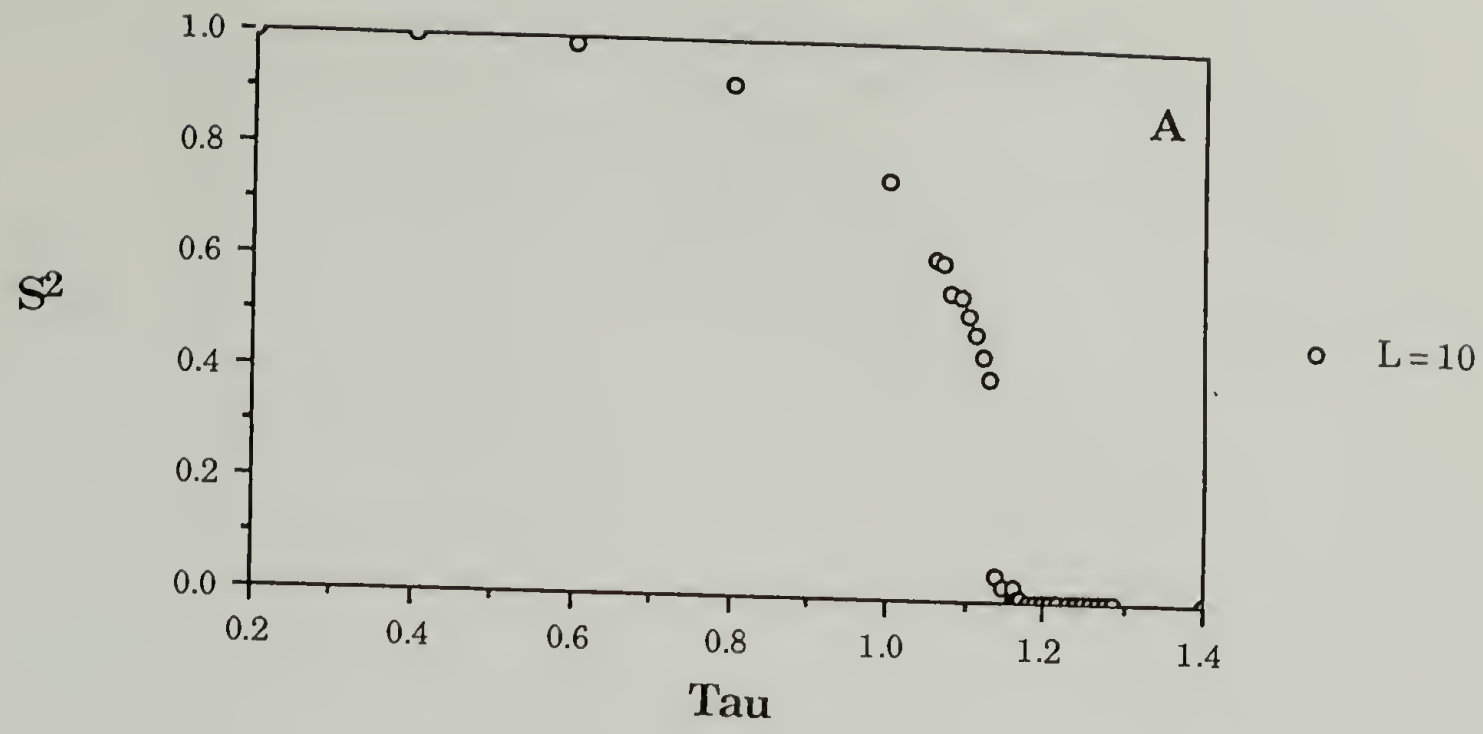
A
S2
1.0
0.8
0.6
0.4
0.2
0.0
0.2
0.4
0.6
0.8
1.0
1.2
1.4
Tau
L = 10

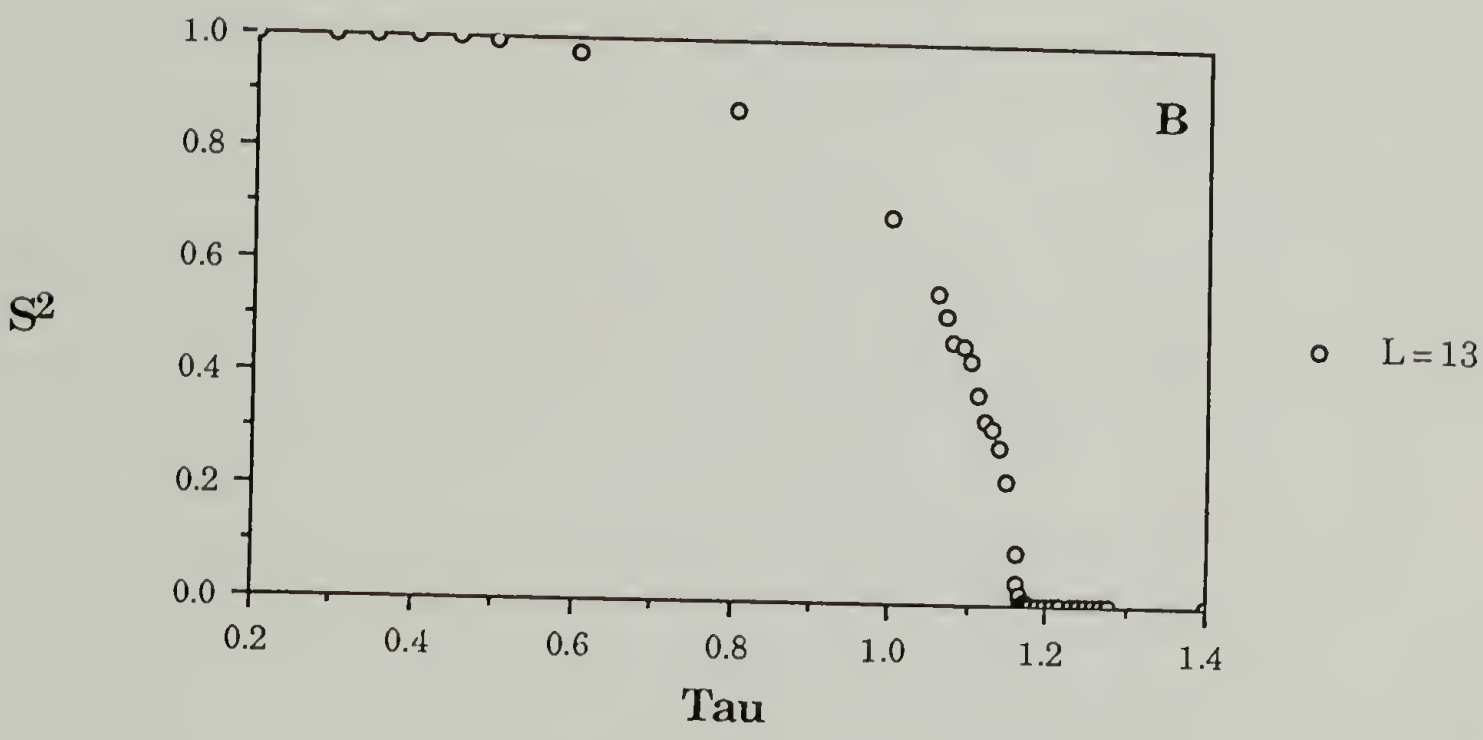
B
S2
1.0
0.8
0.6
0.4
0.2
0.0
0.2
0.4
0.6
0.8
1.0
1.2
1.4
Tau
L = 13

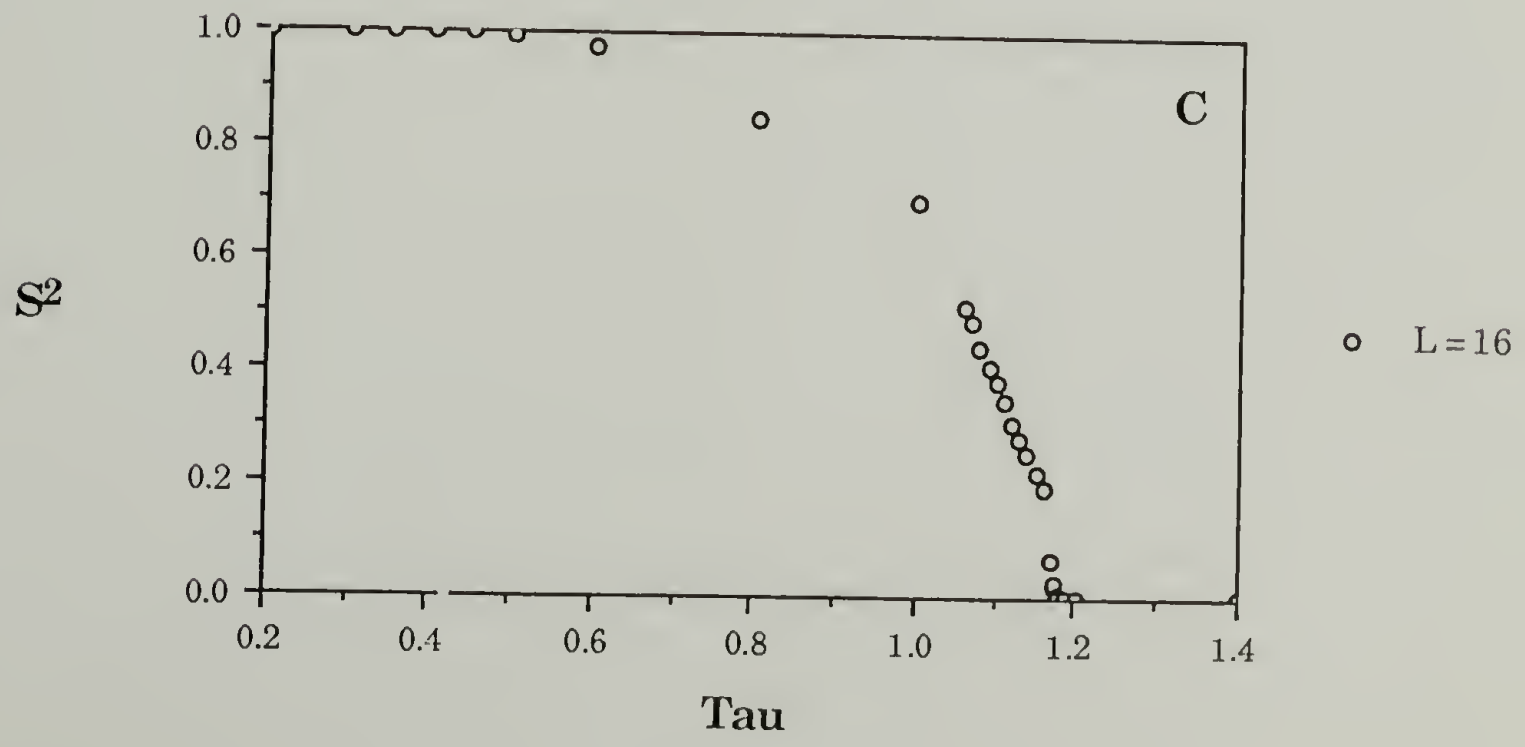
C
S2
1.0
0.8
0.6
0.4
0.2
0.0
0.2
0.4
0.6
0.8
1.0
1.2
1.4
Tau
L = 16

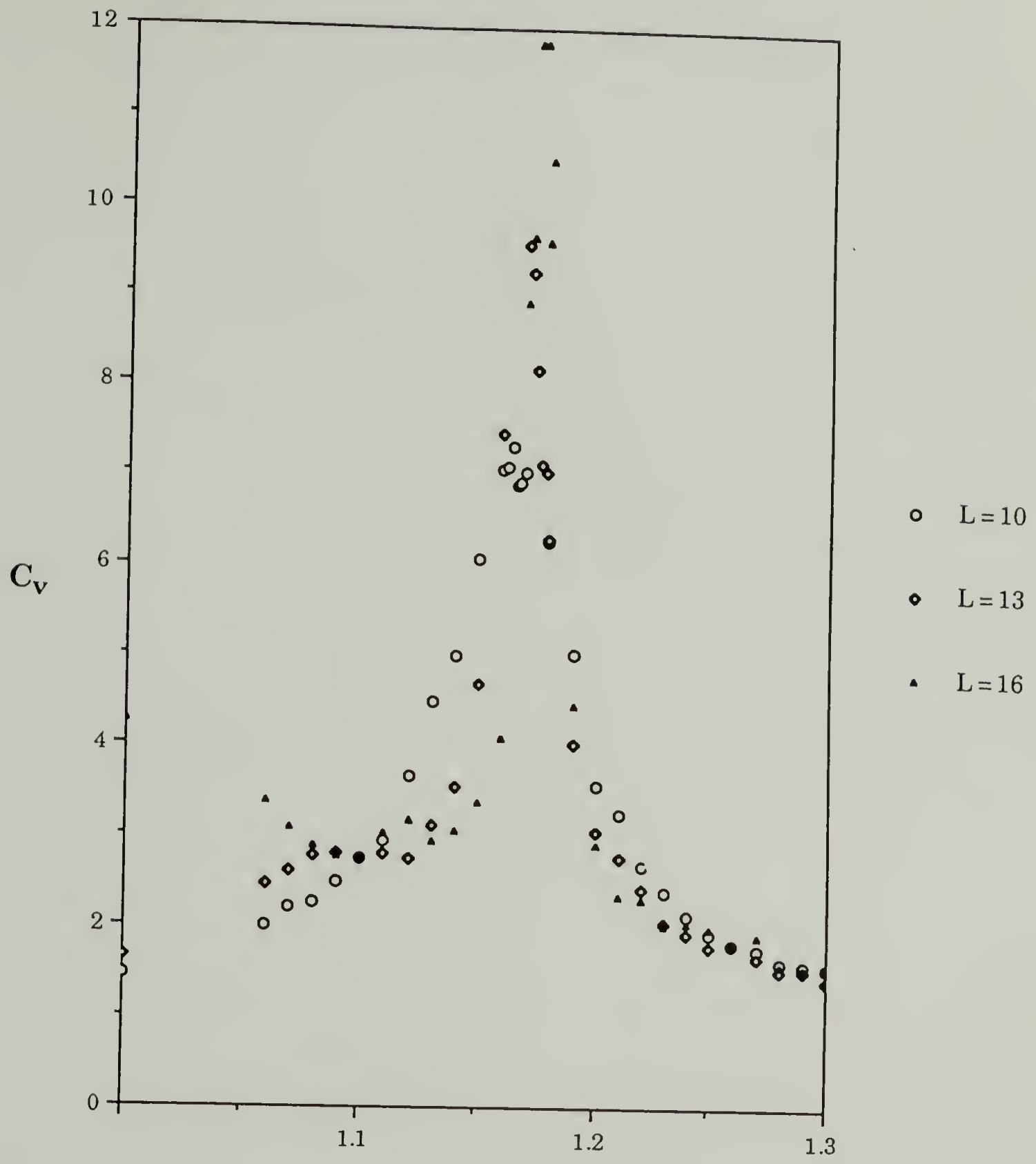

Figure 4.3 The divergence of the heat capacity near the transition for three lattice sizes, L=10, L=13, L=16 for the pure system. Tau = $k_B T/\epsilon_b$.

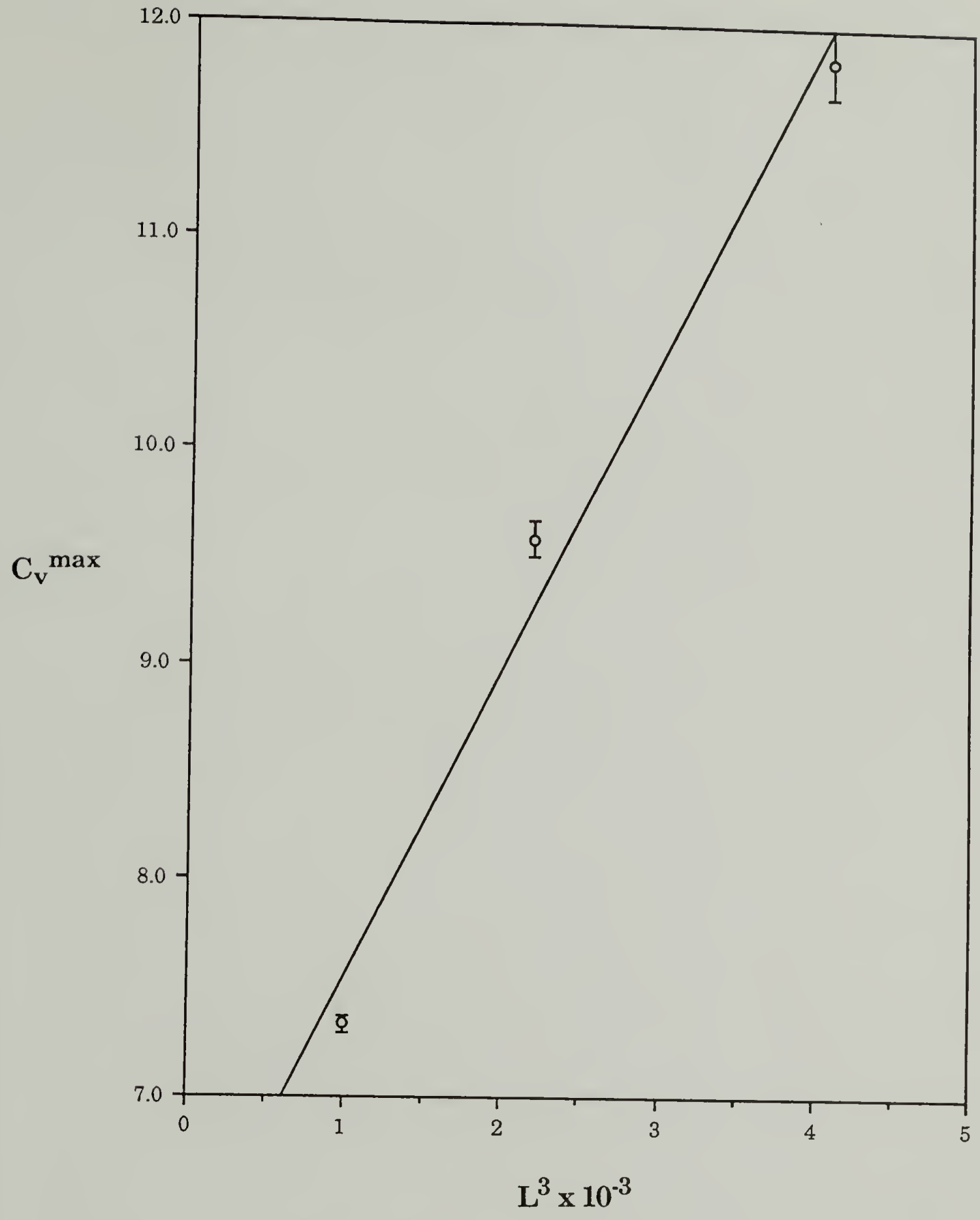

Figure 4.4 The effect of finite size on the heat capacity maximum, C_v^{max}.

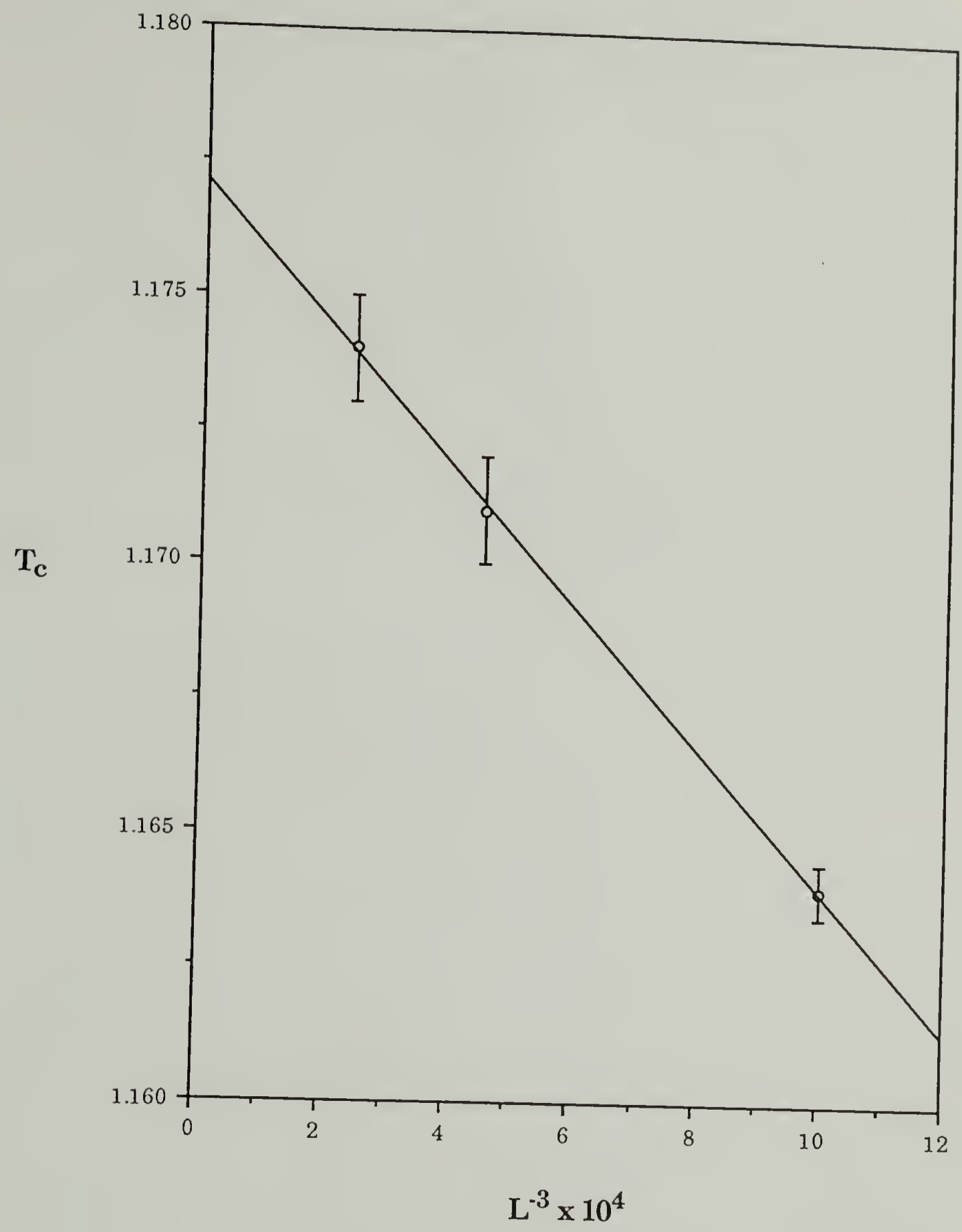

Figure 4.5 The effect of finite size on the transition temperature, T_c. The linearity of this figure and figure 4.4 denotes a first order transition.

Figure 4.6 A view of the change in the heat capacity with reduced temperature, Tau = k_BT/e_b, near the transition temperature. Plot **A** is the pure sample while **B** is for the system with 2.5% impurities, **C** is for 5.0% impurities and **D** is for the system with 7.5% impurities.

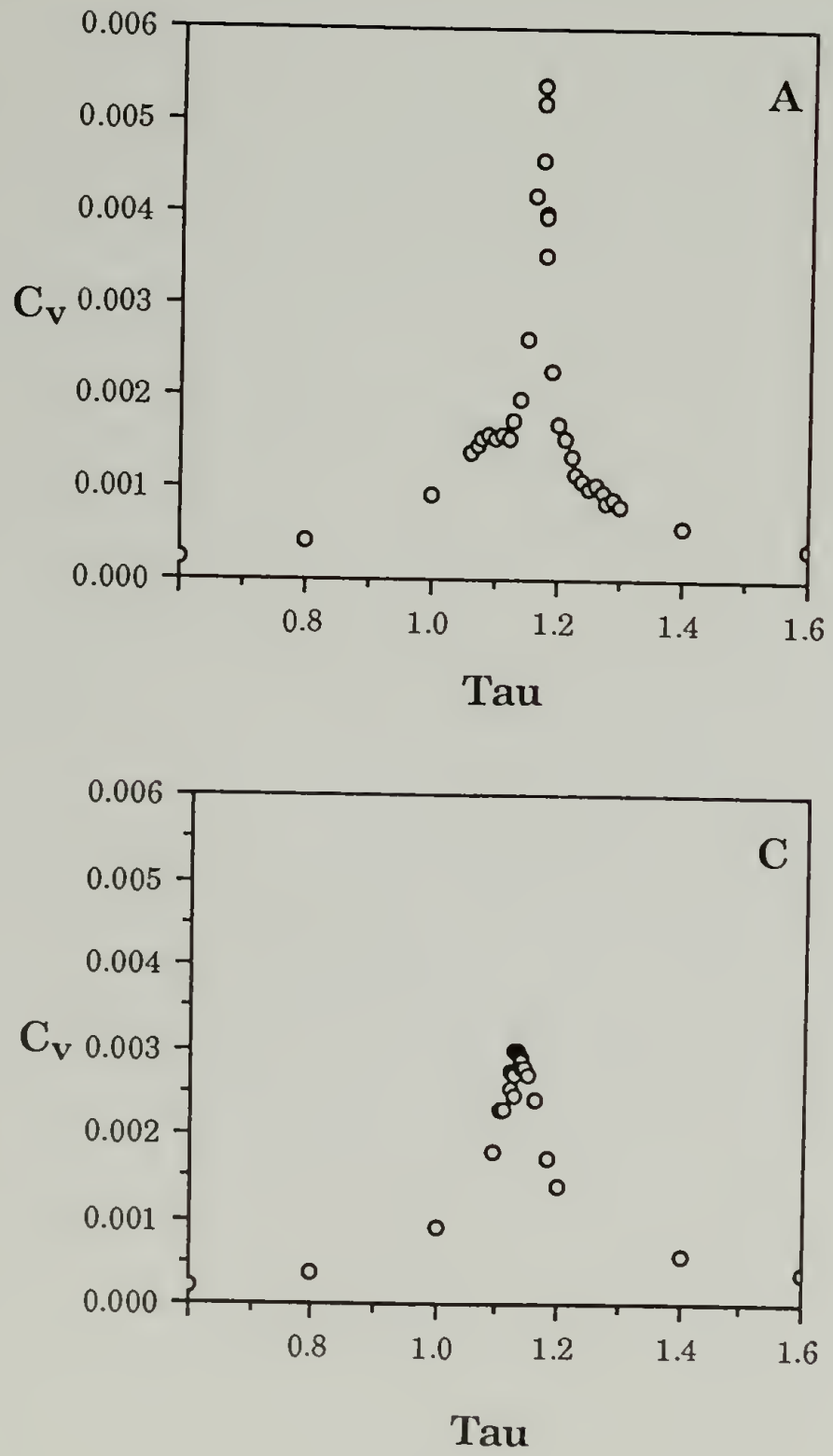

o Pure

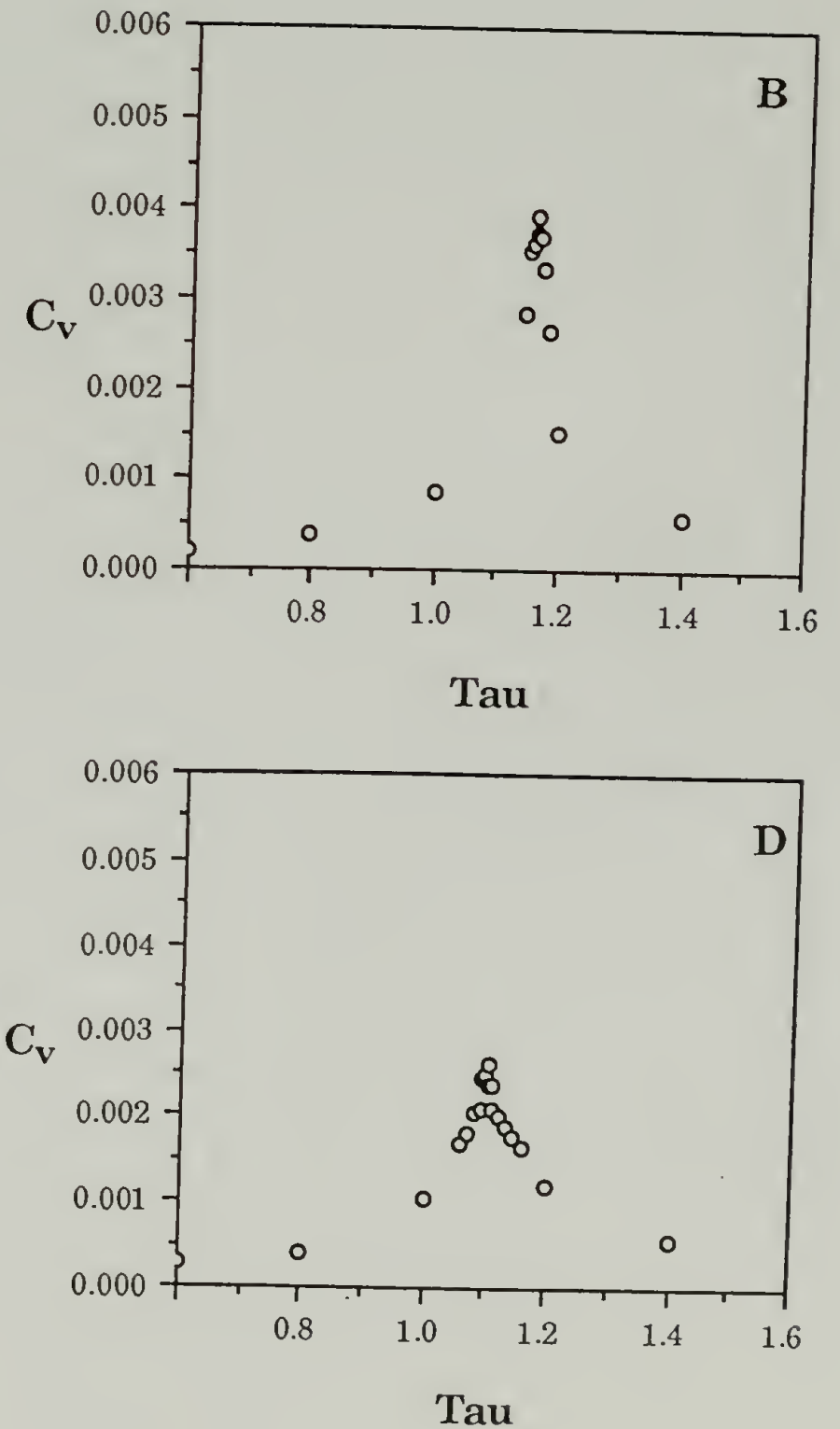

o 2.5%

o 5%

o 7.5%

Figure 4.7 The squared order parameter, S^2, as the impure systems pass through the phase transition. **A.)** 2.5% **B.)** 5.0% **C.)** 7.5%. Tau = k_BT/e_b.

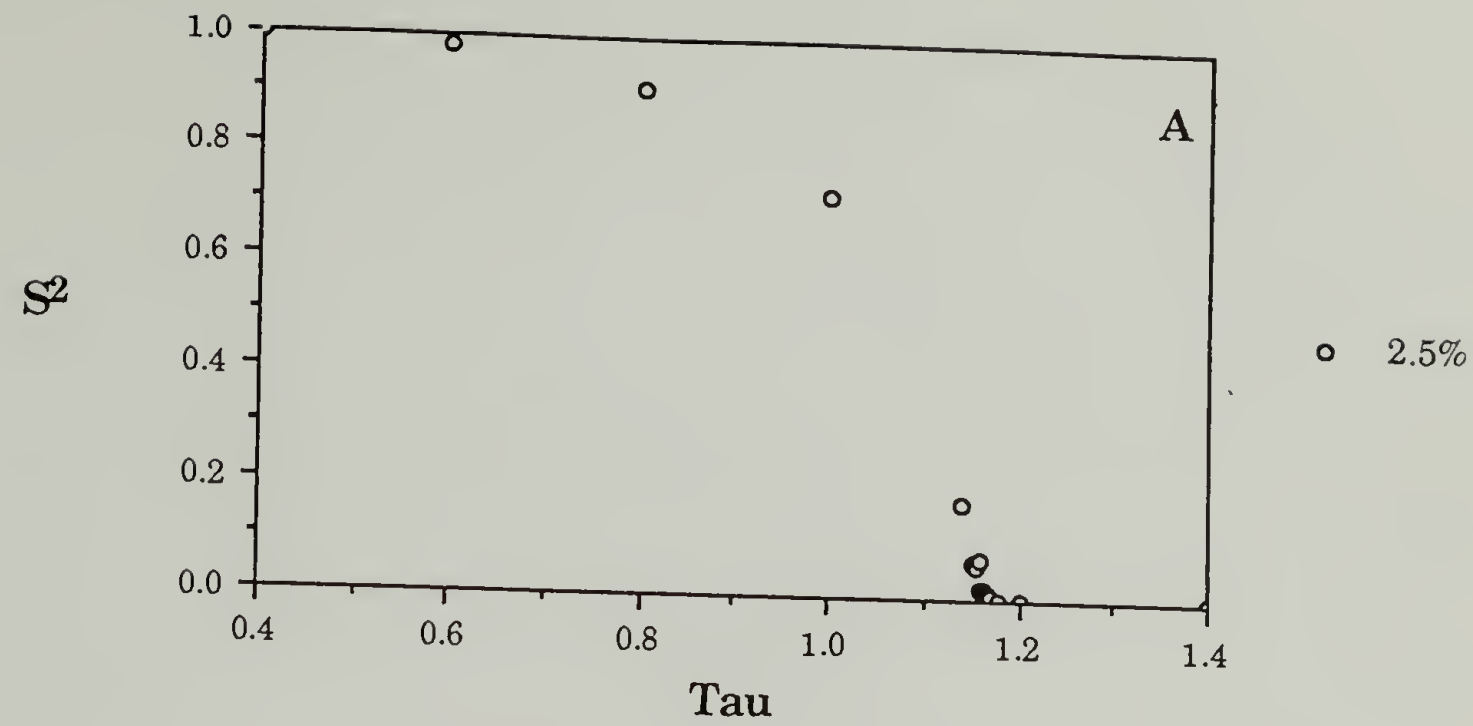
A
B
C
S2
Tau
1.0
0.8
0.6
0.4
0.2
0.0
0.4
0.6
0.8
1.0
1.2
1.4
2.5%
5.0%
7.5%

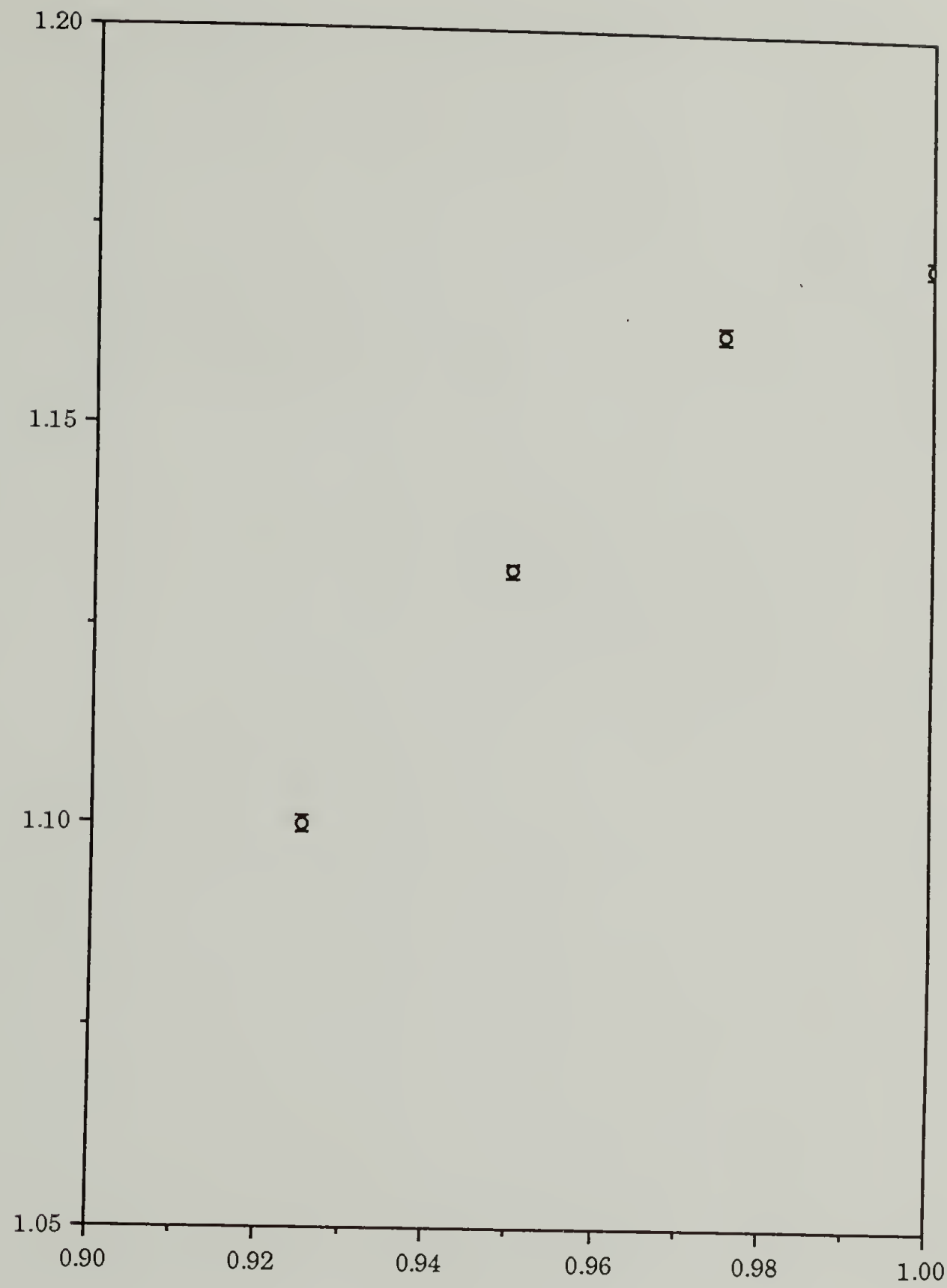

Figure 4.8 The change in the transition temperature with porosity. The system shows a linear change only in the impure region.

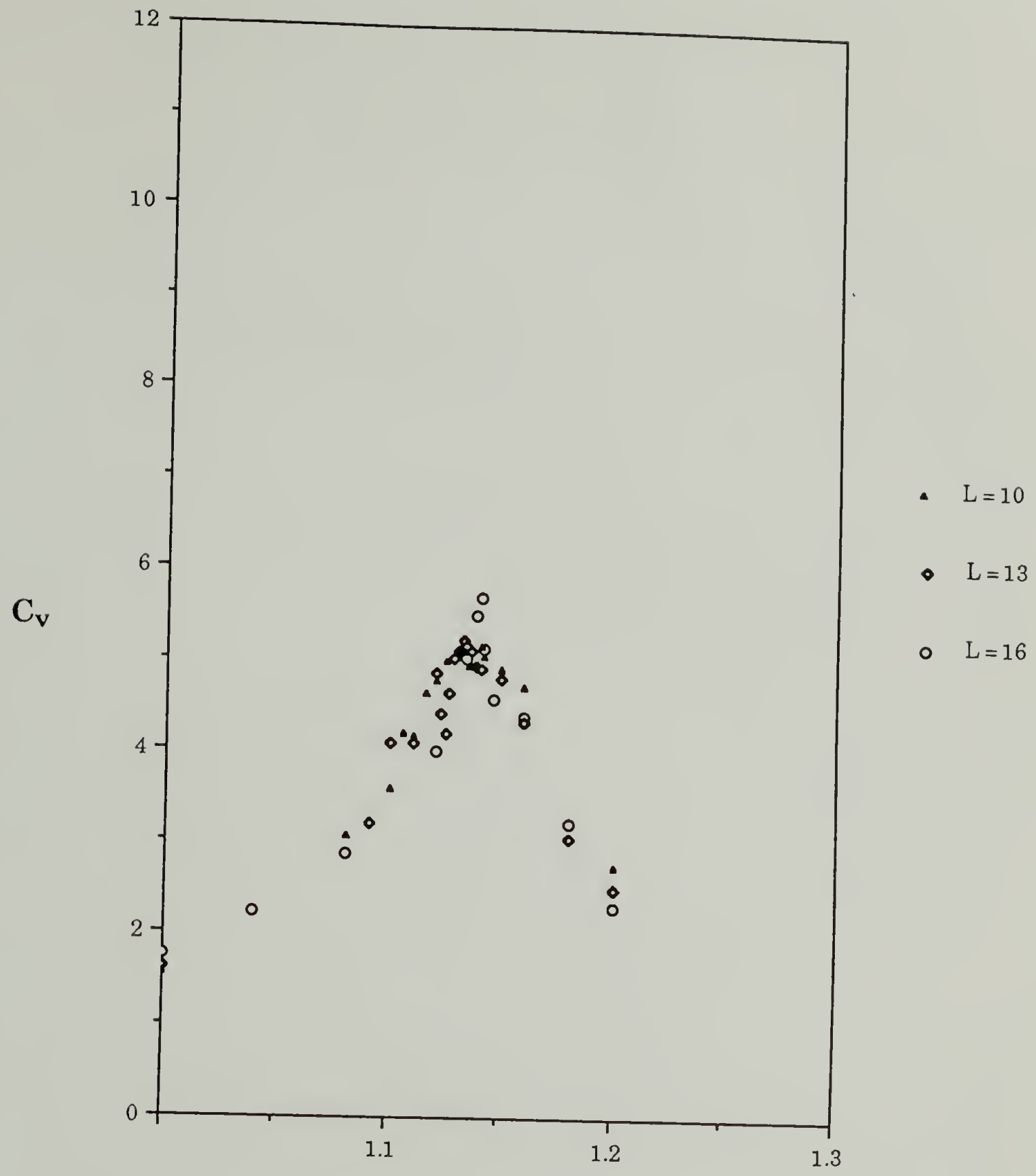

Figure 4.9 The change in the heat capacity near the transition temperature for the three lattice sizes L=10, L=13, and L=16 for the system with 5.0% impurities. Note that the axes scales are identical to Figure 4.3. Tau = $k_B T/\varepsilon_b$.

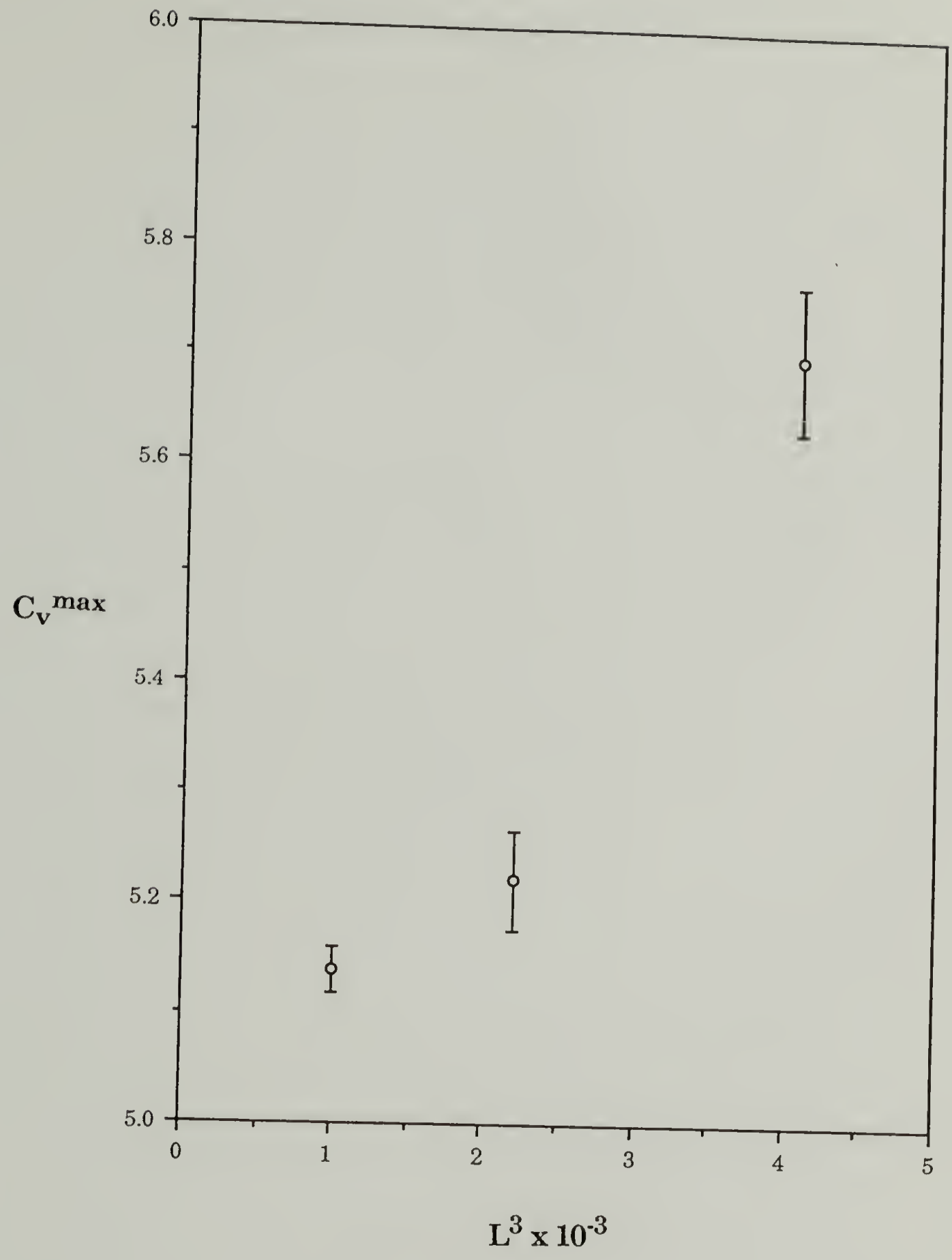

Figure 4.10 The change in the heat capacity maximum with lattice size for the system with 5% impurities.

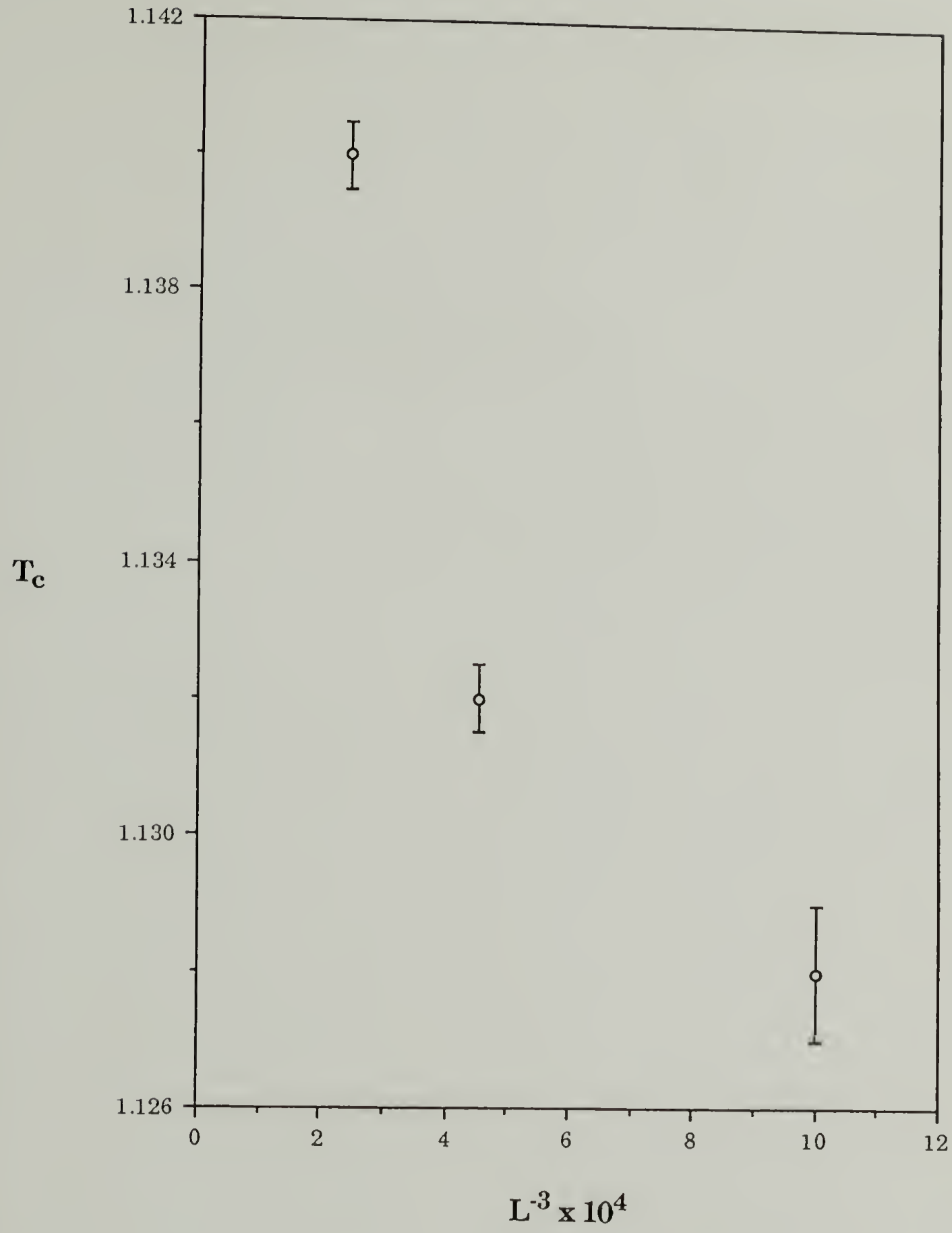

Figure 4.11 The change in T_c with lattice size for the system with 5% impurities. The non-linearity of this figure and figure 4.10 indicates that the presence of impurities changes the order of the transition.

References

1. P.J. Flory, Proc. R. Soc. London **234**, 60 (1956).

2. L. Onsager, Ann. N.Y. Acad. Sci. **51**, 637 (1949).

3. W. Maier and A. Saupe, Z. Naturforsch. Teil A **14**, 882 (1959); **15**, 287 (1960).

4. P.G. DeGennes, The Physics of Liquid Crystals, (Oxford University Press, Oxford 1974).

5. K. Binder and D. Stauffer, in Monte Carlo Methods in Statistical Physics, Ed. K. Binder (Springer Verlag, New York 1978).

6. Y. Imry and S.K. Ma, Phys. Rev. Lett. **333**, 1540 (1974).

7. A. Aharony, Phys. Rev. B **18**, 3318 (1978).

8. Y. Imry, J. Stat. Phys. **34**, 849 (1984).

9. K. Hui and A.N. Berker, Phys. Rev. Lett. **62**, 2506 (1989).

10. A.B. Harris, J. Phys. C **7**, 1671 (1974).

11. U. Krey, Z. Physik. B **26**, 355 (1977).

12. C. Domb, J. Phys. C: Solid State Phys. **5**, 1399 (1972).

13. A. B. Harris, J. Phys. C: Solid State Phys. **7**, 1671 (1974).

14. D. E. Khmel'nitskii, Sov. Phys.–JETP **41**, 981 (1976).

15. V. Wildpaner, H. Rauch, and K. Binder, J. Phys. Chem. Solids **34**, 925 (1973).

16. E. Stoll and T. Schneider, J. Phys. A: Math. Gen. **9**, L67 (1976).

17. D. P. Landau, Physica B **86-88**, 731 (1977).

18. W. Y. Ching and D. L. Huber, Phys. Rev. B **13**, 2962 (1976).

19. R.J. Birgeneau, R.A. Cowley, G. Shirane, and H. Yoshizawa, J. Stat. Phys. **34**, 817 (1984).

20. M.F. Collins, Magnetic Critical Scattering (Oxford University Press, Oxford 1989).

21. Y. Imry and M. Wortis, Phys Rev. B **19**, 3580 (1979).

22. M. Aizenmann and J. Wehr, Phys. Rev. Lett. **62**, 2503 (1989).

23. M. Aizenmann and J. Wehr, Comm. Math. Phys. **130**, 489 (1990).

24. A.N. Berker, Bull. Am. Phys. Soc. **14**, 1990 (1990).

25. A. Baumgartner, J. Chem. Phys. **81**, 484 (1984).

26. A. Baumgartner, J. Chem. Phys. **84**, 1905 (1986).

27. N. Metropolis, A.N. Rosenbluth, M.N. Rosenbluth, A.H. Teller, and E. Teller, J. Chem. Phys. **21**, 1087 (1953).

28. M.S.S. Challa, D.P. Landau, and K. Binder, Phys. Rev. B **34**, 1841 (1986).

29. H.E. Stanley, Introduction to Phase Transitions and Critical Phenomena (Oxford University Press, Oxford 1971).

30. M.E. Fisher and A.E. Ferdinand, Phys. Rev. Lett. **19**, 169 (1967).

31. M.E. Fisher and M.N. Barber, Phys. Rev. Lett. **28**, 1516 (1972).

32. M.E. Fisher and A.N. Berker, Phys. Rev. B **26**, 2507 (1982).

33. O.G. Mouritsen, Computer Studies of Phase Transitions and Critical Phenomena (Springer-Verlag, New York 1984).

34. K. Binder, in Monte Carlo Methods in Statistical Physics, Ed. K. Binder (Springer Verlag, New York 1978).

35. A.B. Harris and T.C. Lubensky, Phys. Rev. Lett. **33**, 1540 (1974).

36. T.C. Lubensky, Phys. Rev. B **11**, 3573 (1975).

37. T.W. Ryan, R.J. Nelmes, R.A. Cowley, and A. Gibaud, Phys. Rev. Lett. **56**, 2704 (1986).

38. R.J. Nelmes, P.E. Hatton, and H. Vass, Phys. Rev. Lett. **60**, 2172 (1988).

39. U.J. Cox, A. Gibaud, and R.A. Cowley, Phys. Rev. Lett. **61**, 982 (1988).

CHAPTER 5

THE NEMATIC TO ISOTROPIC TRANSITION OF A LIQUID CRYSTAL IN A POROUS MATRIX

Introduction

Liquid crystals are a unique phenomena because they exhibit a partially ordered mesophase between the (semi-) crystalline solid and isotropic liquid states.[1] Liquid crystalline polymers have had the most impact on technology because the ordering in the high temperature mesophase results in an increased intermolecular interaction in the low temperature phase and therefore they posses stronger mechanical properties. Because of their technological importance, many theoretical and experimental investigations of the mesophase transitions of liquid crystals have been completed. Original calculations due to Flory [2] and Onsager [3] demonstrated that a state of parallel order can be obtained that is due solely to the anisotropy of the molecule and steric interactions. Intermolecular interactions were of secondary importance. On the other hand, calculations by Maier and Saupe [4] show a definite phase transition from the disordered (isotropic) to ordered state (nematic) due solely to orientational (intermolecular) interactions between molecules with anisotropic polarizabilities. The realistic case is probably a combination of the two effects.

However, most theoretical and analytical calculations have centered on ideal homogeneous systems. As an ideal crystal without defects or impurities does not exist in nature, nor does a purely one or two component liquid crystalline system exist due to surfaces, impurities, and other foreign species. Disorder in real systems can take many different forms, including surfaces, grain boundaries, impurities, disclinations, or the finite size of the system. Because liquid crystals are soft, *i.e.* the energy responsible for long range order is small,[1] disorder will dramatically affect their thermodynamic properties. We are interested in the effect of disorder on the nematic to isotropic transition of a liquid crystal. We have completed the Monte Carlo experiments described in the last chapter and would now like to correlate these results with experimental data. A number of experiments were formulated and attempted before the idea of studying the isotropic–nematic phase transition of a liquid crystal in a porous media was formulated. Using differential scanning calorimetry, the N–I transition was monitored for systems confined to pores of different sizes. The results showed that the confinement of the liquid crystal to the pore did result in a change in the nematic to isotropic transition of the liquid crystal. The results also agree, qualitatively, with the Monte Carlo results as will be explained later.

It is the aim of the present work to undertake an experimental investigation in order to understand the effect of disorder on the nematic to isotropic transition. How will the liquid crystalline system respond to the introduction of disorder? To answer this, an experimental study of the nematic to isotropic transition of a liquid crystal in a controlled pore

glass (CPG) has been studied. It is expected that disorder will manifest itself as surface alignment and finite size effects. Using differential scanning calorimetry (DSC), the nematic-isotropic transition of a small molecule liquid crystal in a CPG has been monitored. The ratio of liquid crystal size to pore size, $\lambda=R_p/R_g$, is an important parameter and is expected to determine the type of disorder that affects the system. At large λ, the surface alignment should strongly affect the transition whereas at small λ finite size effects and the interruption of the ability of the molecules to correlate by confinement to separate pores should dominate.

Experimental

The liquid crystal that was used in these experiments was *p*-azoxyanisole (PAA) purchased from Aldrich and used as received. Thermodynamic parameters of PAA; nematic-isotropic transition, T_c=409 K; Heat of nematic-isotropic transition, ΔH = 0.67 cal/g.

The porous media used was a controlled pore glass for gel permeation chromatography from Electro-Nucleonics. Characteristic data of the porous glass beads used is shown in table 5.1.

Table 5.1

Characteristic Data of Porous Glass

Sample	Pore Size (Å)
CPG1	3,125
CPG2	347
CPG3	156

Each sample was scanned at a rate of 5 K/min with the DSC under nitrogen atmosphere as the sample underwent the nematic to isotropic transition. Each sample was then allowed to anneal at 398 K for 2 hours and then cooled. DSC curves were completed again and compared to the previous thermogram. This process was repeated for each sample until there was no visible change in the DSC curve with further annealing. This method proved satisfactory for all samples but CPG3, the sample with the smallest pore size. It was necessary to anneal this sample at 415 K, above the isotropization temperature, to allow the liquid crystal to diffuse into the small pores. The slow diffusion process allowed us to monitor not only the effect of the pore size on the transition, but also the effect of the amount of liquid crystal in the pores on the transition.

Results

Figures 5.1 through 5.5 show the results of the experiments. Figures 5.1 to 5. 4 are the final DSC thermograms for the four samples. All systems have been annealed so that the equilibrium state has been achieved. In figure 5.1, PAA in the free state shows a sharp peak near the previously reported bulk nematic to isotropic transition with a heat of transition that is similar to the literature enthalpy. As the liquid crystal is confined to the pores, the transition temperature is shifted and the peak is rounded. For the largest pore size, CPG1, figure 5.2, there is an increase in the transition temperature, ΔT=0.2 K and the heat of transition is equal to that of the pure sample. As the pore size and λ decreases, there is a depression of the transition temperature and the heat of transition is less than that of the pure sample. This can be seen in figures 5.3 and 5.4 Note that the ordinate scale in figure 5.4 is shifted.

Figure 5.5 shows the DSC curves for CPG3 at different annealing times. At short times, two peaks are seen. One peak, P2, is at a temperature that is slightly higher than the bulk transition temperature while the other, P1, is slightly lower. As the sample is annealed, P1 grows as P2 diminishes. This continues until in the final state, only P1 remains.

Discussion

Disorder can manifest itself in many ways in real systems and there have been many investigations into the effect of disorder on phase transitions. The effect of one type of disorder, surface alignment, on the

nematic to isotropic transition (N-I) of a liquid crystal has been extensively studied theoretically [5,6] and experimentally.[7-10] The first theoretical work of surface alignment effects on the phase transitions of a liquid crystal was done by Sheng.[6] In this work, the N-I transition of a thin liquid crystalline film was studied. Using the Landau-Degennes theory[1,11] for the free energy density of a liquid crystal, the effect of the thickness of surface aligned thin films was calculated for the N-I transition. By adding a surface potential to the free energy, Sheng showed that the N-I transition temperature will increase as the film thickness decreases until a critical thickness, D_c, is reached. For thicknesses below D_c, the first order N-I phase transition should become continuous. One assumption of this calculation is that the liquid crystal is strongly anchored at the surface wall. Sheng has extended this work[5] by varying the substrate-liquid crystal interaction parameter, g, to include strong and weak surface anchoring. Sheng showed that different regimes exist, each depending on the strength of the interaction parameter. His conclusions included the formation of a 'paranematic' phase analogous to the 'paramagnetic' phase in magnetic systems, a boundary layer phase transition separate from the bulk transition, as well as a three-dimensional g-D-T phase diagram between the nematic, paranematic and isotropic phases. The existence of a separate boundary layer phase transition has been experimentally verified.[7]

Therefore, one type of disorder, surface alignment or surface induced order is expected to raise the transition temperature of an order to disorder transition. This is because there exists a boundary layer that is more ordered than the bulk. This boundary layer will cause an elastic

strain energy as the molecular orientation varies from the bulk value to the boundary value. This additional energy will result in a raising of the transition temperature as more thermal energy is needed to overcome the additional ordering. The temperature increase of the nematic to isotropic transition due to surface alignment of a liquid crystal has been calculated by Sheng[5,6] to be of the order 0.1 to 0.3 K.

Surface tension is also another factor that can change the transition temperature of an order-disorder transition. Over a century ago Thomson[12] deduced the equation that describes the change in the melting temperature of a solid with the radius of a spherical particle.

$$\Delta T = \sigma T_m / R \Delta H \rho$$

where σ is the interfacial surface tension between the two phases, T_m is the melting temperature, R is the radius of the sample, ΔH is the enthalpy of the transition, and ρ is the density of the ordered phase. This equation can be adapted to the nematic to isotropic transition to estimate a temperature depression due to surface tension. Using the values σ = 0.02 erg/cm^2 [13], R = 200 Å, T_{ni} = 408 K, ρ = 1 g/cm^3, and ΔH = 0.67 cal/ g, the change in temperature is expected to be 0.145 K. Even with the smallest pore size, the depression is only expected to be approximately 0.2 K.

The effect of finite size, surface tension and impurities on the N-I transition of a liquid crystal has been less studied. Whereas surface alignment is expected to raise the isotropization temperature, these effects are expected to lower the transition temperature. Many experimental studies have been completed on liquid crystals in confined

spaces, but no attempt has been made to separate the different types of disorder. Both the solid-nematic (S-N) and nematic to isotropic (N-I) transitions have been studied in finite systems.[8,9,14,16] Thin films[14] and cylindrical pores[8,9,15] have been used as model finite systems. In all cases a decrease in the S-N transition with a decrease in characteristic size was observed. The effect of disorder on the N-I transition is less well understood. Some studies[8,10,14,16-18] show a decrease in the N-I transition temperature with characteristic size while others show an increase.[7,9,15] Model finite systems in these studies include porous media, thin films, and polymer dispersed liquid crystalline droplets.

Sheng *et. al.*[19] have studied the effect of finite size on the melting transition. Using positional disorder theory, it was shown that the specific heat of a small, finite cluster of molecules will peak at a temperature lower than the bulk transition temperature and the peak will be broadened. Their calculations served to explain experimental results of a variety of adsorbate systems such as H_2O in porous Al_2O_3. As both the melting and nematic-isotropic phase transitions are first order transitions, if poorly correlated domains exist it is expected that there will be similar finite size effects on the nematic to isotropic transition of a liquid crystal as seen in the melt transition.

Also, if the characteristic size of a system is less than 1 μ, it is not reasonable to invoke the thermodynamic limit and the finite size of the system will alter the phase transition. The effect of finite size on phase transitions and critical phenomena have been studied extensively theoretically. The finite size will shift the transition temperature and round the divergence of the heat capacity for both first and second order

transitions, but for separate reasons. In second order phase transitions the shift of heat capacity peak is due to the limitation of the correlation length to the lattice size, L. Scaling theory therefore[20,21] predicts that the heat capacity maximum, C_v^{max} will diverge as $L^{\alpha/\upsilon}$ while the transition temperature will shift as

$$T_c - T_c^* / T_c^* \sim L^{1/\upsilon}$$

where T_c is the transition temperature of the finite system and T_c^* is the transition temperature of the infinite system.

In first order phase transitions the lattice size dependence is in the form of the volume, L^d. The finite size of the system affects the transition only when the coexisting phases reach the extent of the volume of the lattice. Scaling theory[22,23] then predicts that C_v^{max} will diverge as L^d while the transition temperature will shift as

$$T_c - T_c^* / T_c^* \sim L^{-d}.$$

Unfortunately there is no *a priori* way to determine the direction of the temperature shift. Some transitions are shifted up in temperature while others will be shifted down. The reason for this is still one of the unanswered questions of finite size analysis. Sheng *et al*[19] have studied the effect of finite size clusters on the melting temperature. Using positional disorder theory, they found that a system of small finite clusters will undergo a first order phase transition at an earlier temperature than the bulk sample. Therefore a group of poorly correlated domains will each undergo a phase transition at a temperature below the bulk transition temperature separately, and this

will be manifested as a rounding of the peak in the heat capacity and a decrease in transition temperature. Summarily, an interruption of the ability of the molecules to correlate will result in a lowering of the transition temperature.

Therefore, surface alignment will serve to increase the temperature of the nematic to isotropic phase transition while surface tension will result in a lowering and finite size effects can lower or raise the transition temperature, but the interruption of the correlation of the molecules will result in the system passing through the phase transition at an earlier temperature than the bulk. There exist many other forms of disorder including an applied external field, impurities, and disclinations but it is believed that the observed results can be explained with finite size effects, surface alignment and maybe surface tension.

In order to demonstrate this, examine figure 5.6 This is a sketch of a liquid crystal confined to pores. Figure **A** is an example of the liquid crystal inside a large pore, while **B** is an example of the liquid crystal in a pore that is only slightly larger than the liquid crystal itself. In the first case, there is a surface alignment that causes a boundary layer that is more ordered than the bulk. In this system, the boundary layer experiences a stronger ordering force than the rest of the sample while the rest of the sample experiences little different from the bulk except an elastic strain due to the boundary layer. In the latter case, the ability for the "domains" to correlate in the radial direction is diminished as the pore size decreases. Also, the director within each pore will average to the direction of that pore. As these glasses are created through spinodal decomposition, it is expected that the pores will be a set of interconnected

'tunnels' that are distributed isotropically. Therefore, the director in one pore will, on average, have a different direction than the director in its neighboring pores. Due to this, in the latter system there exists a group of uncorrelated domains or subsystems. If this is the case in our system, how could it explain the observed results?

In figure 5.2, it is seen that for the system with pore size 3,125 Å, λ = 210, there is an increase in the T_{ni} of 0.2 K. For this λ, figure 5.6A is pertinent, *i.e.* there exists an ordered boundary layer and a bulk regime. As the transition is approached, the bulk becomes less ordered and the boundary layer remains ordered. Additional thermal energy is needed to break the boundary layer ordering. The observed heat of transition can also be understood with this explanation. Though additional thermal energy is needed to send the system throught the nematic to isotropic transition, the whole system undergoes the transition, even the boundary layer.The heat of transition is, therefore, equal to that of the pure sample. This serves well to explain observed results. The most compelling fact for this argument is that the magnitude of the temperature shift is in agreement with Sheng. (ΔT_{Exp} = 0.2 K ; ΔT_{Theory} = 0.1 to 0.3 K).

In figure 5.3 the thermogram shows that the transition is depressed 0.77 K. In this system, the pore size is 347 Å, λ = 23. In this case fig 5.6B is relevant. It seems reasonable that the finite size of the system should be important. If this is true then there will exist a group of uncorrelated domains where each will undergo the phase transition separately. In a first order transition, as the transition temperature is approached, the system begins to fluctuate between stable and metastable states. These metastable regions will grow until, at the transition

temperature, the energy difference between the stable and metastable states becomes negligible and they become one to form the new high temperature phase. In this case the metastable regions can only grow to the size of the subsystem and the phase transition will be completed at a lower temperature. The smaller subsystems will undergo the transition sooner, the larger ones later. This causes a smearing of the phase transition that will manifest itself as a broad peak at a lower temperature on the DSC curve. This is what is seen in figure 5.3 Figure 5.4 is an even more graphic example of this for the system with a pore size of 156 Å, λ = 10. In this system, the finite size and small pore size will create more, smaller clusters that will be more poorly correlated. This manifests itself as a larger decrease in the transition temperature and a larger broadening of the discontinuity peak. The decrease in the heat of the transition of these samples can also be explained with this logic. According to this explanation, the system consists of a group of uncorrelated domains that each undergo the transition separately. These domains do join together, however. As is illustrated in figure 5.6, the area where two or more pore, or domains, connect will be disordered due to the convergence of two or more directors. Being disordered, this interdomain region can not form the nematic structure and therefore can not undergo the nematic to isotropic transition. This small region will undergo a solid to isotropic transition at the melting temperature. The heat of the isotropic to nematic transition of these samples is lowered because only a portion of the PAA is undergoing the nematic to isotropic transition. From the observed results it can be seen that 84% of the liquid crystal undergoes the N–I transition while only 40% of the PAA is able to undergo the transition for sample CPG3.

This result agrees, qualitatively, with the results of the Monte Carlo simulation described in chapter 3. In that experiment, the interruption of the ability for the liquid crystal to correlate over the whole system resulted in the depression of the transition temperature and the rounding of the heat capacity peak. In this experiment, the liquid crystal can not correlate over a large length scale because of the presence of the porous glass and the result is a depression of the transition temperature and a rounding of the heat capacity peak. Though the extent and method of the interruption of the correlation of the molecules differs in the two experiments, the results are the same and lends strength to the argument that the presence of fluctuations and perturbations will strongly affect the nematic to isotropic transition of a liquid crystal.

Surface tension may also contribute to the change in the transition temperature in each of the systems. But as stated before, the lowering of the transition temperature due to surface temperature will range from 0.1 K to 0.2 K, depending on the pore size. For CPG1, it seems that there is not enough surface tension to affect the transition as an increase, not a decrease is seen. Even if it does have an effect , the calculated value for the temperature decrease due to surface tension from the Thomson equations is 9.28×10^{-03} K, an order of magnitude less than the observed increase. As the pore size gets smaller it is expected that the surface tension effects will become more important. On the other hand, as the system becomes smaller, finite size effects result in the coexistence of uncorrelated regimes, become important, and overshadows both surface alignment and surface tension effects. This can be seen as the transition temperature decreases for the smaller pore sizes. The decrease due to

surface tension as calculated from the Thomson equation will only reach values of 0.08 K and 0.018 K for samples CPG2 and CPG3 respectively. Therefore, though surface tension may play a minor role in the shifting of the transition temperature, its effect on the phase transition in this system is negligible.

The evolution of figure 5.4 is also an interesting study. Figure 5.5 shows a history of the phase transition as the sample is annealed. After a very short annealing times, two peaks are seen in the thermogram. If two peaks are seen in the melting of a crystalline substance by DSC, it is concluded that two different crystal structures coexist. By analogy, two different liquid crystalline regions must coexist. Using previous arguments, we believe that there exist two regions; 1. Inside the pores 2. Outside the porous glass in a semi-infinite film on its surface. The logic of this explanation is as follows, P1 is lower than the bulk transition temperature, while the other P2 is slightly higher. Therefore, P1 must represent liquid crystal that is confined to the pores while P2 represents liquid crystal that is surface aligned. As the system is annealed, more liquid crystal penetrates the pores and peak P1 grows at the expense of peak P2. Finally we see a single peak as the liquid crystal completely penetrates the pores at the longest annealing time.

Conclusion

We have presented a study of the effect of surface alignment and finite size on the nematic to isotropic transition of a liquid crystal. It was shown that, at large pore sizes (~ 3000 Å), alignment by the surface will cause the creation of a boundary layer that causes an increase in the

transition temperature T_{ni}. As the pore size gets smaller, the surface effects are overshadowed by the finite size of the system. The finite size serves to create uncorrelated domains that cause a lowering of the transition temperature and broadening of the heat capacity peak.

We also have seen the simultaneous presentation of surface and finite size effects on the nematic to isotropic transition of the liquid crystals as the evolution of the confinement to the porous media occurs. In the smallest pore size, two regimes exist at small annealing times as manifested by the two peaks in the DSC curve. We conclude that the two regimes consist of a constrained regime inside the pores while the other is a semi-infinite layer on the outside surface of the porous glass. As the liquid crystal penetrates the pores, the lower temperature peak grows at the expense of the high temperature peak demonstrating the penetration of the pores by the liquid crystal. This system demonstrates the unique characteristics of identification and examination of different types of disorder simultaneously. Hopefully this result will encourage the further study of the effect of disorder on phase transitions.

We have found that the introduction of disorder to a liquid crystalline system will result in a dramatic change in the nematic to isotropic phase transition, not only a shifting of the transition temperature but also a rounding of the discontinuity peak. This is in agreement with the results of the Monte Carlo simulation that show that the presence of impurities will decrease the transition temperature, round the heat capacity peak, and change the order of the phase transition from first order to continuous. The results of this experiment are not precise enough to determine if the rounding is only partial *i.e.* it

is still a first order transition, or complete, *i.e.* it is a continuous transition. It seems that liquid crystals are very susceptible to the introduction of perturbations and this must be considered when studying liquid crystals experimentally or theoretically. From this, it can also be concluded that liquid crystals may be an ideal model system to study the effect of heterogeneity on phase transitions. Hopefully, this will lead to a better understanding of the nature and response of the phase transitions of liquid crystals.

Figure 5.1 The DSC thermogram for fully annealed pure PAA.

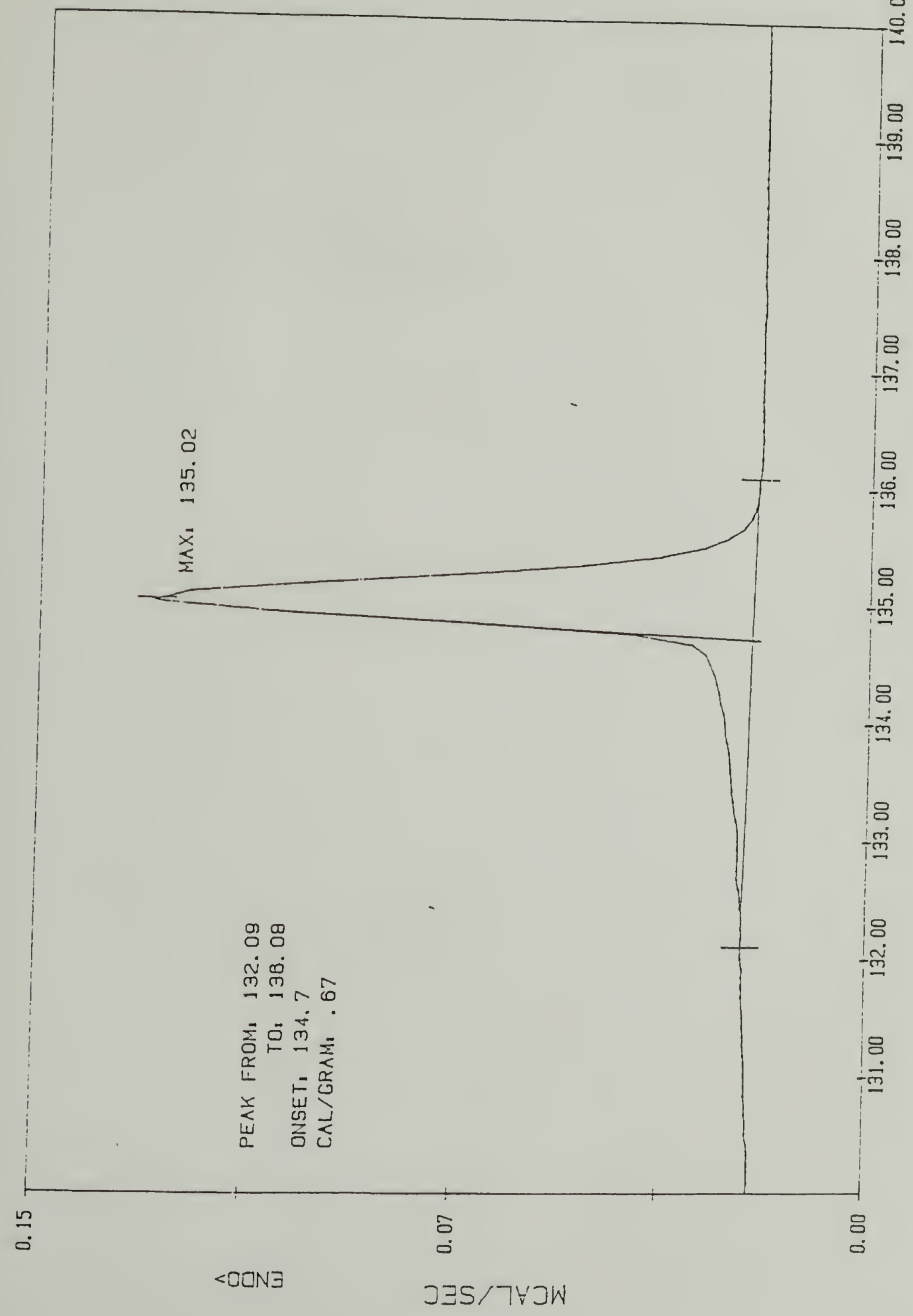
MAX: 135.02
PEAK FROM: 132.09
TO: 138.08
ONSET: 134.7
CAL/GRAM: .67
0.15
0.07
0.00
MCAL/SEC
ENDO>
135.00
136.00
137.00
138.00
139.00
140.00
131.00
132.00
133.00
134.00
TEMPERATURE (C)

Figure 5.2 The DSC thermogram for fully annealed system PAA in CPG1, pore size 3,125 Å.

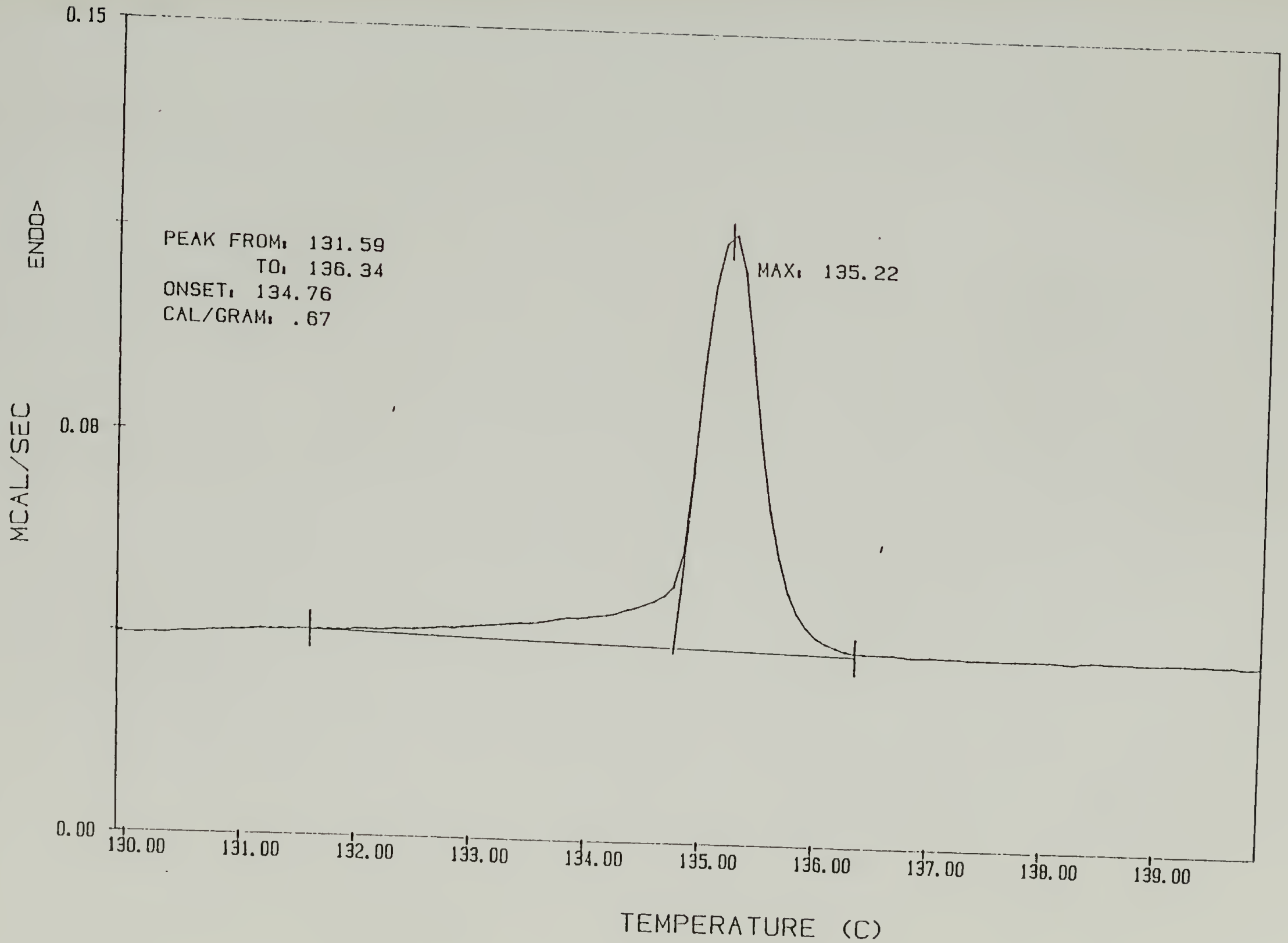
0.15
ENDO>
PEAK FROM: 131.59
TO: 136.34
ONSET: 134.76
CAL/GRAM: .67
MAX: 135.22
MCAL/SEC
0.08
0.00
130.00
131.00
132.00
133.00
134.00
135.00
136.00
137.00
138.00
139.00
TEMPERATURE (C)

Figure 5.3 The DSC thermogram for fully annealed system PAA in CPG2, pore size 347 Å.

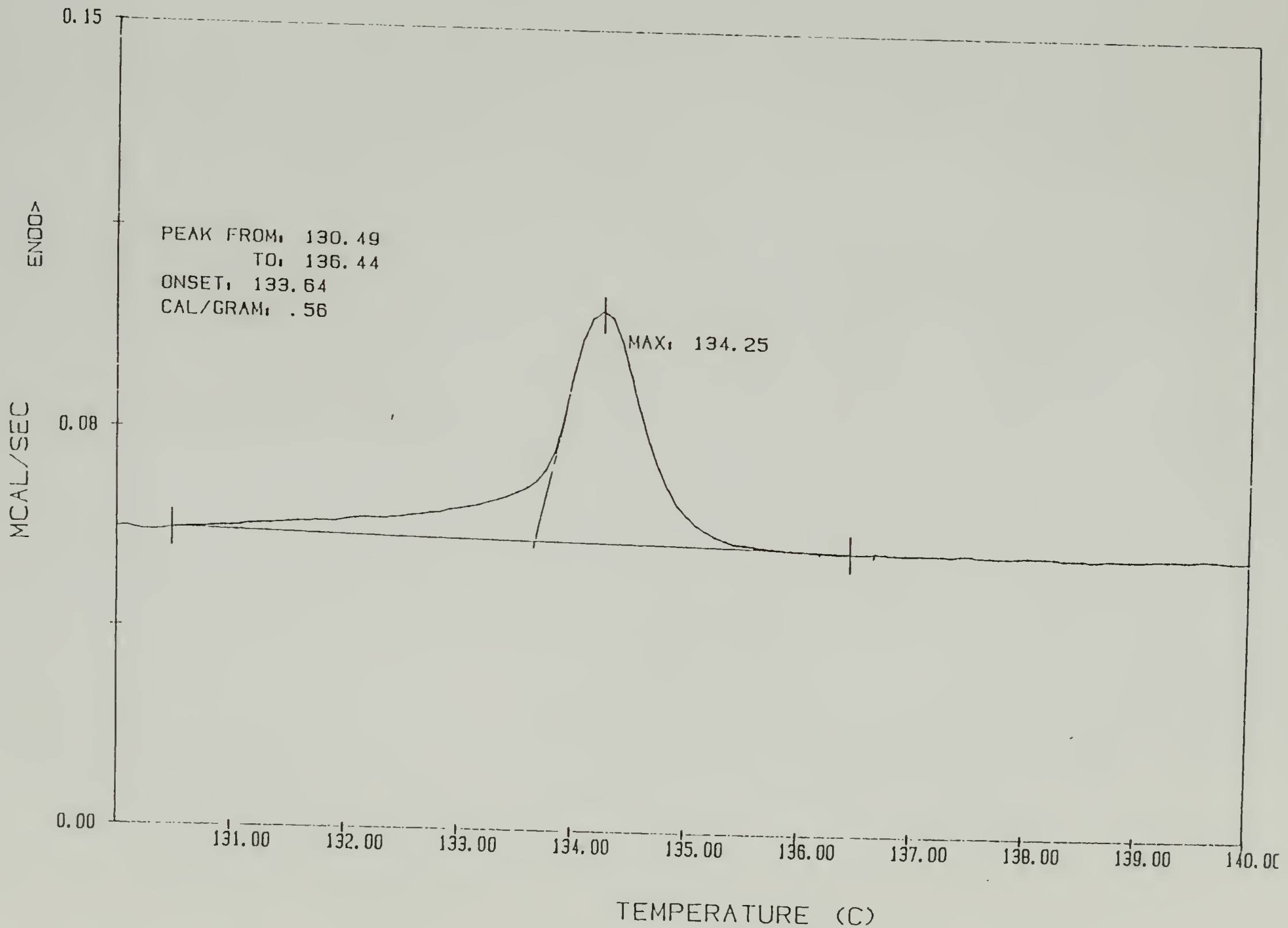
0.15
0.08
0.00
ENDO>
MCAL/SEC
PEAK FROM: 130.49
TO: 136.44
ONSET: 133.64
CAL/GRAM: .56
MAX: 134.25
131.00
132.00
133.00
134.00
135.00
136.00
137.00
138.00
139.00
140.00
TEMPERATURE (C)

Figure 5.4 The DSC thermogram for fully annealed system PAA in CPG3, pore size 156 Å.

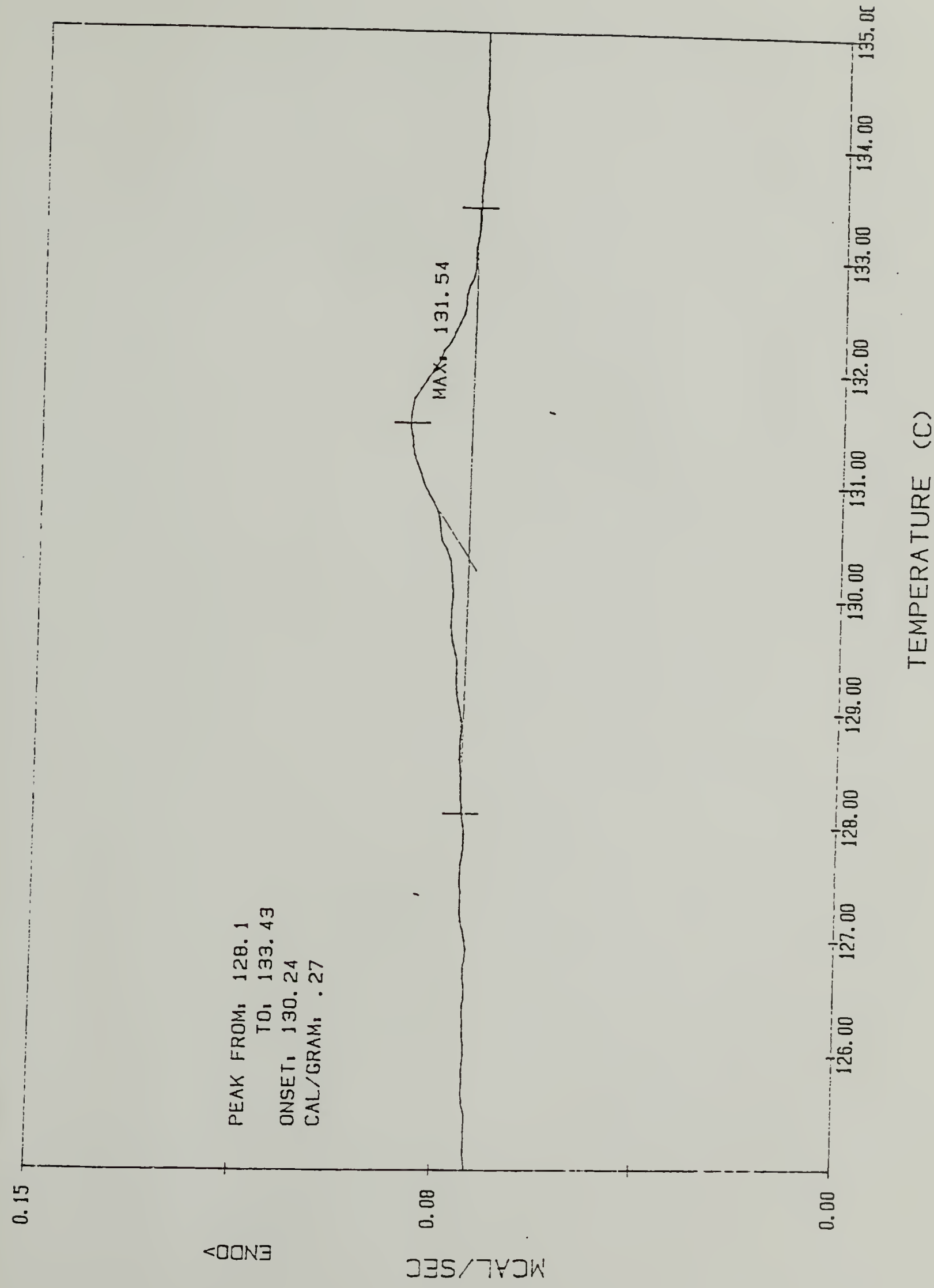
ENDO▽
0.15
0.00
MCAL/SEC
PEAK FROM: 128.1
TO: 133.43
ONSET: 130.24
CAL/GRAM: .27
MAX. 131.54
126.00
127.00
128.00
129.00
130.00
131.00
132.00
133.00
134.00
135.00
TEMPERATURE (C)

Figure 5.5 DSC thermograms for PAA in CPG3, pore size 156 Å at different annealing times. A) 2 Hours, B) 4 Hours, C) 26 Hours, D) 74 hours, E) 5 Days, F) 8 Days, G) 10 Days, H) 16 Days.

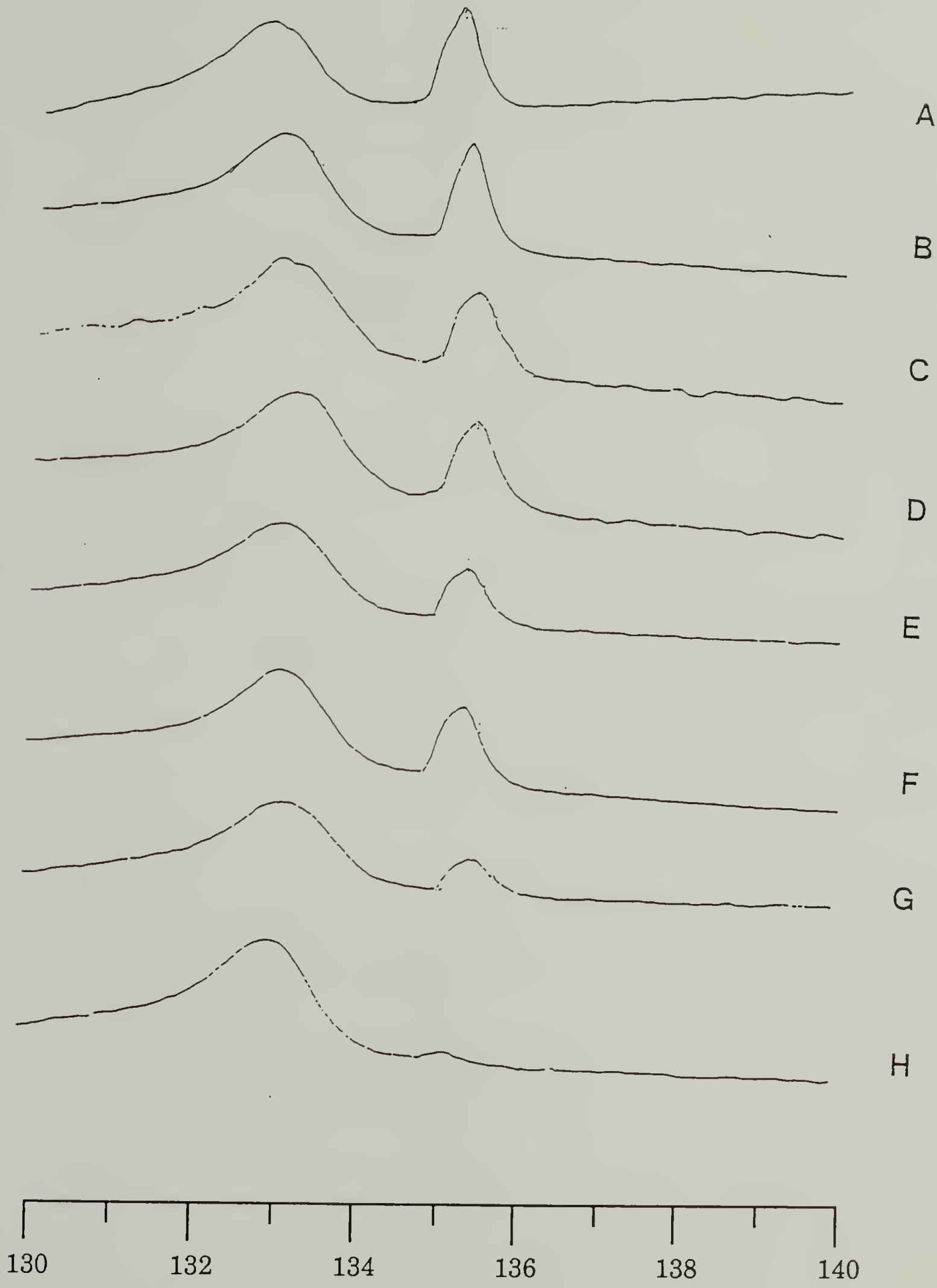
A
B
C
D
E
F
G
H
130
132
134
136
138
140
Temperature (°C)

A.)

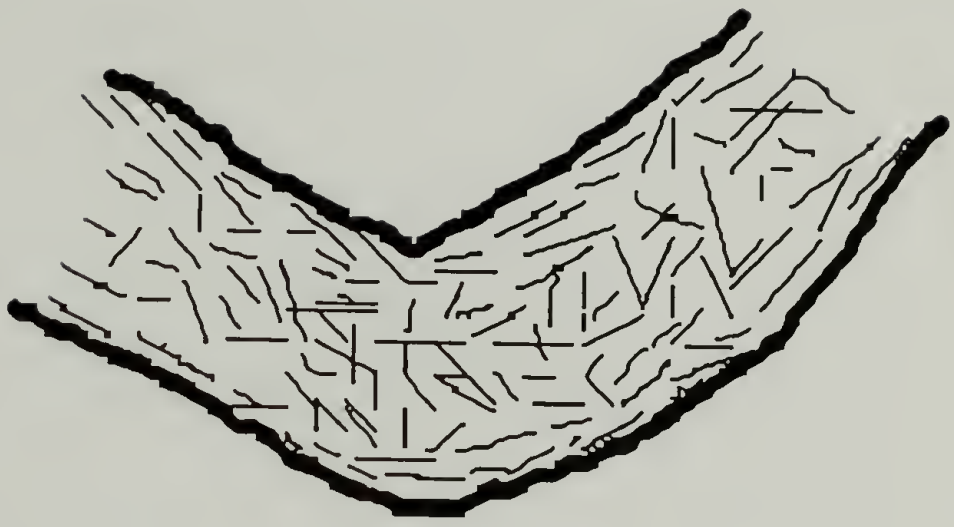

B.)

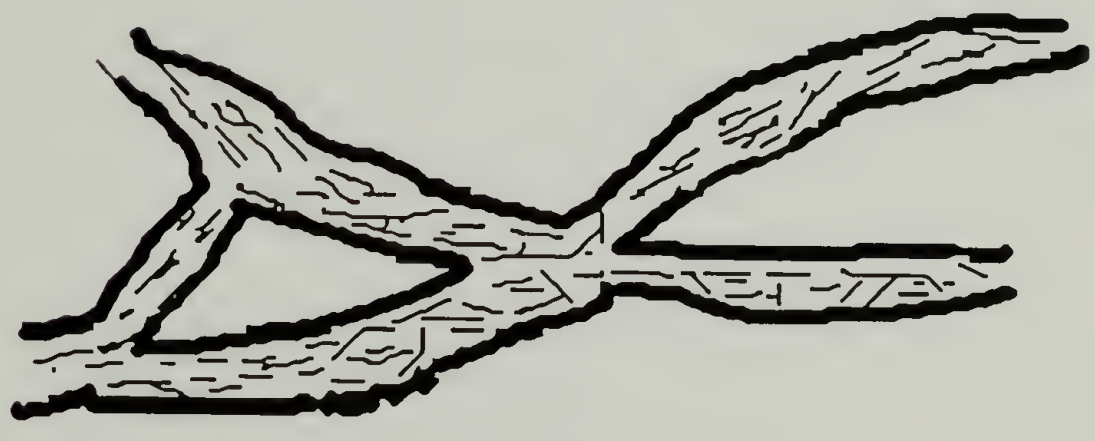

Figure 5.6 Diagrammatic sketch of a liquid crystal confined to large (**A**) and small (**B**) pores.

References

1. P. G. DeGennes, *The Physics of Liquid Crystals* (Oxford University Press, Oxford, 1974).

2. P.J. Flory, Proc. R. Soc. London **234**, 60 (1956).

3. L. Onsager, Ann. N.Y. Acad. Sci. **51**, 637 (1949).

4. W. Maier and A. Saupe, Z. Naturforsch. Teil A **14**, 882 (1959); **15**, 287 (1960).

5. P. Sheng, Phys. Rev. A **26**, 1610 (1982).

6. P. Sheng, Phys. Rev. Lett. **37**, 1059 (1976).

7. Y. IImure, H. Mada, and S. Kobayashi, Phys. Lett. **103A**, 342 (1984).

8. D. Armitage and F. P. Price, Chem. Phys. Lett. **44**, 305 (1976).

9. F. M. Aliev, Sov. Phys. Cryst. **33**, 573 (1988).

10. A. Golemme, S. Zumer, D. W. Allender, and J. W. Doane, Phys. Rev. Lett. **61**, 2937 (1988).

11. P. G. DeGennes, Mol. Cryst. Liq. Cryst. **12**, 193 (1971).

12. J. Thomson, Proc. Roy. Soc. London **A20**, 1 (1871).

13. D. Armitage and F.P. Price, Chem Phys. Lett. **44**, 305 (1976).

14. M.V. Kurik, Sov. Phys. Solid State **19**, 1081 (1977).

15. F.M. Aliev and M.N. Breganov, Sov. Phys. JETP **68**, 70 (1989).

16. D. Armitage and F.P Price, Mol. Cryst. and Liq. Cryst. **44**,33 (1978).

17. D. Armitage and F.P Price, J. Polym. Sci. Polym. Symp. **63**, 95 (1978).

18. M. Kuzma and M.M. Labes, Mol. Cryst. and Liq. Cryst. **100**, 103 (1983).

19. P. Sheng, R.W. Cohen, and J.R. Schrieffer, J. Phys. C: Solid State Phys. **14**, L565 (1981).

20. M.E. Fisher and A.E. Ferdinand, Phys. Rev. Lett. **19**, 169 (1967).

21. M.E. Fisher and M.N. Barber, Phys. Rev. Lett. **28**, 1516 (1972).

22. M.E. Fisher and A.N. Berker, Phys. Rev. B **26**, 2507 (1982).

23. M.S.S. Challa, D.P. Landau, and K. Binder, Phys. Rev. B **34**, 1841 (1986).

CHAPTER 6

CONCLUSIONS AND FUTURE WORK

Conclusions

Our objective in this study is to increase the knowledge of the phase transitions of liquid crystalline polymers. The main part of this study has centered on the gelation of poly (γ-benzyl l-glutamate) in benzyl alcohol. The phenomenon of gelation is used extensively in the processing of rod-like polymers, yet the processes that occur that result in gelation are not well understood nor theoretically predicted. We are, therefore, interested in understanding the processes that occur that result in the formation of a gel from a solution of poly (γ-benzyl l-glutamate) in benzyl alcohol.

The results of our study have helped to elucidate the processes that occur in the high temperature phase that result in gelation, as well as the relationship between polymer size and annealing time in the isotropic phase to the local structure of the resultant gel. Our results show that there exists an aggregation of PBLG in the isotropic phase up to 80 °C in benzyl alcohol. As the temperature is lowered towards the gelation threshold, the size of the aggregate changes little for the time scales of our experiments (2–10 hours/temperature). However as the

gelation transition is crossed, the size of the polymer aggregate increases substantially, indicating that further aggregation occurs at this point.

The annealing procedure in the isotropic phase will affect the local structure of the resultant gel. For a sudden quench method, where the temperature is brought from 75 °C to room temperature directly, the local structure of the gel is rather open and resembles an aggregate that is formed through the clustering of clusters mechanism. For a step quench annealing procedure, where the system is allowed to equilibrate at successive temperatures as the temperature is lowered through the isotropic phase, the local structure becomes more compact, indicating the tendency of the aggregate to relax or rearrange into a denser structure.

It has also been shown that the local rotational dynamics of the PBLG molecule in the cholesteric phase will undergo continuous reorientational motion but as the system is brought into the gel phase the motion becomes more constrained and jump-like. Deep in the gel phase, the only motion that is possible is a dumbbell like reorientation between two points. This indicates that in the cholesteric phase, though there is correlation between molecules, the local dynamics are unhindered while the transition into the gel phase constrains the local motions of the polymer.

The phenomenon of gelation is very complex and not well understood. While we have increased the knowledge of the processes that occur that result in gelation, we have not solved the problem of gelation. As the next step, we decided to step back and examine the more

general subject of the phase transitions of liquid crystals. We have completed experiments on the effect of quenched disorder on the nematic–isotropic (N–I) transition of liquid crystals. Using Monte Carlo simulation we have shown that the introduction of quenched impurities will alter the N–I transition in the following ways; it will lower the transition temperature, it will lower and round the heat capacity peak of the transition, and it will change the order of the transition. To corroborate these results, we have completed a simple experiment. Using differential scanning calorimetry, we have monitored the nematic to isotropic transition of a small molecule liquid crystal that has been confined to a controlled pore glass. These experiments show that at large pore size, the transition temperature is increased slightly due to surface induced order. At smaller pore sizes, however, the transition temperature is depressed and the heat capacity peak is lowered and rounded due to the interruption of the ability of the molecules to correlate. The results of the Monte Carlo and differential scanning calorimetry experiments give the same conclusion, that the introduction of quenched disorder can interrupt the ability of the molecules to correlate to such an extent that the transition temperature will be decreased, the heat capacity peak lowered and rounded, and the order of the transition may be changed.

Future Work

Gelation of Poly (γ-benzyl l-glutamate)

The gelation of rod-like polymers is an important step in the processing of many high strength materials. Yet, it is a phenomena that

is not well understood, or even theoretically predicted. We have attempted to characterize the dynamics and physics on a molecular level in order to understand the processes that occur that result in the gelation of the molecules. We have used small angle and quasi-elastic neutron scattering in order to view the molecule on the length scale of 10s to 100s of angstroms. We have used deuterated benzyl alcohol to increase the contrast. But, one of the greatest powers of neutron scattering is the strength of isotopic substitution. We have not fully utilized the potential of isotopic substitution and this seems to be the direction that could yield the greatest results.

A study of the radius of gyration and persistence length of the PBLG molecule at different concentrations and temperatures would allow a better characterization of the shape and reaction of the molecule to changes in temperature and concentration as the system approaches gelation. Through isotopic substitution, a deuterated PBLG molecule can be created. Addition of a small fraction of deuterated PBLG into a solution of hydrogenated PBLG and benzyl alcohol will result in an ideal system for neutron scattering. Small angle neutron scattering could then be used to determine the radius of gyration and persistence length of the deuterated PBLG molecule for all concentrations and temperatures in the phase diagram. This will allow an understanding of the structure of a single PBLG molecule as the gelation threshold is approached from the isotropic and liquid crystalline regions as well as the configuration of the macromolecule in the gel.

The results of the quasi-elastic neutron scattering could also be clarified with the help of isotopic substitution. In the PBLG molecule

there exist eight dynamically different types of hydrogen atoms; the α-methylene and the β-methylene protons on the side chain, the benzyl hydrogens, the meta phenyl hydrogens, ortho phenyl hydrogens, para phenyl hydrogen, the backbone methine hydrogen, and the amido proton. Through selective isotopic substitution,quasi-elastic neutron scattering could measure the dynamics of each proton sparately. By deuteration of all but the para position on the phenyl ring, the dynamics of that proton, and therefore the dynamics of the para axis of the phenyl ring, can be determined with quasi-elastic neutron scattering. By deuteration of all hydrogens but the α-methylene protons, the dynamics of that pair of hydrogens and therefore the dynamics of the side chain near the α-helix could be deduced. A repetition of this procedure for all sets of protons could lead to a complete characterization of the local dynamics of the PBLG molecule. Completion of these measurements at various temperatures and concentrations throughout the phase diagram will lead to an insight into the local dynamics that occur as the polymer molecule is subjected to gelation conditions.

Characterization of the gel that is formed upon solvent quality reduction of solutions of PBLG has been widely utilized as a method in understanding the gelation process. Optical microscopy[1] and electron microscopy[2,3] have been used to observe the gel while scanning electron microscopy[4,5] has been used to examine the microcellular foam that remains after removal of the solvent from the gel. These methods all examine the gel down to the length scale of microns. Using SANS, we have shown that the gel is self-similar over the length scale of 20–500 Å. We have shown that the fractal dimension of the gel is dependent on the

originating phase, the molecular weight of the macromolecule, and the thermal history of the system. Other factors that may effect the morphology of the resultant gel are shear flow and application of external fields such as magnetic or electric fields. While we have extensively studied the gels that are formed from the isotropic phase, examination of the fractal dimension for a series of molecular weights throughout the temperatures and concentrations of the phase diagram will allow a better comprehension of the gel. A detailed study of the fractal dimension of the gel formed in the presence of shear flow or external fields would also be an interesting study of the morphology of the resultant gel and possibly result in the ability to tune in a specific morphology of the gel.

The Response of Semi-flexible Liquid Crystals to Quenched Random Disorder

The study of the response of liquid crystals to the introduction of quenched random disorder provides insight into the phase transitions of liquid crystals and, also, more generally, the response of first order phase transitions to the introduction of quenched disorder. We have shown that the introduction of disorder will destroy the first order nature of the nematic-isotropic transition of a liquid crystal. This is in agreement with previous calculations that have shown that quenched random disorder can eliminate or decrease the discontinuity associated with a first order transition. There are two aspects of our results that deserve further study. We have shown that the first order nature of the transition is eliminated by the introduction of disorder, but we have not attempted to define the order of the transition that occurs in the impure

system. A more thorough analysis of the impure system as it passes through the nematic to isotropic transition can determine the order of the transition, whether it exhibits critical behavior, and, if so, the critical exponents. In this manner a more complete understanding of the nematic to isotropic transition in the presence of impurities can be achieved. The other aspect of our results that deserves elucidation is the minimum impurity concentration at which the first order nature of the transition is destroyed. We have shown that the transition occurs below 2.5% impurities, but does it occur at a finite level of impurity concentration or does it occur at the introduction of an infinitesimal amount of disorder? The answer to the question will also further explain the effect of the addition of quenched impurities to a liquid crystalline system.

We are interested in the transitions of polymeric liquid crystals, but have used a trimer as a model system in this experiment. It would take a long stretch of the imagination to assume that a trimer sufficiently models a polymer. There exist many differences in the physics of small molecule liquid crystals (SMLC) and thermotropic liquid crystalline polymers (TLCP). One example is that when TLCP are brought into the nematic state, imperfections in the ordering result in defects known as disclinations. The annihilation of these defects proceeds with annealing, but due to the high viscosity and long relaxation times of the polymer, complete elimination of these defects does not occur. For SMLC, the elimination of disclinations can proceed to completion. Therefore, creating a monodomain of a TLCP is extremely difficult, while a monodomain is readily formed in SMLC. Another example is that a

surface will order a small molecule liquid crystal after surface rubbing or surface modification. TLCP, on the other hand, will not be ordered by a surface with simple surface modification or surface rubbing, though a larger amount of order in a TLCP has been found in the presence of a magnetic field and a grooved surface than just the magnetic field. It is apparent that the connectivity of the polymer manifests itself as an increased viscosity and relaxation time which in turn affects the response of the liquid crystal to an external perturbation. It seems, therefore, that an extension of this study to a system of polymers is necessary in order to draw conclusions concerning the response of a thermotropic liquid crystalline polymer to the introduction of quenched impurities. In any case, a simple extrapolation of the reported results is not valid for liquid crystalline polymers.

<u>The Nematic-Isotropic Transition of a Liquid Crystal in a Porous Matrix.</u>

We have also completed experiments of the effect of confinement to pores on the nematic to isotropic transition of a small molecule liquid crystal. We have shown that the confinement results in an increase or decrease of the transition temperature, T_{ni}, dependent upon the ratio of the pore size to molecular size, λ. An increase in T_{ni} occurs at large λ due to surface ordering while a decrease in T_{ni} at small λ is a result of the interruption by the pores of the ability of the molecules to correlate. We have attempted to account for these results with theory. We have not, however provided direct evidence that surface ordering occurs at large λ or that many uncorrelated regimes exist at small λ. This direct evidence would be of great interest and possibly shed new light on the development

of this system, especially the processes that occur during the annealing of sample CPG3.

Using small angle neutron scattering, it could be possible to observe the liquid crystal on a local length scale as the silica porous glass beads should be nearly invisible to neutrons. If not, a more complicated system will exist, but it is still characterizable. Particularly interesting would be description of the system at a temperature between the two peaks that are present throughout the annealing of CPG3 (see figure 5.5).

As was described in the previous section, there exist many differences between the physics of small molecule liquid crystals and polymeric liquid crystal, mostly due to the long relaxation times and increased viscosity of the liquid crystalline polymer. Therefore, a more thorough understanding of the response of all liquid crystals can only be found if this study is extended to include larger liquid crystals, including polymeric liquid crystals. By lowering λ through increasing the molecular size rather than decreasing the pore size, the universality of the parameter, λ, can also be tested.

Another possible experiment that would help us to understand our results more fully would be a Monte Carlo simulation study on the effect of a wall that orders a liquid crystal on the nematic to isotropic transition of that liquid crystal. Using Monte Carlo methods, the strength of the wall–liquid crystal interaction can be specifically controlled. By changing the size of the liquid crystal a molecular weight–substrate/liquid crystal interaction–temperature phase diagram could be constructed.

References

1. P. S Russo, P. Magestro, and W. G. Miller in *Reversible Polymeric Gels and Related Systems, ACS Symposium Series* #350 edited by P.S. Russo, (American Chemical Society, Washington D.C., 1987).

2. W. G. Miller, L. Kou, K. Tohyama, and V. Voltagio, Journ. Poly. Sci.: Polym. Symp. **65**, 91 (1978).

3. K. Tohyama and W. G. Miller, Nature **289**, 813 (1981).

4. C. L. Jackson, E. T. Samulski, and M. T. Shaw, Polym. Mater. Sci. Eng. **57**, 107 (1987).

5. C. L. Jackson and M. T. Shaw, Polymer **31**, 1070 (1990).

BIBLIOGRAPHY

Berker, A. N., "Quenched Fluctuation-Induced Second Order Phase Transitions," Bull. Am. Phys. Soc. **14**, 1990 (1990).

Binder, K., *Monte Carlo Methods in Statistical Physics*, Springer–Verlag, New York (1974).

Block, H., *Poly (γ-benzyl l-glutamate) and Other Glutamic Acid Containing Polymers*, Gordon & Breach Science Publishers, New York (1983).

DeGennes, P. G., *The Physics of Liquid Crystals,* Oxford University Press, Oxford (1974).

Flory, P. J., "Phase Equilibria in Solutions of Rod-like Particles," Proc. Roy. Soc. (London). **A234**, 73 (1956).

Harris, A. B., "Effect of Random Defects on the Critical Behavior of Ising Models," J. Phys. C: Solid State Phys. **7**, 1671 (1974).

Imry, Y., and Wortis, M., "Influence of Quenched Impurities on First Order Phase Transitions," Phys Rev. B **19**, 3580 (1979).

Janik, J. A., and Riste, T., "Liquid Crystals," in *Methods in Experimental Physics, Vol 23B*, Ed. Sköld, K. and Rice, D. L. Academic Press, Boston (1986).

Leadbetter, A. J. and, Lechner, R. E., "Neutron Scattering Studies," in *The Plastically Crystalline State*, Ed. Sherwood, J.N. Wiley, New York (1979).

Mandelbrot, B., *Fractals, Form, Chance, and Dimension*, Freeman, San Francisco (1977).

Miller, W. G., Rai, J. H., and Wee, E. L., "Liquid Crystal–Isotropic Phase Equilibria in Stiff Chain Polymers," in *Liquid Crystals and Ordered Fluids*, Ed. Porter, R., and Johnston, J. Plenum, New York (1974).

Mouritsen, O.G., *Computer Studies of Phase Transitions and Critical Phenomena,* Springer–Verlag, New York (1984).

Onsager, L., "The Effect of Shapes on the Interaction of Colloidal Particles," Ann. N.Y. Acad. Sci. **51**, 627 (1949).

Russo, P. S , Magestro, P., and Miller W. G., "Gelation of Poly (γ-benzyl-α,L-glutamate)," in *Reversible Polymeric Gels and Related Systems, ACS Symposium Series* #350 Ed. Russo, P.S. American Chemical Society, Washington D.C. (1987).

Sheng, P., "Boundary Layer Phase Transition in Nematic Liquid Crystals," Phys. Rev. A **26**, 1610 (1982).

Sheng, P., "Phase Transition in Surface-Aligned Nematic Films," Phys. Rev. Lett. **37**, 1059 (1976).

Wee, E. L., and Miller, W. G., "Liquid Crystal–Isotropic Phase Equilibria in the System Poly-γ-benzyl-α, L-glutamate-Dimethylformamide," J. Phys. Chem. **75**, 1446 (1971).